Supplementary Materials for

Circularly polarized chemiluminescence from planarly chiral bis(adamantylidene-1,2-dioxetane)s

Minglin Shi,[ab] Mo Xie,[c] Shigang Wan,[b] Chao Zou,[b] Yuliang Liu,[b] Xinyan Zhou,[b] Peng Yang,[b] Xiaoyong Chang,[b] and Wei Lu*[b]

[a] School of Chemistry and Chemical Engineering, Harbin Institute of Technology, Harbin 150001, Heilongjiang, P. R. China

[b] Department of Chemistry, Southern University of Science and Technology, Shenzhen 518055, Guangdong, P. R. China. E-mail: luw@sustech.edu.cn

[c] College of Chemistry and Materials Science, Jinan University, Guangzhou 510632, Guangdong, P. R. China

Experimental Section

Materials. All starting materials were purchased from commercial sources and used as received. The solvents used for synthesis were of analytical grade unless stated otherwise. The solvents used for photophysical measurements were of HPLC grade. The reactions were performed at room temperature and under atmosphere unless states otherwise.

Characterization. ^{1}H-NMR, ^{13}C-NMR, COSY-NMR spectra were recorded with Bruker Avance 400 FT-NMR, 500 FT-NMR and/or 600 FT-NMR with Prodigy Platform spectrometers. UV-vis absorption spectra were recorded on a Thermo Scientific Evolution 201 UV-visible Spectrophotometer (all the absorption data were recorded in a 1 cm cell). High resolution mass spectra (HR-MS) were obtained on a Thermo Scientific Q Exative mass spectrometer, operated in heated electrospray ionization (HESI) mode, coupled with Thermo Scientific Ultimate 3000 system (the HR-MS signals were very weak for some dioxetanes). Single crystal of **6R** suitable for X-ray diffraction analysis was obtained by slowly evaporation of n-hexane/dichloromethane solution at ambient temperature. The diffraction data were collected on a Bruker D8 Venture single crystal X-ray diffractometer. The crystal was kept at 100 K during data collection. Using Olex2, the structure was solved with the ShelXT structure solution program using Intrinsic Phasing and refined with the SHELXL refinement package using Least Squares minimization.

Measurement. Photoluminescent (PL) spectra were recorded via Edinburgh Spectrometer FLS-980 equipped with MCP-PMT detector. Emission lifetime measurements were performed with Hamamatsu compact fluorescence lifetime spectrometer C11367. Absolute photoluminescent quantum yields (PLQY) were recorded with Hamamatsu absolute PL quantum yield spectrometer C11347. Circularly polarized photoluminescence (CP-PL) and circularly polarized chemiluminescence (CP-CL) spectra were recorded on JASCO CPL-300 at rt. Electronic circular dichroism (ECD) spectra were recorded on Applied Photophysics Chirascan at rt. Chemiluminescent (CL) spectra and kinetic scans were recorded on FLS-980 with stirring and temperature controlling. The excitation Xe lamp was off when CL measurements were performed. CL spectra were recorded about 60 s after the dioxetane solution (in DMSO, 2 mL, 0.1 mM) was added TBAF solution (in DMSO, 0.4 mL, 1 mM or 0.5 mM). The kinetic scans were started before the addition. CP-CL kinetic scans were started after a cuvette containing dioxetane solution (in DMSO, 0.8 mL, 0.5 mM) was added TBAF solution (in DMSO, 1.6 mL, 1 mM or 0.5 mM). When CP-CL spectra were recorded, the slit of the excitation arm was adjusted to the minimum and the excitation beam was block with a mask. Chemiluminescent quantum yields (CLQY) were recorded on Ultra Weak Chemiluminescent Analyzer

BPCL-GP21Q with tert-butyl(3-((1r,3r,5r,7r)-4'-methoxyspiro[adamantane-2,3'-[1,2]dioxetan]-4'yl)phenoxy) dimethylsilane (**A0**, Scheme S1) as standard (Φ_{CL} = 29%).[1] The records were started before dioxetane solution (in DMSO, 0.5 mL, 0.1 μM) was added TBAF solution (in DMSO, 0.5 mL, 1 mM).

Computational Methods

All calculations were performed with Gaussian16 suite of program[2] employing density functional theory (DFT) and time-dependent density functional theory (TDDFT). The hybrid functional M062X[3] and triple zeta basis set 6-311G(d,p)[4] were applied here. The geometries of complex **5R** and **7R** in ground state were full optimized based on the X-ray crystal structures. The singlet vertical excitation energy, rotatory strength and corresponding electron transitions as well as the frontier molecular orbital analysis was based on the ground state geometry. Based on the excitation energy, $E_{n\rightarrow m}$, and rotatory strength, the electrostatic circular dichroisms were simulated using Gaussian functions. A full width at half-maximum (FWHM), that is, the broadening of each peak (individual transition) of 0.67 eV was applied.

Abbreviations. **Et_3N** – triethylamine, **$Pd(PPh_3)_2Cl_2$** – bis(triphenylphosphine) palladium(II) chloride, **$Pd(PhCN)_2Cl_2$** – bis(benzonitrile)palladium chloride, **CuI** – Copper(I) iodide, **Et_2O** – diethyl ether, **^{n}BuLi** – n-butyllithium, **THF** – tetrahydrofuran, **MeOH** – methanol, **DIPA** – diisopropylamine, **PE** – petroleum ether, **EtOAc** – ethyl acetate, **DMSO** – dimethyl sulfoxide, **$MgSO_4$** – magnesium sulfate, **Na_2SO_3** – sodium sulfite.

Synthesis and Characterization

The compounds tert-butyl(3-((1r,3r,5r,7r)-4'-methoxyspiro [adamantane-2,3'-[1,2]dioxetan]-4'-yl)phenoxy)dimethylsilane (**A0**)[5], 3-(((1r,3r,5R,7S)-adamantan-2-ylidene)(methoxy)methyl)-2-chloro-6-iodophenol (**A10**)[6], (*R/S*)-4,12-diiodo[2.2]paracyclophane (**A13**)[7], (*R/S*)-4-iodo[2.2]paracyclophane (**A14**)[7] and were prepared according to modified literature methods.

Ref

[1] Adam, W. *et al*. *Photochem. Photobiol.* **1996,** *63*, 463-467.

[2] M. J. Frisch, H. B. Schlegel, G. E. Scuseria, M. A. Robb, J. R. Cheeseman, G. Scalmani, V. Barone, G. A. Petersson, H. Nakatsuji, X. Li, M. Caricato, A. V. Marenich, J. Bloino, B. G. Janesko, R. Gomperts, B. Mennucci, H. P. Hratchian, J. V. Ortiz, A. F. Izmaylov, J. L. Sonnenberg, D. Williams-Young, F. Ding, F. Lipparini, F. Egidi, J. Goings, B. Peng, A. Petrone, T. Henderson, D. Ranasinghe, V. G. Zakrzewski, J. Gao, N. Rega, G. Zheng, W. Liang, M. Hada, M. Ehara, K. Toyota, R. Fukuda, J. Hasegawa, M. Ishida, T. Nakajima, Y. Honda, O. Kitao, H. Nakai, T. Vreven, K. Throssell, J. A. Montgomery, Jr., J. E. Peralta, F. Ogliaro, M. J. Bearpark, J. J. Heyd, E. N. Brothers, K. N. Kudin, V. N. Staroverov, T. A. Keith, R. Kobayashi, J. Normand, K. Raghavachari, A. P. Rendell, J. C. Burant, S. S. Iyengar, J. Tomasi, M. Cossi, J. M. Millam, M. Klene, C. Adamo, R. Cammi, J. W. Ochterski, R. L. Martin, K. Morokuma, O. Farkas, J. B. Foresman, and D. J. Fox, *Gaussian 16, Revision B.01, Gaussian Inc. Wallingford CT,* **2016**.

[3] Y. Zhao, D. G. Truhlar, *J. Chem. Phy.* **2006**, *125*, 194101.

[4] P. C. Hariharan, J. A. Pople, *Theor. Chim. Acta* **1973**, *28*, 213-222.

[5] Hisamatsu, S. *et al*. *Tetrahedron* **2017**, *73*, 3993-3998.

[6] Shabat, D. *et al*. *ACS Cent Sci* **2017**, *3*, 349-358.

[7] Lützen, A. *et al. Eur. J. Org. Chem.* **2013***,* 4523–4532.

Synthetic Procedures

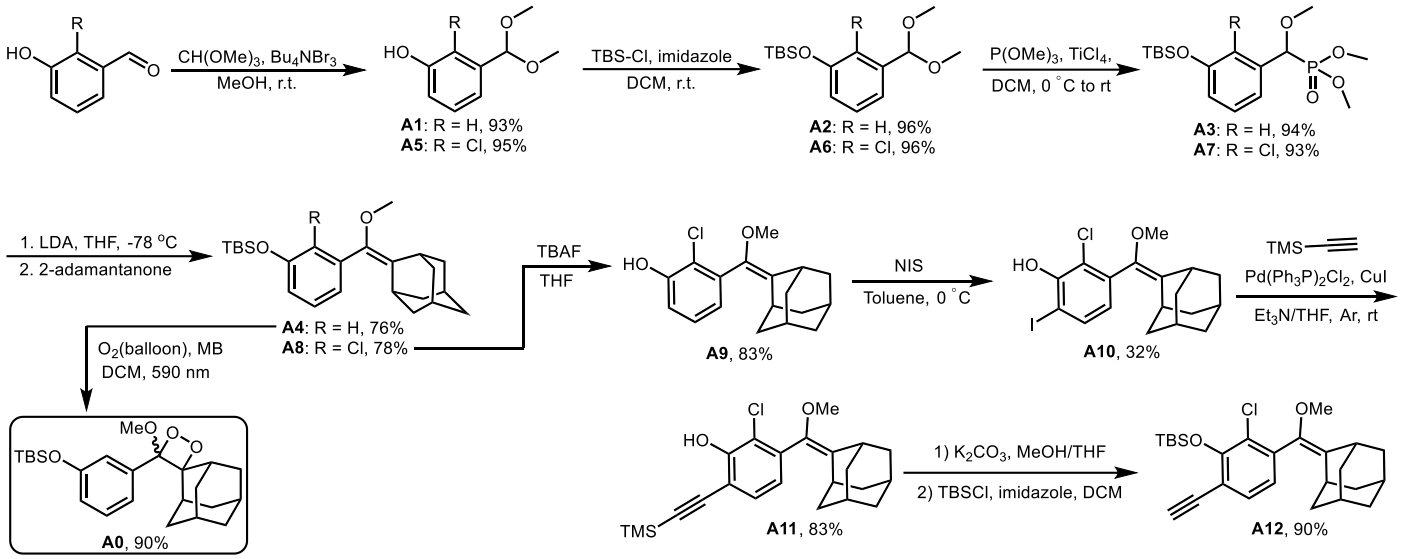

Scheme S1 The synthetic procedures of dioxetane standard **A0** and precursor **A12**.

Compound A1 and A5:

3-hydroxybenzaldehyde (2.5 g, 20 mmol) was dissolved in methanol (20 mL), Trimethyl orthoformate (3.3 ml, 30 mmol) and tetrabutylammonium tribromide (482 mg, 1.0 mmol) were adde respectively. The mixture was stirred at room temperature and monitored by thin layer chromatography (TLC) until completion. After 4 h, the solution was diluted with EtOAc and washed with 0.01M $NaHCO_3$ (100 mL). Organic phase was dried with anhydrous sodium sulfate, concentrated under reduced pressure and purified by column chromatography on silica gel (PE:EA = 90:10 , R_f = 0.39) to afford **A1** as a colorless oil (3.12 g, 93% yield). The NMR data were matched with the literature's value.[5] **A5** was obtained by the same method as a colorless oil (3.85 g, 95% yield). ^{1}H NMR (400 MHz, $CDCl_3$) δ 7.25 – 7.19 (m, 1H), 7.06 – 7.04 (m, 1H), 5.76 (s, 1H), 5.59 (s, 1H), 3.40 (s, 6H).

Compound A2 and A6:

Compound **A1** (3.02 g, 18 mmol) and imidazole (2.45 g, 36 mmol) were dissolved in DCM (40 mL). Tert-butyldimethylsilyl chloride (4.05 g, 27 mmol) was then added and the mixture was stirred and monitored by TLC. After 8 h, the white precipitate was filtered-off. The residue was evaporated under reduced pressure and purified by column chromatography on silica gel (PE:EA = 98:2 , R_f = 0.36) to afford **A2** as colorless oil. (4.87 g, 96% yield). The NMR data were matched with the literature's value.[5] **A6** was obtained by the same method as a colorless oil (5.48 g, 96% yield). ^{1}H NMR (400 MHz, $CDCl_3$) δ 7.25 (dd, J = 7.8, 1.4 Hz,

1H), 7.17 (t, *J* = 7.9 Hz, 1H), 6.90 (dd, *J* = 8.0, 1.5 Hz, 1H), 5.66 (s, 1H), 3.40 (s, 6H), 1.06 (s, 9H), 0.25 (s, 6H).

Compound A3 and A7:

Compound **A2** (4.51 g, 16 mmol) and trimethyl phosphite (2.45 ml, 20.8 mmol) were dissolved in DCM (80 mL). Reaction mixture was stirred at 0 ℃ and titanium (IV) chloride (2.11 ml, 19.2 mmol) was added dropwise. The solution was monitored by TLC. After 7 h, the reaction mixture was poured into the suspension of celite (30 g) in DCM (100 mL), after stirring 10 min, saturated $NaHCO_3$ solution (10 mL) was added at 0 ℃. The mixture stirred for 1 h before filtered, the filtrate was added saturated $NaHCO_3$ solution (80 mL) and stirred for 30 min, then the phases were separated. Organic phase was dried with anhydrous sodium sulfate, concentrated under reduced pressure and purified by column chromatography on silica gel (PE:EA 50:50, R_f = 0.45) to afford **A3** as colorless oil (5.41 g, 94% yield). ^{1}H NMR (400 MHz, $CDCl_3$) δ 7.24 (t, *J* = 8.0 Hz, 1H), 7.02 (d, *J* = 8.0 Hz, 1H), 6.95 (q, *J* = 2.0 Hz, 1H), 6.84 – 6.80 (m, 1H), 4.49 (d, *J* = 15.6 Hz, 1H), 3.71 (d, *J* = 10.4 Hz, 3H), 3.67 (d, *J* = 10.4 Hz, 3H), 3.38 (s, 3H), 0.98 (s, 9H), 0.20 (s, 6H). **A7** was obtained by the same method as a colorless oil (5.86 g, 93% yield). ^{1}H NMR (400 MHz, $CDCl_3$) δ 7.30 (dt, *J* = 7.9, 1.6 Hz, 1H), 7.22 (t, *J* = 7.9 Hz, 1H), 6.91 (dt, *J* = 7.9, 1.5 Hz, 1H), 5.22 (d, *J* = 15.7 Hz, 1H), 3.81 (d, *J* = 10.6 Hz, 3H), 3.67 (d, *J* = 10.5 Hz, 3H), 3.38 (s, 3H), 1.06 (s, 9H), 0.25 (s, 6H).

Compound A4 and A8:

Compound **A3** (5.04 g, 14 mmol) was dissolved in anhydrous THF (60 mL) under argon atmosphere at -78 ℃. LDA (2.0 M in THF, 9.0 ml, 18 mmol) was added and the solution was stirred for about 20 minutes. A solution of 2-adamantanone (3.0 g, 20 mmol) in THF (20 mL) was added at the same temperature. The reaction was kept for 15 minutes and then warmed to room temperature slowly. The mixture was monitored by TLC. After 9 h, the solution was diluted with EtOAc and washed with brine. Organic phase was dried with anhydrous sodium sulfate, concentrated under reduced pressure and purified by column chromatography on silica gel (PE:EA 99:1, R_f = 0.30) to afford **A4** as a white solid. (4.08 g, 76% yield). ^{1}H NMR (400 MHz, $CDCl_3$) δ 7.20 (t, *J* = 8.0 Hz, 1H), 6.92 – 6.90 (m, 1H), 6.80 – 6.75 (m, 2H), 3.29 (s, 3H), 3.24 (s, 1H), 2.63 (s, 1H), 2.02 – 1.78 (m, 12H), 0.99 (s, 9H), 0.19 (s, 6H). **A8** was obtained by the same method as a white solid (4.57 g, 78% yield). ^{1}H NMR (400 MHz, $CDCl_3$) δ 7.14 – 7.10 (m, 1H), 6.90 – 6.88 (m, 2H), 3.33 (s, 3H), 3.29 (s, 1H), 2.04 (s, 1H), 2.00 – 1.66 (m, 12H), 1.06 (s, 9H), 0.25 (s, 6H).

Compound A0:

Compound **A4** (76 mg, 0.2 mmol) and methylene blue (2 mg) were dissolved in DCM (4 mL). Oxygen was bubbled into the solution which was irradiated by a yellow light source (590 nm). The solution was monitored by TLC. After 15 min, the reaction mixture was purified by column chromatography on silica gel (PE:EA 98:2, R_f = 0.35) to afford **A0** as a white solid (75 mg, 90% yield). The NMR data were matched with the literature's value.[5]

Compound A9:

Compound **A8** (5.03 g, 12 mmol) was dissolved in THF (30 mL). Tetrabutylammonium fluoride (1.0 M in THF, 13 mL, 13 mmol) was added. The solution was stirred at room temperature for 2 h. The solution was diluted with EtOAc and washed with 1M HCl (15 mL). Organic phase was dried with anhydrous sodium sulfate, concentrated under reduced pressure and purified by column chromatography on silica gel (PE:EA 95:5, R_f = 0.30) to afford **A9** as a white solid (3.03 g, 83% yield). ^{1}H NMR (400 MHz, $CDCl_3$) δ 7.20 – 7.16 (m, 1H), 7.02 (dd, J = 8.2, 1.6 Hz, 1H), 6.86 (dd, J = 7.5, 1.5 Hz, 1H), 5.72 (s, 1H), 3.33 (s, 3H), 3.30 (s, 1H), 2.04 (s, 1H), 2.02 – 1.73 (m, 12H).

Compound A10:

Compound **A9** (3.05 g, 10 mmol) was dissolved in 100 ml of toluene at 0 ℃. N-Iodosuccinimide (NIS) (2.48 g, 11 mmol) was added in several portions. Reaction was stirred for 4 hours at 0 ℃ and monitored by TLC. Before byproduct was formed, the reaction mixture was carefully purified by column chromatography on silica gel (PE:EA 95:5, R_f = 0.34) to afford **A10** as white solid (1.38 g, 32% yield). The unreacted **A9** was recovered. **A10**: ^{1}H NMR (400 MHz, $CDCl_3$) δ 7.63 (d, J = 8.1 Hz, 1H), 6.64 (d, J = 8.1 Hz, 1H), 6.18 (s, 1H), 3.33 (s, 3H), 3.28 (s, 1H), 2.11 (s, 1H), 2.01 – 1.69 (m, 12H).

Compound A11:

Compound **A10** (430 mg, 1 mmol) was dissolved in Et_3N (5 ml), then $PdCl_2(PPh_3)_2$ (35 mg, 0.05 mmol) and CuI (9.5 mg, 0.05 mmol) were added successively under nitrogen atmosphere. A solution of trimethylsilylacetylene (150 mg, 1.5 mmol) in THF (5 ml) was injected to the flask. The mixture was stirred at room temperature, monitored by TLC. After 10 h, the reaction mixture was concentrated and purified by column chromatography (PE:EA = 95:5, R_f = 0.45) to give the desired product **A11** (333 mg, 83% yield) as pale-yellow solid. ^{1}H NMR (400 MHz, $CDCl_3$) δ 7.28 (d, J = 8.2 Hz, 1H), 6.81 (d, J = 8.0 Hz, 1H), 6.21 (s,

1H), 3.32 (s, 3H), 3.28 (s, 1H), 2.08 (s, 1H), 1.96 – 1.69 (m, 12H), 0.30 (s, 9H). ^{13}C NMR (126 MHz, $CDCl_3$) δ 153.2, 139.4, 136.6, 132.1, 129.6, 123.3, 120.8, 110.4, 102.6, 98.6, 57.1, 39.1, 39.0, 38.6, 38.6, 37.1, 32.9, 29.7, 28.4, 28.2, –0.1. HRMS (ESI) m/z : $[M+H]^+$ calc. for $C_{23}H_{30}ClO_2Si^+$, 401.1704; found, 401.1697.

Compound A12:

Compound **A11** (200 mg, 0.5 mmol) was dissolved in MeOH/THF (5 mL/5 mL). Potassium carbonate (345 mg, 2.5 mmol, 5.0 equiv.) was added to the solution, then the mixture was stirred at room temperature overnight. TLC was used to indicate completion of the reaction. After 9 h, the mixture was filtered through celite and washed with EtOAc. The filtrate was washed with 0.1 M HCl. The organic layer was dried by anhydrous sodium sulfate, concentrated, and used for next step without further purification. The obtained residue was dissolved in 5 ml CH_2Cl_2, then imidazole (68 mg, 1 mmol, 2 equiv.) and ter-butyldimethylsilyl chloride (113 mg, 0.75 mmol, 1.5 equiv.) were added successively. White precipitate was produced immediately. The solution was stirred at room temperature and monitored by TLC. After 4 h, the precipitate was filtered off. The residue was concentrated under reduced pressure and purified by column chromatography (PE:EA = 98:2, R_f = 0.45) to afford a white solid **A12** (199 mg, 90% yield). ^{1}H NMR (500 MHz, $CDCl_3$) δ 7.31 (d, J = 8.0 Hz, 1H), 6.83 (d, J = 8.0 Hz, 1H), 3.30 (s, 3H), 3.25 (s, 1H), 3.23 (s, 1H), 2.04 – 1.64 (m, 13H), 1.05 (s, 9H), 0.30 (s, 6H). ^{13}C NMR (126 MHz, $CDCl_3$) δ 153.5, 139.7, 136.9, 131.5, 131.2, 127.0, 124.4, 115.6, 82.4, 80.9, 56.9, 39.1, 39.0, 38.6, 38.5, 37.1, 32.9, 29.6, 28.4, 28.3, 26.0, 25.7, 18.8, –2.9, –2.9, –3.6. HRMS (ESI) m/z : $[M+H]^+$ calc. for $C_{26}H_{36}ClO_2Si^+$, 443.2173; found, 443.2168.

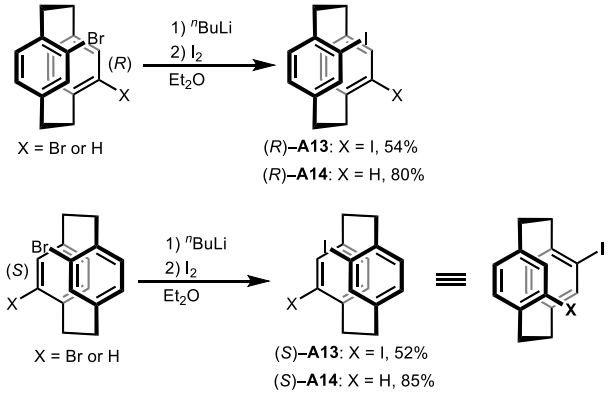

Scheme S2 The synthetic procedures of chiral scaffold (*R*/*S*)−**A13** and (*R*/*S*)−**A14**.

Compound *(R/S)*-**A13**:

4,12-dibromo[2.2]paracyclophane (366 mg, 1 mmol) was dissolved in anhydrous Et_2O (20 mL) and cooled to 0 °C, then ^{n}BuLi (2.5 M in hexane, 1.2 mL, 3 mmol) was added slowly by using a syringe and the solution was stirred for 20 min. Iodine (1.02 g, 4 mmol) was added, then the solution was warmed to room temperature and stirred for 2 h. The reaction mixture was diluted with EtOAc and water and the layers separated. The organic layer was washed with Na_2SO_3, water, and brine, and dried with $MgSO_4$. The solvent was evaporated, and the crude product was purified by column chromatography on silica gel (EtOAc/PE, 1%; R_f = 0.31) to give the product **A13** as a colorless powder.

(*R*)-4,12-diiodo[2.2]paracyclophane *(R)*-**A13**: 248 mg colourless powder, 54% yield. ^{1}H NMR (400 MHz, $CDCl_3$) δ 7.50 (d, *J* = 2.0 Hz, 2H), 6.56 – 6.49 (m, 4H), 3.40 – 3.35 (m, 2H), 3.16 – 3.05 (m, 2H), 3.00 – 2.89 (m, 4H). HRMS (ESI) m/z : $[M-H]^-$ calc. for $C_{16}H_{13}I_2^-$, 458.9112; found, 458.9114.

(*S*)-4,12-diiodo[2.2]paracyclophane *(S)*-**A13**: 239 mg colourless powder, 52% yield. ^{1}H NMR (400 MHz, $CDCl_3$) δ 7.50 (d, *J* = 2.0 Hz, 2H), 6.56 – 6.49 (m, 4H), 3.40 – 3.35 (m, 2H), 3.16 – 3.05 (m, 2H), 3.00 – 2.89 (m, 4H). HRMS (ESI) m/z : $[M-H]^-$ calc. for $C_{16}H_{13}I_2^-$, 458.9112; found, 458.9115.

Compound *(R/S)*-**A14**:

4-bromo[2.2]paracyclophane (287 mg, 1 mmol) was dissolved in anhydrous Et_2O (15 mL) and cooled to 0 °C, then ^{n}BuLi (2.5m in hexane, 0.5 mL, 1.25 mmol) was added slowly by using a syringe and the solution was stirred for 10 min. Iodine (381 mg, 1.5 mmol) was added, then the solution was warmed to room temperature and stirred for 2 h. The reaction mixture was diluted with EtOAc and washed with water and the layers separated. The organic layer was washed with Na_2SO_3 aqueous solution, water, and brine, and dried with $MgSO_4$. The solvent was evaporated, and the crude product was purified by column chromatography on silica gel (EA/PE, 1%; R_f = 0.30) to give the product **A14** as a white powder.

(*R*)-4-iodo[2.2]paracyclophane (*R*)-**A14**: 267 mg white solid, 80% yield. ^{1}H NMR (400 MHz, $CDCl_3$) δ 7.24 (dd, *J* = 8.0 Hz 2.0 Hz, 1H), 6.82 (d, *J* = 1.6 Hz, 1H), 6.58 – 6.45 (m, 4H), 6.41 (d, *J* = 7.6 Hz, 1H), 3.42 – 3.35 (m, 1H), 3.26 – 3.19 (m, 1H), 3.14 – 2.87 (m, 6H). HRMS (ESI) m/z : $[M+H]^+$ calc. for $C_{16}H_{16}I^+$, 335.0297; found, 335.0290.

(*S*)-4-iodo[2.2]paracyclophane (*S*)-**A14**: 284 mg white solid, 85% yield. ^{1}H NMR (400 MHz, $CDCl_3$) δ 7.24 (dd, *J* = 8.0 Hz 2.0 Hz, 1H), 6.82 (d, *J* = 1.6 Hz, 1H), 6.58 – 6.45 (m, 4H), 6.41 (d, *J* = 7.6 Hz, 1H), 3.41 – 3.35 (m, 1H), 3.26 – 3.19 (m, 1H), 3.15 – 2.88 (m, 6H). HRMS (ESI) m/z : $[M+H]^+$ calc. for $C_{16}H_{16}I^+$, 335.0297; found, 335.0292.

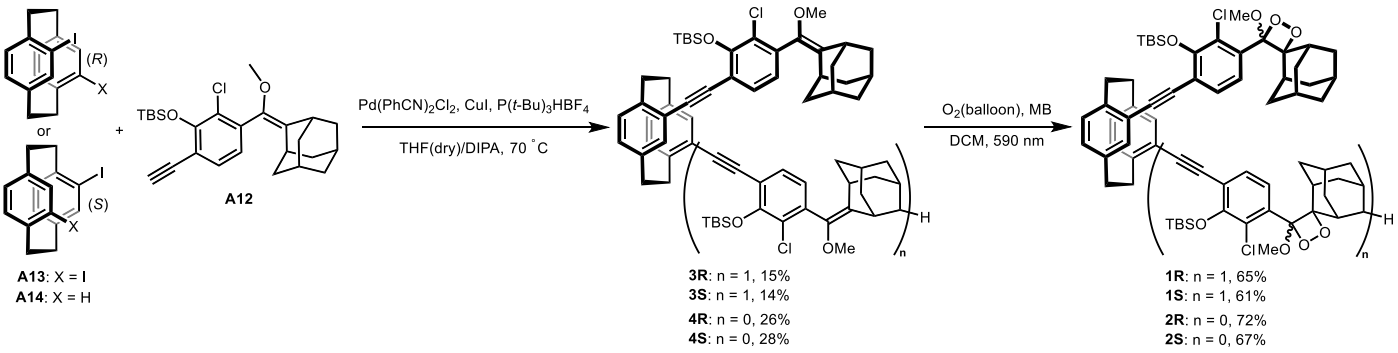

Scheme S3 The synthetic procedures of chiral dioxetanes **1R**, **1S**, **2R** and **2S**.

Compound 3R/3S and 4R/4S:

A mixture of (*R*)-**A13** (46 mg, 0.1 mmol), **A12** (97 mg, 0.22 mmol), $Pd(PhCN)_2Cl_2$ (7.7 mg, 0.02 mmol), (t-Bu)$_3$P·HBF_4 (11.6 mg, 0.04 mmol), CuI (1.9 mg, 0.01 mmol) was placed in a round-bottom flask equipped with magnetic stirring bar. After degassing the reaction mixture three times, dry THF (4 mL) and dry DIPA (4 mL) were added to the mixture via a syringe. The reaction was carried out at 70 °C overnight. After the reaction mixture was cooled to room temperature, precipitates were removed by filtration, and the solvent was evaporated. The residue was purified by column chromatography on SiO_2 (EtOAc/petroleum ether = 1/50 v/v as an eluent, R_f = 0.21) to afford **3R** (16.3 mg, 15%) as a light brown solid, further purification was performed by prep-TLC. **3S** (15.3 mg, 14%) was prepared by same methods with (*S*)-**A13** (46 mg, 0.1 mmol) and **A12** (97 mg, 0.22 mmol) as materials. **4R** and **4S** were prepared by same methods.

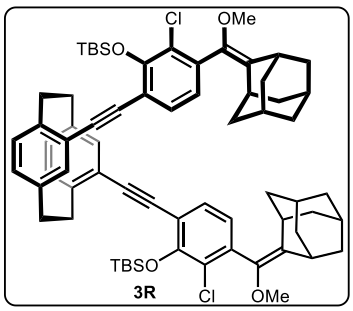

3R: 16.3 mg pale-yellow solid, 15% yield.^{1}H NMR (400 MHz, $CDCl_3$) δ 7.47 – 7.44 (m, 2H), 7.08 (s, 2H), 6.91 (d, J = 8.0 Hz, 2H), 6.57 (s, 4H), 3.72 – 3.66 (m, 2H), 3.34 (s, 6H), 3.28 (s, 2H), 3.21 – 3.12 (m, 4H), 2.91 – 2.86 (m, 2H), 2.13 – 2.12 (m, 2H), 1.96 – 1.71 (m, 24H), 0.95 (s, 18H), 0.24 – 0.21 (m, 12H). ^{13}C NMR (101 MHz, $CDCl_3$) δ 152.3, 142.4, 139.9, 139.7, 136.1, 133.7, 133.0, 131.2, 130.9, 127.2, 124.8, 124.5, 119.2, 117.5, 104.8, 94.09, 57.1, 56.9, 39.2, 39.0, 38.6, 37.2, 34.6, 33.8, 33.0, 29.6, 28.4, 28.3, 25.9, 22.7, 18.7, –2.9, –3.3. HRMS (ESI) m/z : $[M+Na]^+$ calc. for $C_{68}H_{82}O_4Cl_2Si_2Na^+$, 1111.5026; found, 1111.5031.

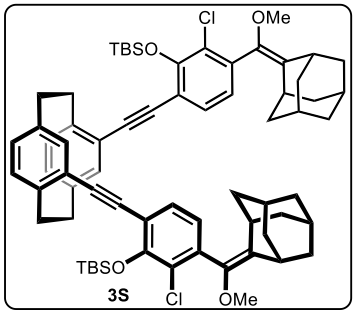

3S: 15.3 mg pale-yellow solid, 14% yield.^{1}H NMR (500 MHz, $CDCl_3$) δ 7.46 – 7.43 (m, 2H), 7.08 (s, 2H), 6.90 (d, J = 8.0 Hz, 2H), 6.57 (s, 4H), 3.72 – 3.67 (m, 2H), 3.34 (s, 6H), 3.28 (s, 2H), 3.21 – 3.12 (m, 4H), 2.91 – 2.86 (m, 2H), 2.12 – 2.12 (m, 2H), 1.98 – 1.70 (m, 24H), 0.95 (s, 18H), 0.23 – 0.21 (m, 12H). ^{13}C NMR (126 MHz, $CDCl_3$) δ 152.3, 142.5, 139.9, 139.7, 136.1, 133.9, 133.0,

131.2, 131.0, 127.2, 124.8, 124.5, 119.2, 117.6, 104.8, 94.1, 77.3, 77.0, 76.8, 57.1, 56.9, 39.2, 39.0, 38.6, 37.2, 34.7, 34.6, 33.8, 33.0, 29.6, 28.4, 28.3, 26.9, 25.9, 18.7, –2.9, –3.3. HRMS (ESI) m/z : $[M+Na]^+$ calc. for $C_{68}H_{82}O_4Cl_2Si_2Na^+$, 1111.5026; found, 1111.5019.

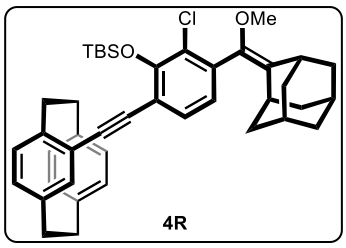

4R: 16.8 mg pale-yellow solid, 26% yield. ^{1}H NMR (500 MHz, $CDCl_3$) δ 7.48 (d, *J* = 7.5 Hz, 1H), 7.00 (d, *J* = 8.0 Hz, 1H), 6.95 (d, *J* = 8.0 Hz, 1H), 6.59 – 6.45 (m, 6H), 3.67 (t, *J* = 10.5 Hz, 1H), 3.37 (d, *J* = 4.5 Hz, 3H), 3.33 – 3.23 (m, 2H), 3.17 – 3.05 (m, 4H), 3.03 – 2.96 (m, 1H), 2.94 – 2.89 (m, 1H), 2.14 (s, 1H), 2.06 – 1.73 (m, 12H), 1.10 (s, 9H), 0.36 – 0.34 (m, 6H). ^{13}C NMR (101 MHz, $CDCl_3$) δ 152.2, 142.6, 139.9, 139.7, 139.4, 139.3, 136.4, 136.2, 134.0, 133.2, 132.9, 132.7, 132.4, 131.2, 131.0, 130.3, 127.3, 124.8, 124.6, 117.5, 94.4, 90.2, 56.9, 39.2, 39.0, 38.6, 38.6, 37.2, 35.5, 35.2, 34.5, 34.4, 33.0, 29.6, 28.4, 28.3, 26.0, 25.9, 18.8, –3.0, –3.1.

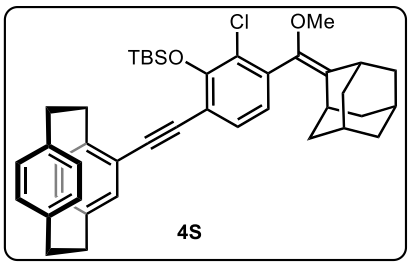

4S: 18.2 mg pale-yellow solid, 28% yield.^{1}H NMR (400 MHz, $CDCl_3$) δ 7.48 (d, *J* = 7.5 Hz, 1H), 7.00 (d, *J* = 8.0 Hz, 1H), 6.95 (d, *J* = 8.0 Hz, 1H), 6.59 – 6.44 (m, 6H), 3.67 (t, *J* = 12.4 Hz, 1H), 3.36 (d, *J* = 2.8 Hz, 3H), 3.32 – 3.22 (m, 2H), 3.17 – 3.07 (m, 4H), 3.05 – 2.99 (m, 1H), 2.96 – 2.87 (m, 1H), 2.13 (s, 1H), 1.97 – 1.72 (m, 12H), 1.09 (s, 9H), 0.35 – 0.33 (m, 6H). ^{13}C NMR (101 MHz, $CDCl_3$) δ 152.3, 142.6, 139.9, 139.7, 139.5, 139.4, 136.5, 136.2, 134.0, 133.3, 132.9, 132.7, 132.4, 131.2, 131.0, 130.3, 127.3, 124.9, 124.6, 117.5, 94.5, 90.3, 56.9, 39.2, 39.0, 38.6, 38.6, 37.2, 35.5, 35.2, 34.6, 34.5, 33.0, 29.7, 28.5, 28.3, 26.0, 18.9, –3.0, –3.1.

Compound 1R/1S and 2R/2S:

The dioxetanes were synthesized using photocatalytic oxidation pathway. Precursor **3R** (21.8 mg, 0.02 mmol) and methylene blue (MB, 1 mg) were dissolved in of CH_2Cl_2 (4 ml). Oxygen was bubbled into the solution which was irradiated by a yellow light source (590 nm) for 15 min. The reaction was monitored by TLC and purified by column chromatography (PE:EA = 20:1, R_f = 0.20) to obtain **1R** as a mixture of three diastereoisomers which are same spots on TLC plate and difficult to separate by column chromatography, their structures are illustrated in **Figure S2**. **1S**, **2R** and **2S** were obtained with same procedures.

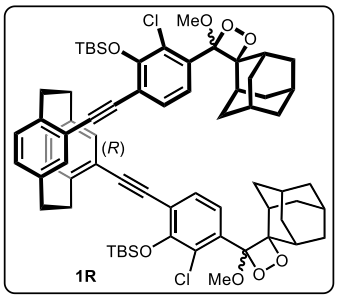

1R: 15.0 mg white solid, 65% yield. ^{1}H NMR (400 MHz, $CDCl_3$) δ 7.72 (d, *J* = 8.4 Hz, 2H), 7.55 (d, *J* = 8.0 Hz, 2H), 7.07 (d, *J* = 8.0 Hz, 2H), 6.59 (s, 4H), 3.71 – 3.66 (m, 2H), 3.24 – 3.13 (m, 10H), 3.02 (s, 2H), 2.94 – 2.88 (m, 2H), 2.37 – 2.34 (m, 2H), 2.12 (s, 2H), 1.93 – 1.57 (m, 22H), 0.97 – 0.93 (m, 18H), 0.24 – 0.18 (m, 12H). ^{13}C NMR (126 MHz, $CDCl_3$) δ 152.9, 152.9, 142.6, 142.6, 139.7, 139.7, 134.0, 134.0, 133.9, 133.8, 133.4, 133.3, 133.2, 131.4, 131.3, 131.2, 125.6, 124.8, 124.5, 119.4, 119.4, 119.4, 112.4, 105.1, 96.4, 96.4, 95.2, 95.1, 90.2, 90.1, 90.1, 77.3, 77.0, 76.8, 49.6, 49.6, 44.6, 42.4, 39.3, 39.0, 38.8, 36.7, 34.8, 34.6, 33.9, 33.9, 33.8, 33.5, 32.7, 32.7, 32.3, 32.3, 32.3, 31.6, 31.5, 29.7, 29.5, 26.9, 26.3, 26.2, 25.9, 25.9, 25.9, 25.8, 25.3, 23.0, 23.0, 21.2, 20.2, 19.2, 18.8, 18.7, 18.7, 14.4, 14.2, 11.4, –2.8, –2.9, –2.9, –3.1, –3.1, –3.2, –3.2. HRMS (ESI) m/z : $[M+H]^+$ calc. for $C_{68}H_{83}Cl_2O_8Si_2^+$, 1153.5004; found, 1153.5021.

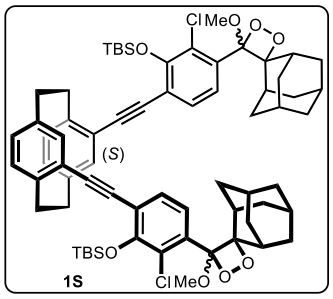

1S 14.1 mg white solid, 61% yield. ^{1}H NMR (400 MHz, $CDCl_3$) δ 7.72 (d, *J* = 8.4 Hz, 2H), 7.55 (d, *J* = 8.0 Hz, 2H), 7.07 (d, *J* = 8.0 Hz, 2H), 6.59 (s, 4H), 3.72 – 3.66 (m, 2H), 3.24 – 3.10 (m, 10H), 3.02 (s, 2H), 2.94 – 2.88 (m, 2H), 2.37 – 2.34 (m, 2H), 2.12 (s, 2H), 1.93 – 1.48 (m, 22H), 0.96 – 0.93 (m, 18H), 0.24 – 0.18 (m, 12H). ^{13}C NMR (126 MHz, $CDCl_3$) δ 153.0, 142.6, 139.7, 134.0, 134.0, 133.9, 133.8, 133.4, 133.3, 131.4, 131.3, 125.7, 124.8, 124.5, 119.4, 112.1, 105.1, 96.4, 96.4, 95.2, 90.1, 90.0, 77.3, 77.2, 77.0, 76.8, 49.6, 49.6, 47.0, 39.3, 36.7, 36.3, 34.5, 33.9, 33.5, 32.7, 32.7, 32.3, 32.3, 31.6, 31.5, 27.5, 26.9, 26.3, 25.9, 25.9, 25.9, 25.9, 22.7, 20.2, 18.8, 18.7, –2.9, –3.2, –3.2. HRMS (ESI) m/z : $[M]^+$ calc. for $C_{68}H_{83}Cl_2O_8Si_2^+$, 1153.5004; found, 1153.4999.

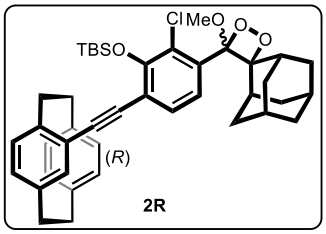

2R: 9.8 mg white solid, 72% yield. ^{1}H NMR (400 MHz, $CDCl_3$) δ 7.79 (d, *J* = 8.0 Hz, 1H), 7.62 (d, *J* = 8.4 Hz, 1H), 7.01 – 6.98 (m, 1H), 6.62 – 6.47 (m, 6H), 3.69 (t, *J* = 11.8 Hz, 1H), 3.32 – 3.24 (m, 4H), 3.19 – 2.92 (m, 7H), 2.39 (d, *J* = 13.2 Hz, 1H), 2.17 (d, *J* = 7.2 Hz, 1H), 1.95 (d, *J* = 12.4 Hz, 1H), 1.87 (d, *J* = 13.2 Hz, 1H), 1.80 – 1.73 (m, 3H), 1.70 – 1.63 (m, 4H), 1.43 – 1.41 (m, 2H), 1.11 (d, *J* = 2.0 Hz, 9H), 0.37 – 0.31 (m, 6H). ^{13}C NMR (101 MHz, $CDCl_3$) δ 152.8, 142.8, 142.8, 139.8, 139.4, 139.4, 139.3, 136.5, 136.4, 134.0, 133.2, 133.2, 133.2, 132.7, 132.4, 132.4, 131.3, 130.4, 130.3, 125.7, 124.8, 124.5, 124.5, 119.4, 112.0, 96.4, 95.5, 95.5, 89.8, 89.7, 77.3, 77.0, 76.7, 49.6, 36.6, 35.5, 35.2, 34.5, 34.4, 33.9, 33.5, 32.7, 32.6, 32.3, 31.6, 31.5, 26.9, 26.2, 26.0, 25.8, 18.8, –2.9, –2.9, –3.0, –3.0.

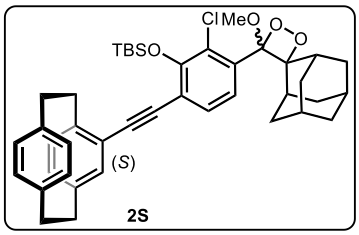

2S: 9.1 mg white solid, 67% yield. ^{1}H NMR (500 MHz, $CDCl_3$) δ 7.79 (d, *J* = 8.5 Hz, 1H), 7.62 (d, *J* = 8.5 Hz, 1H), 7.00 (t, *J* = 7.0 Hz, 1H), 6.62 – 6.47 (m, 6H), 3.69 (t, *J* = 11.8 Hz, 1H), 3.30 – 3.24 (m, 4H), 3.19 – 2.92 (m, 7H), 2.39 (d, *J* = 12.5 Hz, 1H), 2.17 (d, *J* = 10.5 Hz, 1H), 1.95 (d, *J* = 13.5 Hz, 1H), 1.87 (d, *J* = 13 Hz, 1H), 1.80 – 1.77 (m, 3H), 1.70 – 1.63 (m, 4H), 1.43 – 1.41 (m, 2H), 1.11 (d, *J* = 2.0 Hz, 9H), 0.36 – 0.31 (m, 6H). ^{13}C NMR (101 MHz, $CDCl_3$) δ 152.8, 142.8, 142.8, 139.8, 139.4, 139.4, 139.3, 136.5, 136.4, 134.0, 133.2, 133.2, 133.2, 132.7, 132.4, 132.4, 131.3, 130.4, 130.3, 125.7, 124.8, 124.5, 124.5, 119.4, 112.0, 96.4, 95.5, 95.5, 89.8, 89.7, 77.3, 77.2, 77.0, 76.7, 49.6, 36.6, 35.5, 35.2, 34.5, 34.4, 33.9, 33.5, 32.7, 32.6, 32.3, 31.6, 31.5, 26.9, 26.2, 26.0, 26.0, 25.8, 18.8, –2.9, –2.9, –3.0, –3.0.

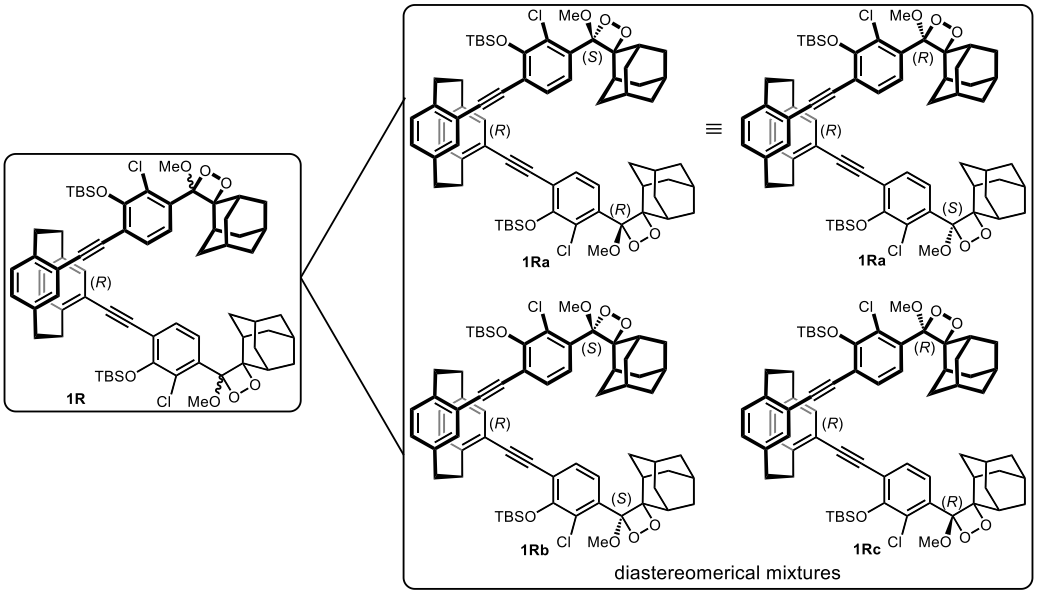

Figure S1 The chemical structures of three diastereoisomers of **1R**.

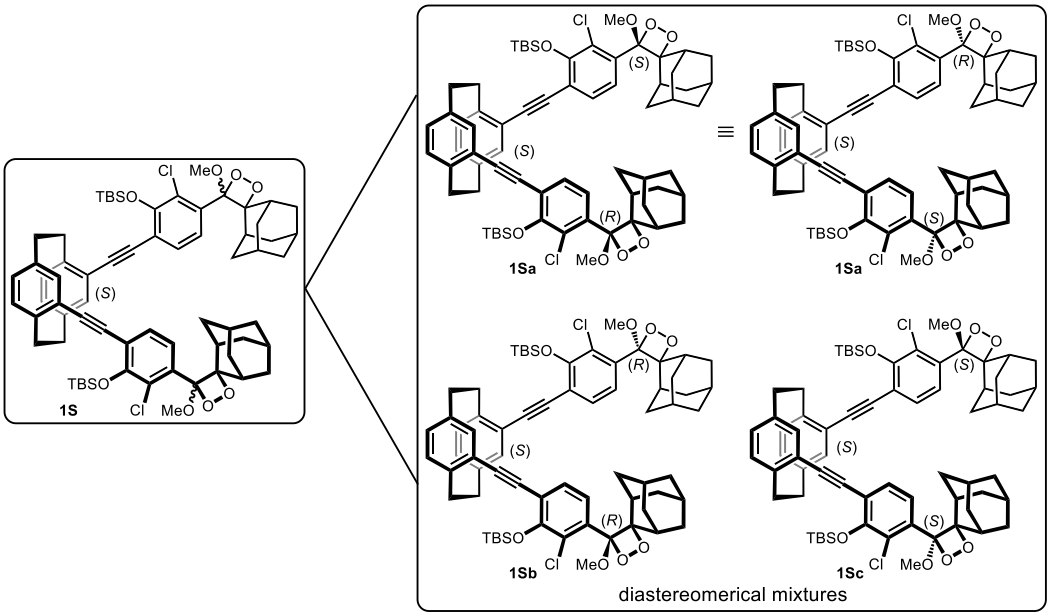

Figure S2 The chemical structures of three diastereoisomers of **1S**.

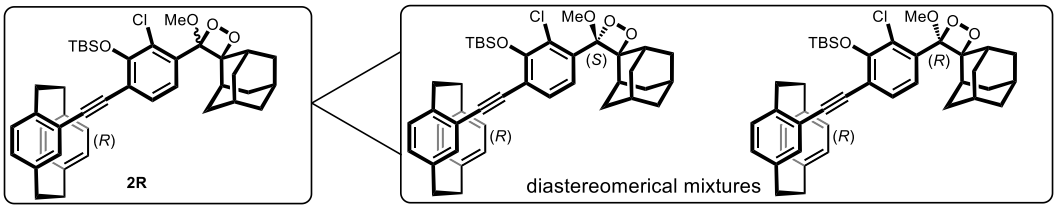

Figure S3 The chemical structures of two diastereoisomers of **2R**.

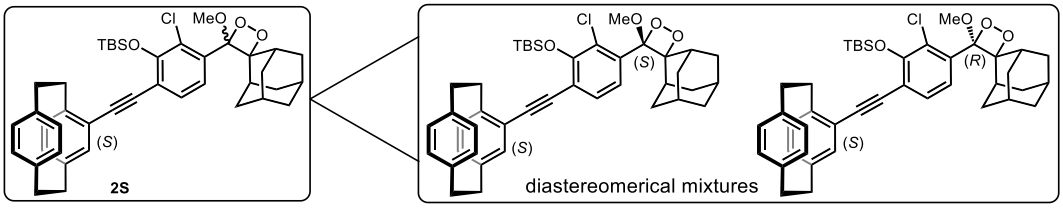

Figure S4 The chemical structures of two diastereoisomers of **2S**.

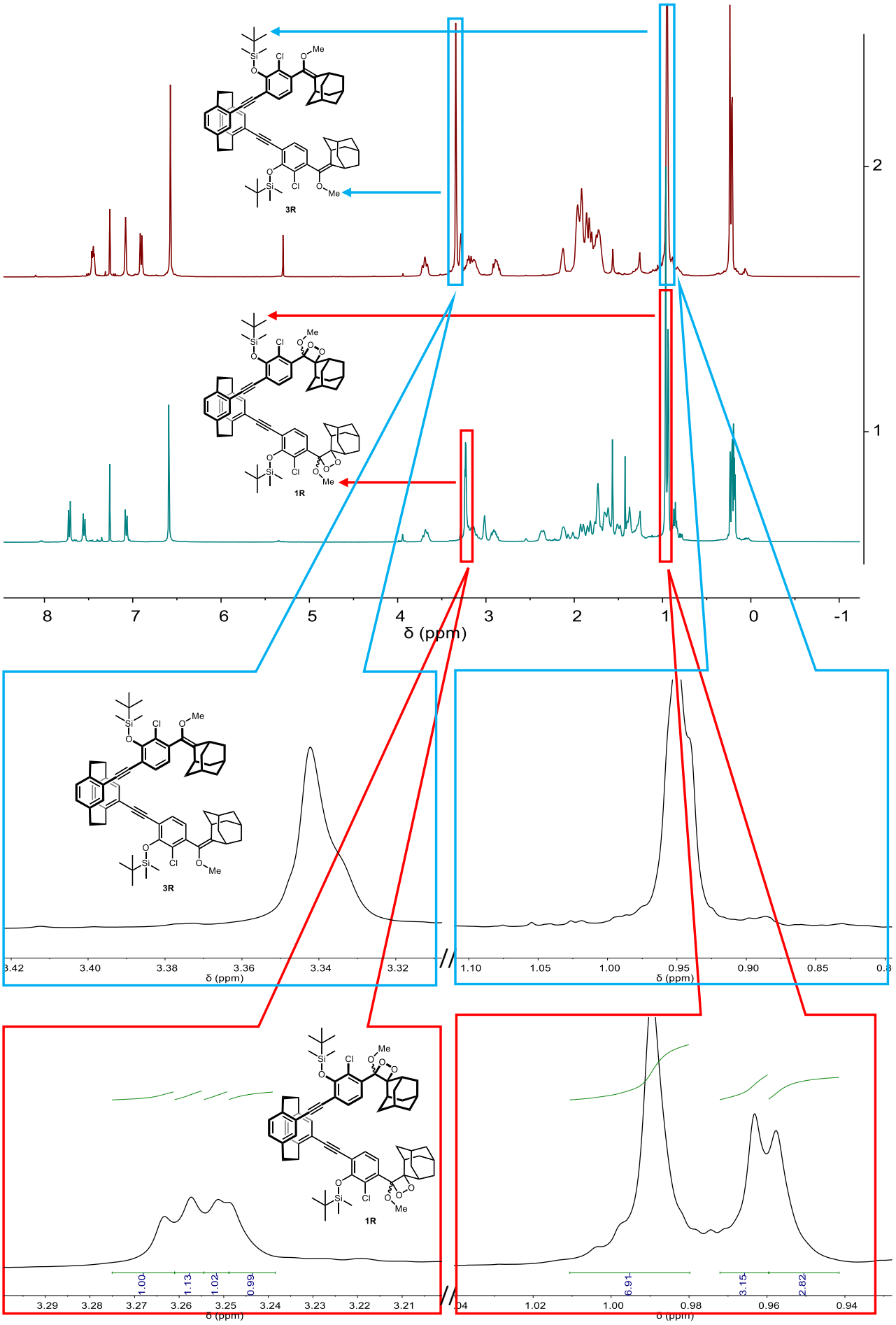

Figure S5 Illustration of the diastereoisomer ratio determined by ^{1}H-NMR spectra of **1R**.

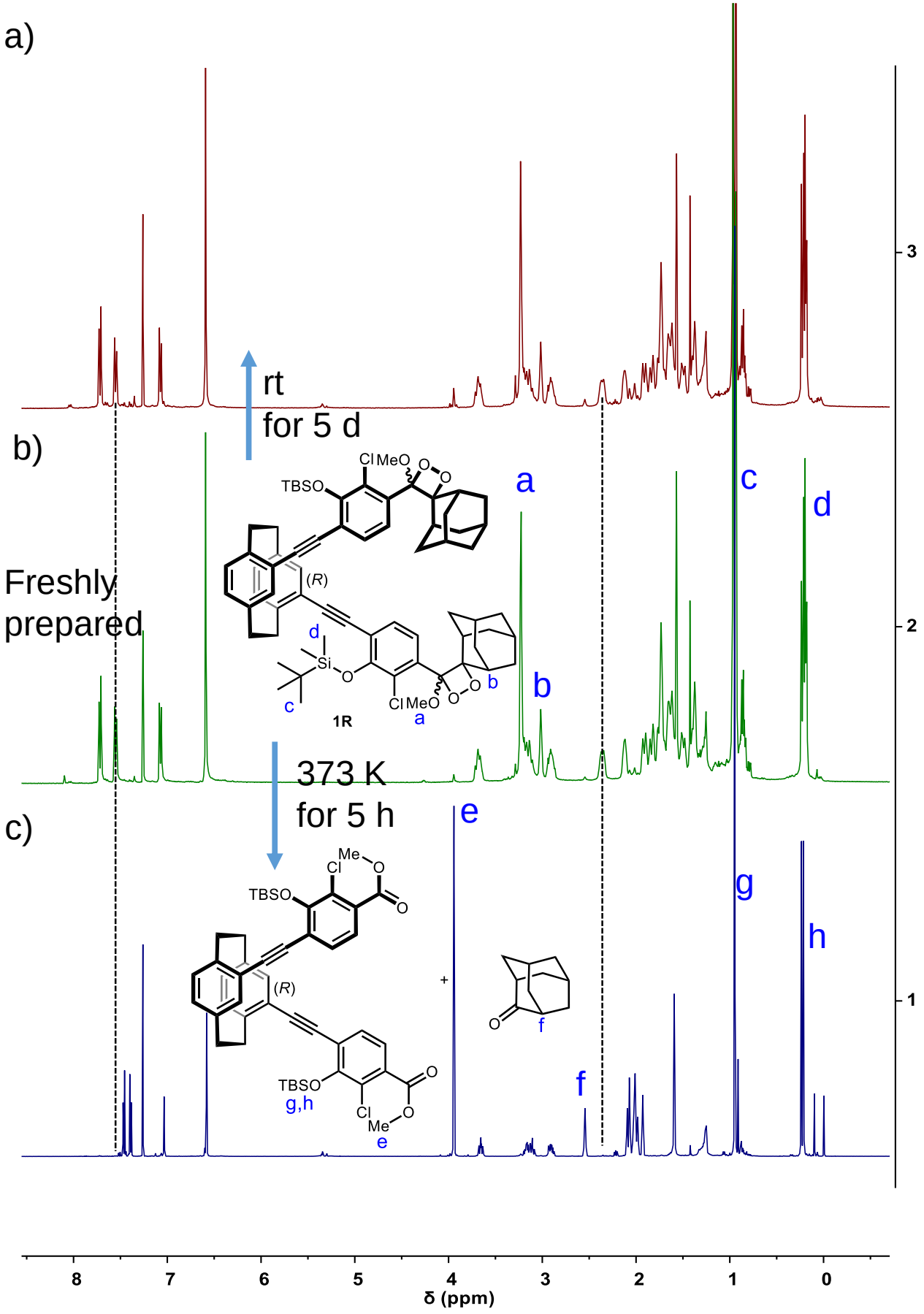

Figure S6 Comparison of ^{1}H-NMR spectra (500 MHz, $CDCl_3$): (a) **1R** stored at rt for 5 days, (b) freshly prepared **1R**, and (c) the mixture of **1R** heated at 100 ℃ for 5 hours.

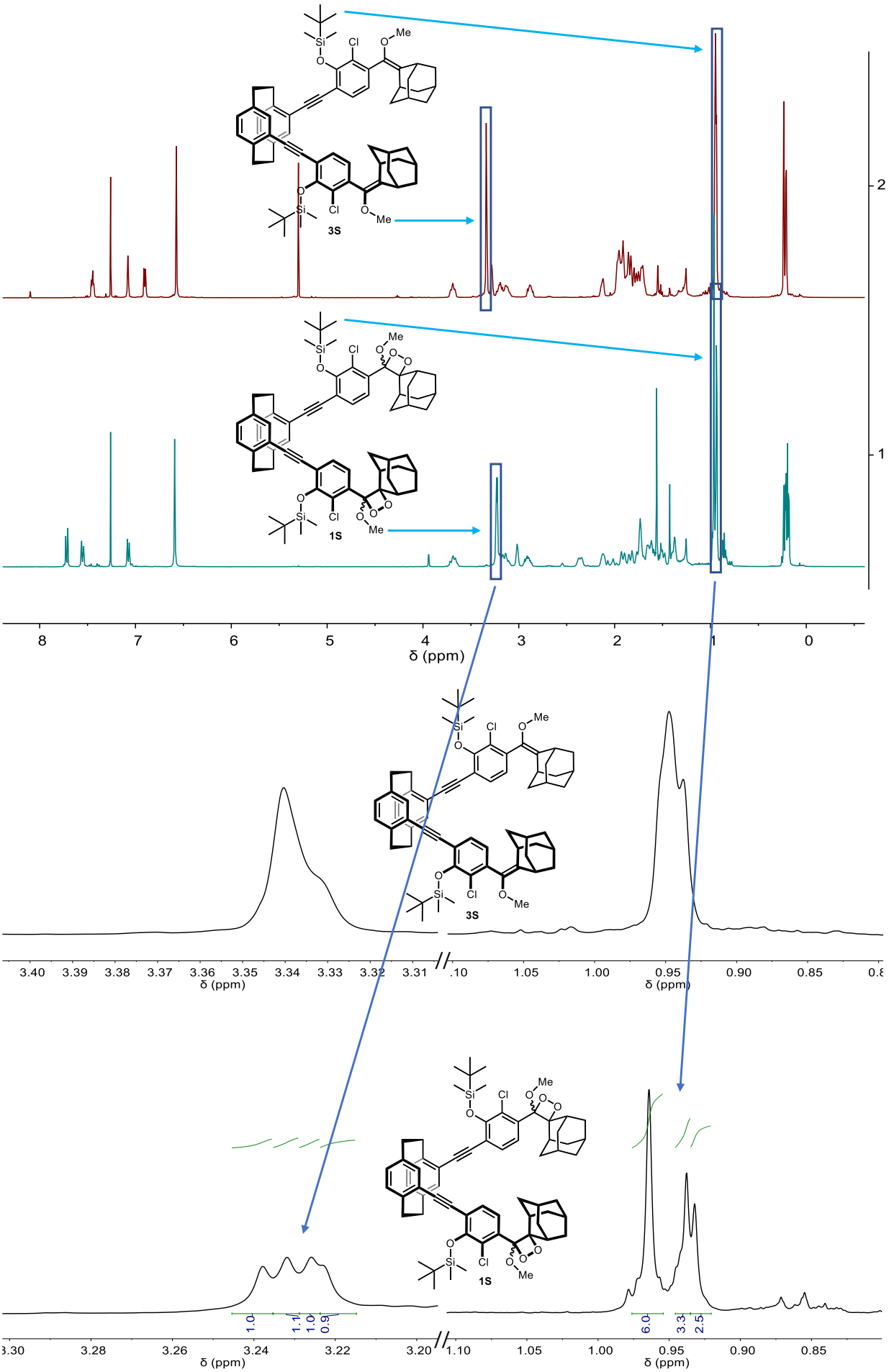

Figure S7 Illustration of the diastereoisomer ratio determined by ^{1}H-NMR spectra of **1S**.

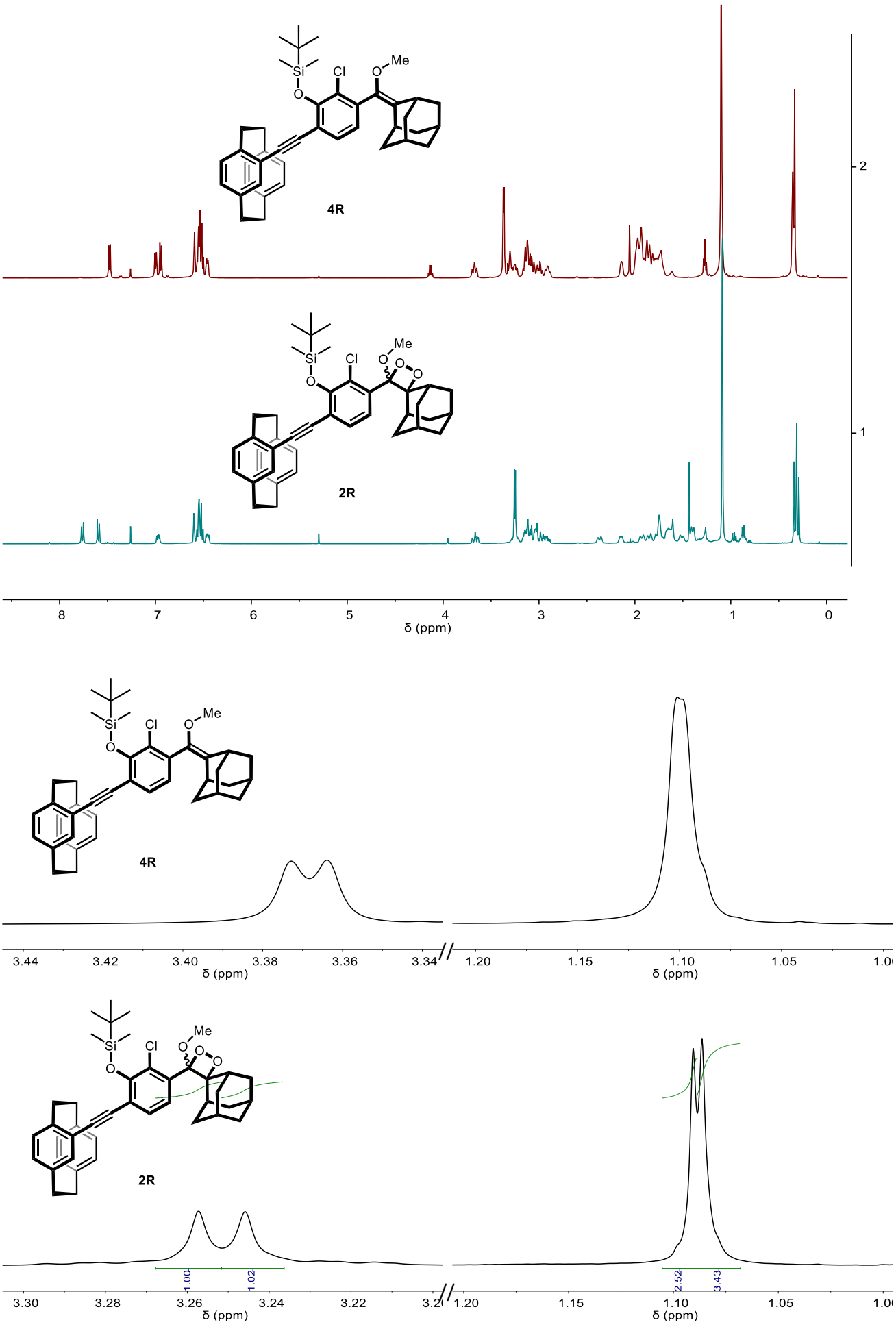

Figure S8 Comparison of ^{1}H-NMR spectra between **4R** and **2R**.

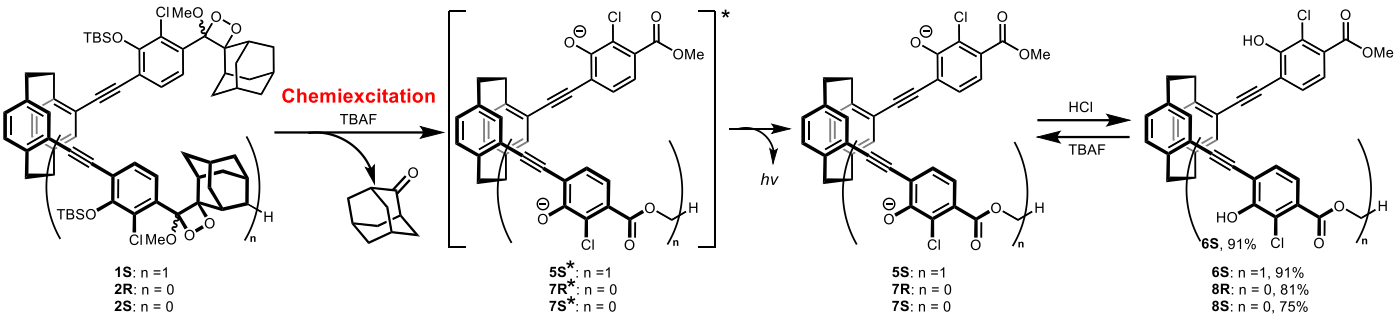

Scheme S4 The chemiexcitation of **1S**, **2R**/**2S** and synthetic procedures of **6S**, **8R**/**8S**.

Compound 6R/6S and 8R/8S:

To a solution of **1R** (23.1 mg, 0.02 mmol) in THF (5 mL) was added TBAF (0.2 mL, 1 M in THF), light emitted immediately, and the mixture stirred for 60 min for completely conversion, then extracted with EtOAc and acidified with 1 M HCl. The organic layer was washed with brine, dried with $MgSO_4$. The solvent was evaporated, and the crude product was purified by column chromatography on silica gel (EA/PE, 20 %; R_f = 0.3) to give **6R** as pale-yellow solid. **6S**, **8R** and **8S** were prepared by same methods.

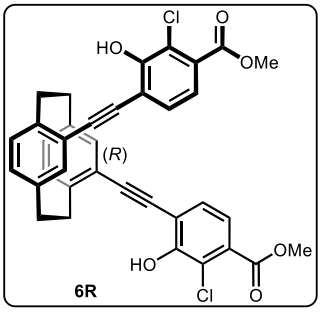

6R: 11.2 mg pale-yellow solid, 90% yield. ^{1}H NMR (500 MHz, $CDCl_3$) δ 7.45 (s, 4H), 7.16 (s, 2H), 6.62 – 6.58 (m, 4H), 6.53 (s, 2H), 3.95 (s, 6H), 3.70 – 3.65 (m, 2H), 3.26 – 3.21 (m, 2H), 3.11 – 3.06 (m, 2H), 2.97 – 2.91 (m, 2H). ^{13}C NMR (126 MHz, $CDCl_3$) δ 165.5, 153.2, 142.6, 139.9, 134.1, 134.1, 133.8, 130.0, 129.8, 123.8, 122.7, 120.0, 115.2, 98.0, 86.8, 52.6, 34.3, 33.7. HRMS (ESI) m/z : $[M-H]^-$ calc. for $C_{36}H_{25}Cl_2O_6^-$, 623.1034; found, 623.1036.

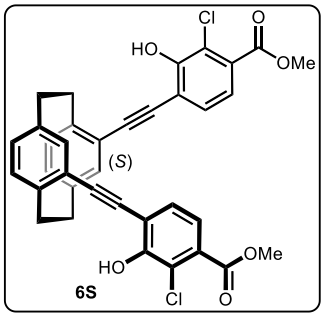

6S: 11.3 mg pale-yellow solid, 91% yield.^{1}H NMR (500 MHz, $CDCl_3$) δ 7.46 (s, 4H), 7.16 (s, 2H), 6.62 – 6.58 (m, 4H), 6.52 (s, 2H), 3.96 (s, 6H), 3.70 – 3.65 (m, 2H), 3.27 – 3.21 (m, 2H), 3.12 – 3.07 (m, 2H), 2.97 – 2.91 (m, 2H). ^{13}C NMR (126 MHz, $CDCl_3$) δ 165.5, 153.2, 142.6, 139.8, 134.1, 134.0, 133.7, 130.0, 129.7, 123.7, 122.7, 120.0, 115.1, 97.9, 86.7, 52.6, 34.2, 33.6. HRMS (ESI) m/z : $[M-H]^-$ calc. for $C_{36}H_{25}Cl_2O_6^-$, 623.1034; found, 623.1037.

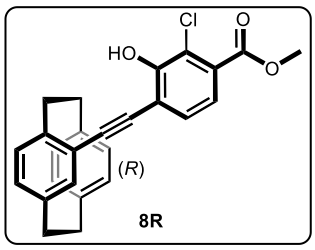

8R: 6.7 mg pale-yellow solid, 81% yield. ^{1}H NMR (400 MHz, $CDCl_3$) δ 7.48 (d, *J* = 8.4 Hz, 1H), 7.45 (d, *J* = 8.8 Hz, 1H), 7.01 (dd, *J* = 8.0 Hz 1.6 Hz, 1H), 6.63 – 6.48 (m, 6H), 6.43 (s, 1H), 3.96 (s, 3H), 3.71 – 3.64 (m, 1H), 3.33 – 3.26 (m, 1H), 3.16 – 2.89 (m, 6H). ^{13}C NMR (101 MHz, $CDCl_3$) δ 165.5, 153.1, 142.9, 140.0, 139.5, 139.4, 137.1, 134.1, 133.7, 133.4, 132.8, 132.4, 130.1, 129.8, 123.8, 122.8, 120.0, 115.4, 98.3, 86.5, 52.6, 35.5, 35.1, 34.5, 34.3. HRMS (ESI) m/z : $[M+H]^+$ calc. for $C_{26}H_{22}ClO_3^+$, 417.1257; found, 417.1248.

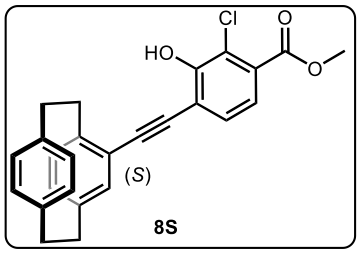

8S: 6.2 mg pale-yellow solid, 75% yield. ^{1}H NMR (400 MHz, $CDCl_3$) δ 7.48 (d, *J* = 8.4 Hz, 1H), 7.45 (d, *J* = 8.4 Hz, 1H), 7.01 (dd, *J* = 8.0 Hz 1.6 Hz, 1H), 6.63 – 6.48 (m, 6H), 6.43 (s, 1H), 3.96 (s, 3H), 3.71 – 3.64 (m, 1H), 3.33 – 3.26 (m, 1H), 3.16 – 2.89 (m, 6H). ^{13}C NMR (101 MHz, $CDCl_3$) δ 165.5, 153.1, 142.9, 140.0, 139.5, 139.4, 137.1, 134.1, 133.7, 133.4, 132.8, 132.4, 130.1, 129.8, 129.8, 123.8, 122.8, 120.0, 115.4, 98.3, 86.5, 52.6, 35.5, 35.1, 34.5, 34.3. HRMS (ESI) m/z : $[M+H]^+$ calc. for $C_{26}H_{22}ClO_3^+$, 417.1257; found, 417.1247.

NMR and HRMS Spectra

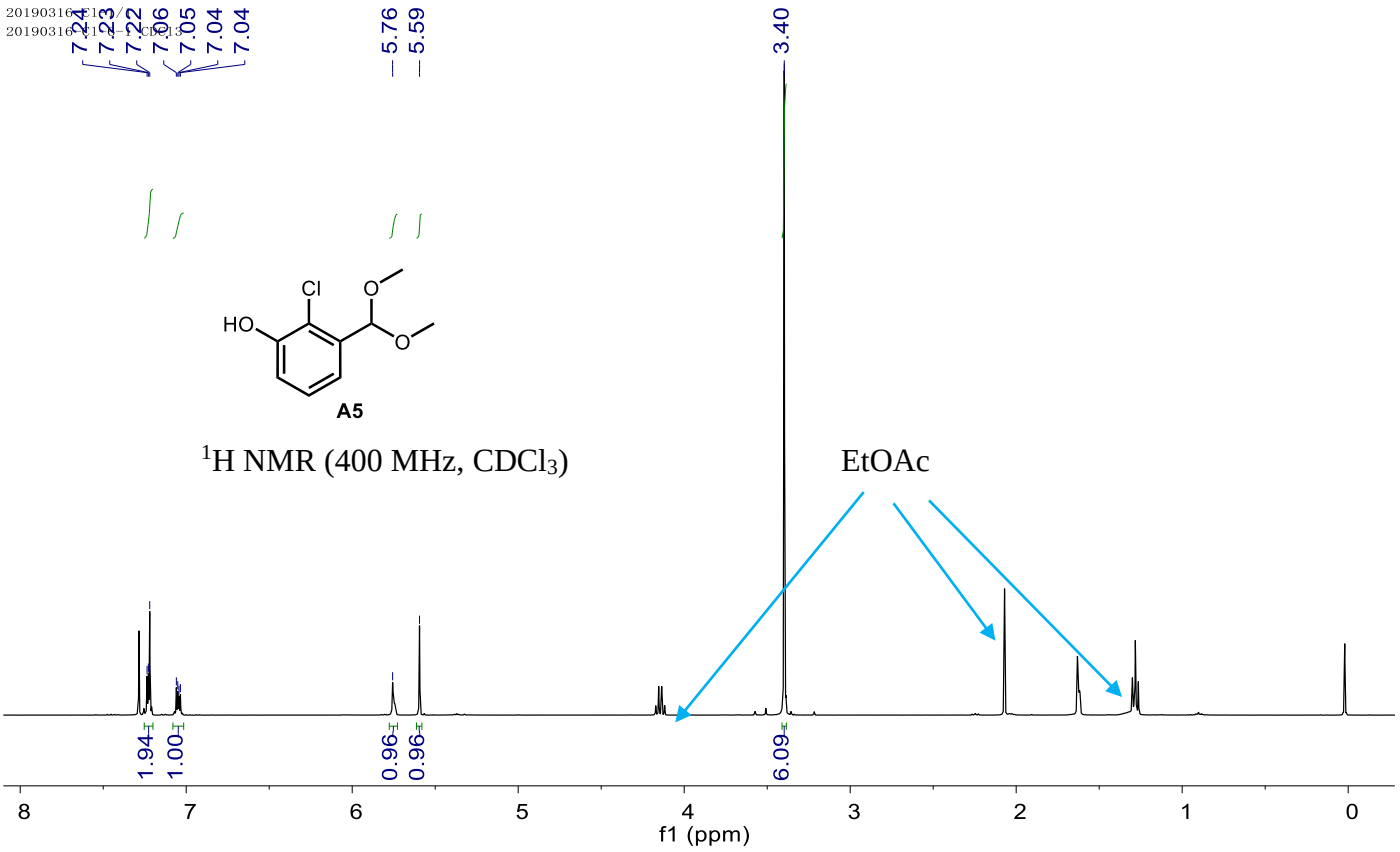

^{1}H NMR (400 MHz, $CDCl_3$)

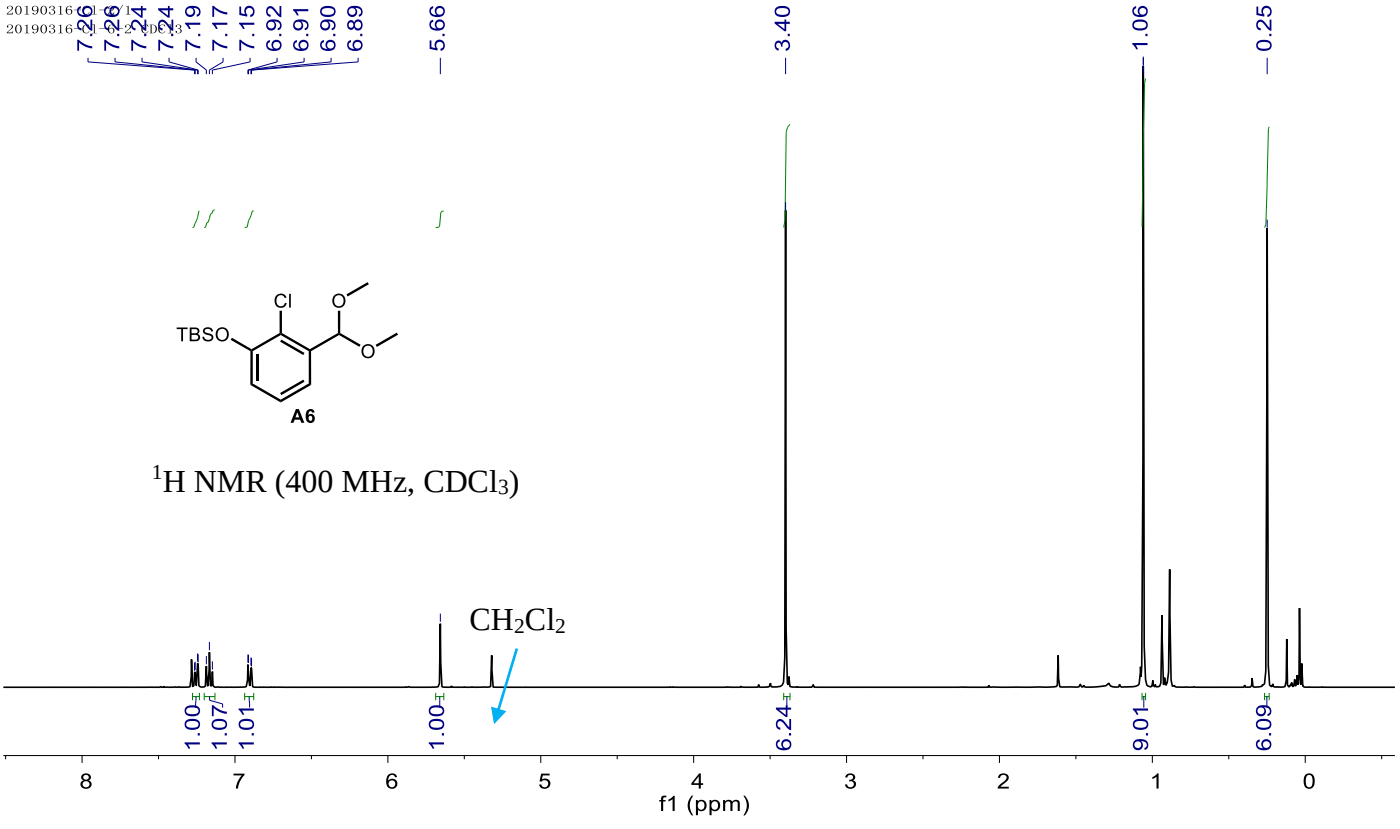

^{1}H NMR (400 MHz, $CDCl_3$)

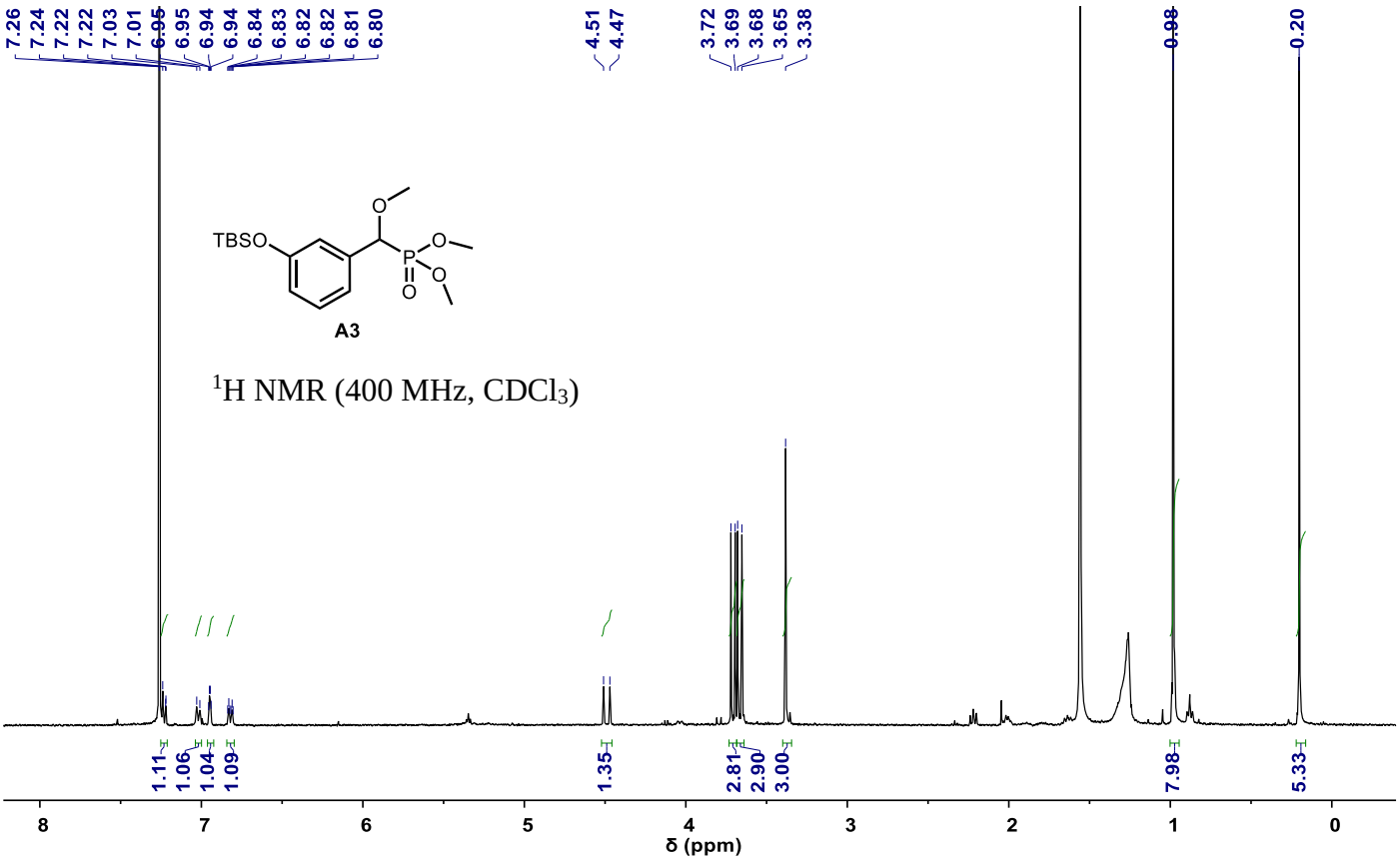

A3

^{1}H NMR (400 MHz, $CDCl_3$)

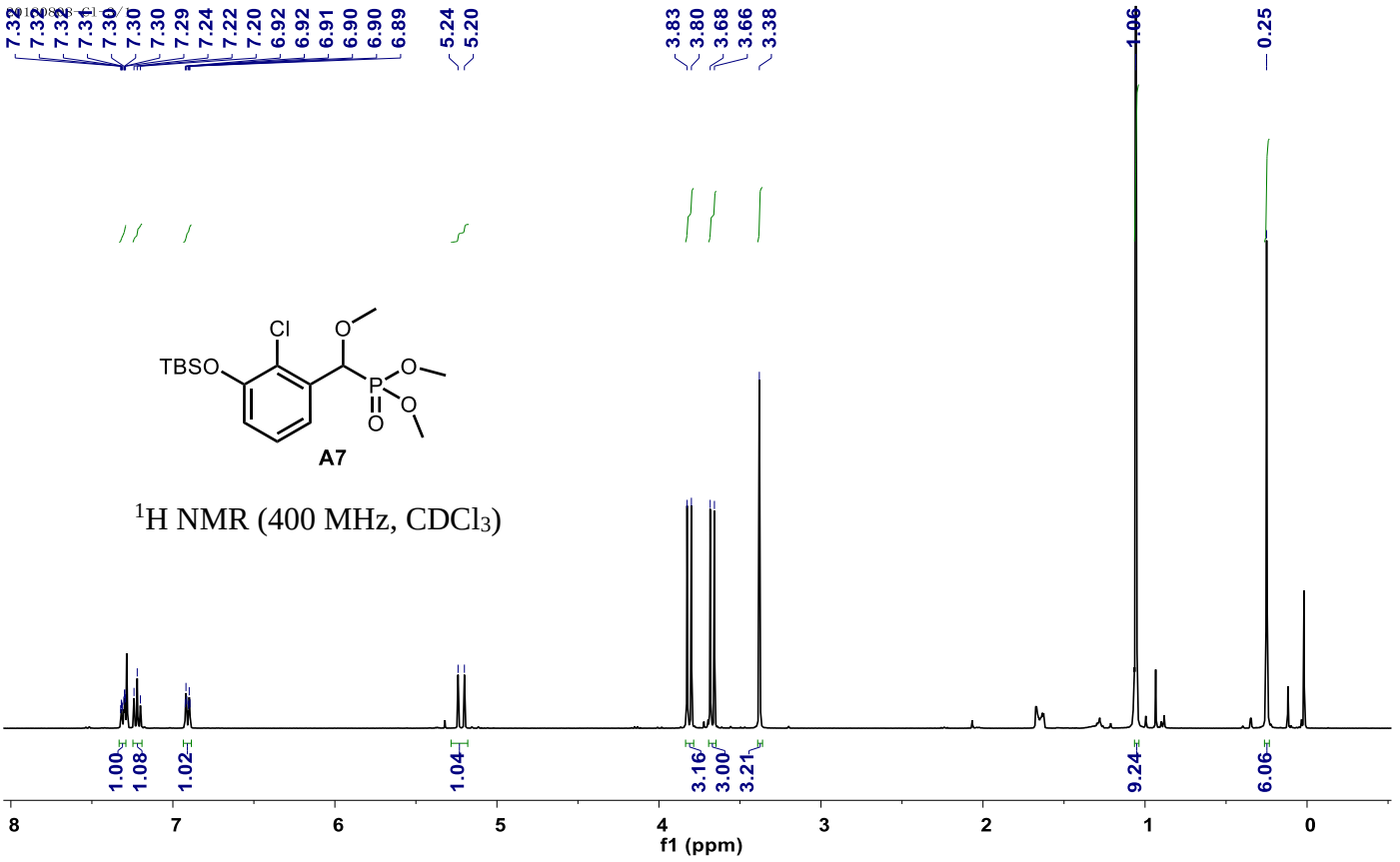

A7

^{1}H NMR (400 MHz, $CDCl_3$)

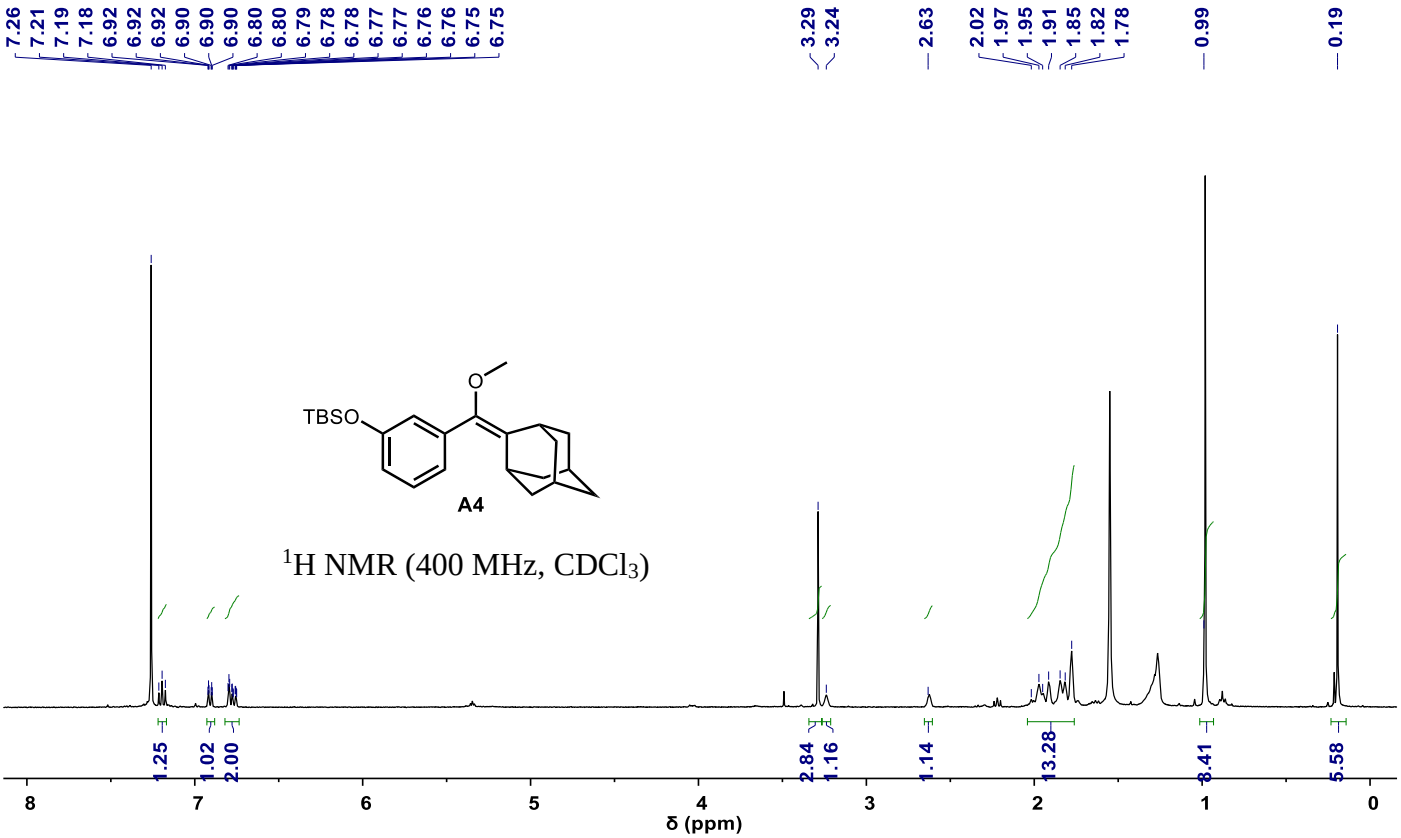

^{1}H NMR (400 MHz, $CDCl_3$)

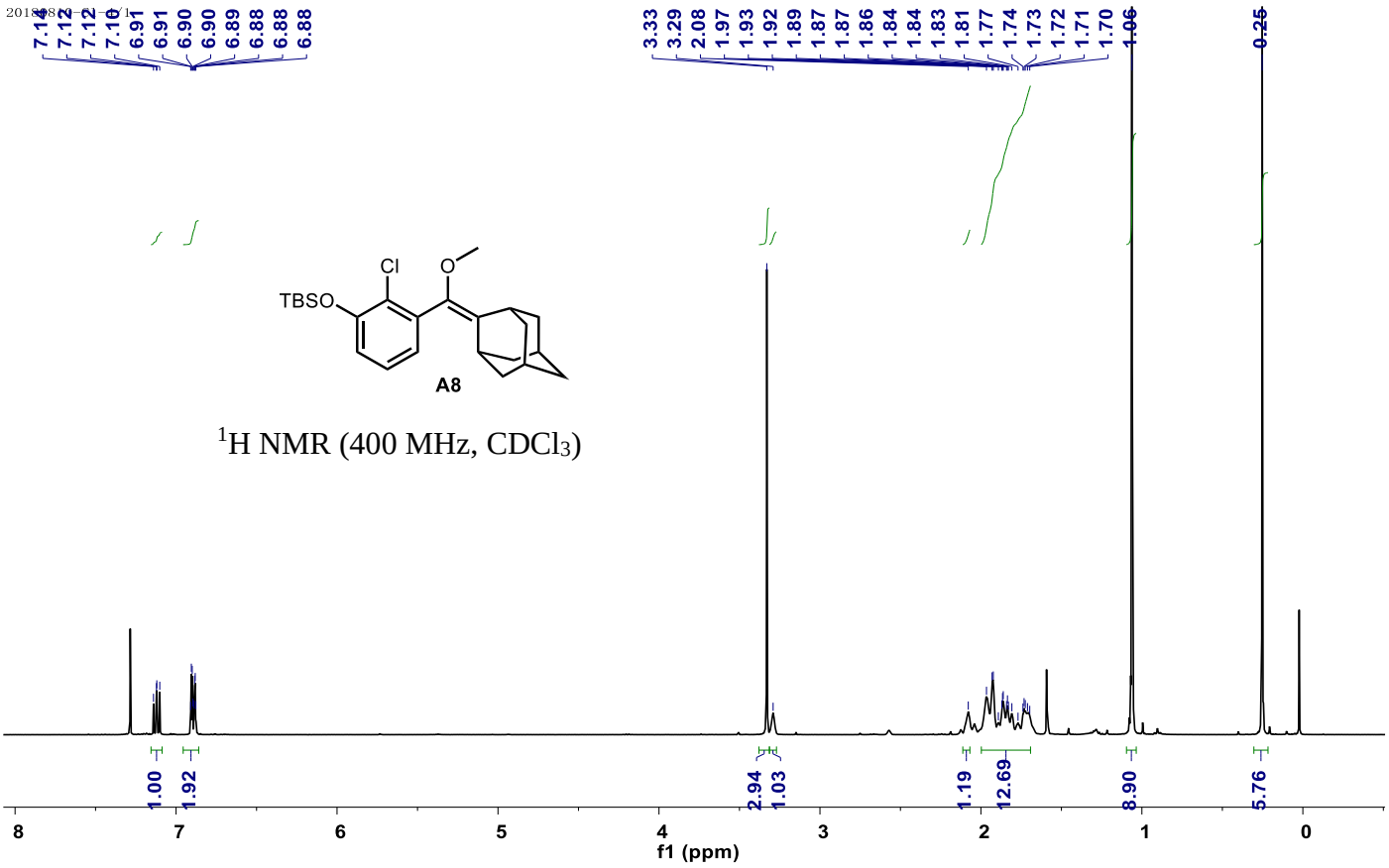

^{1}H NMR (400 MHz, $CDCl_3$)

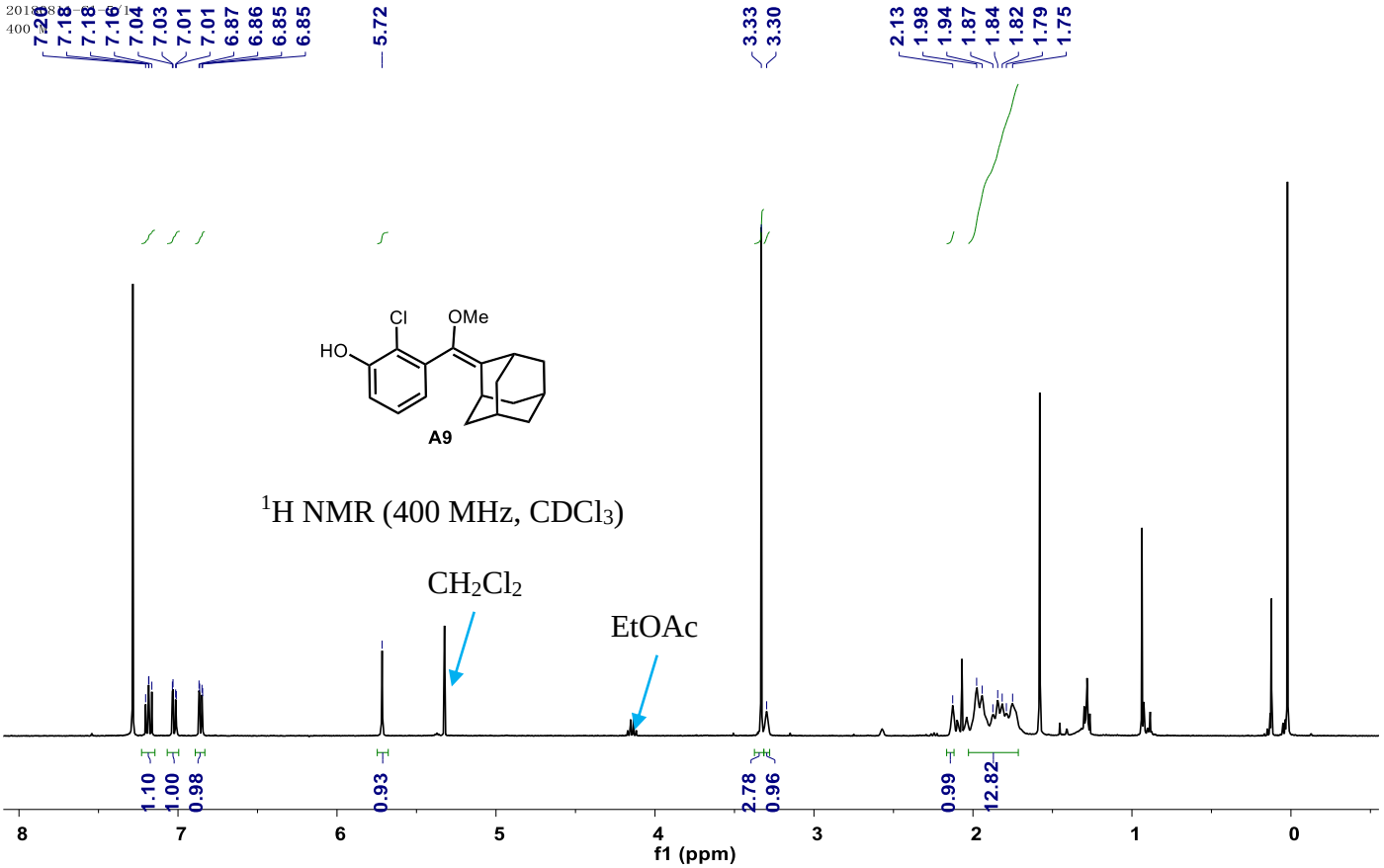
7.20
7.18
7.18
7.16
7.04
7.03
7.01
7.01
6.87
6.86
6.85
6.85
5.72
3.33
3.30
2.13
1.98
1.94
1.87
1.84
1.82
1.79
1.75
Cl
OMe
HO
A9
1H NMR (400 MHz, CDCl3)
CH2Cl2
EtOAc
1.10
1.00
0.98
0.93
2.78
0.96
0.99
12.82
8
7
6
5
4
3
2
1
0
f1 (ppm)

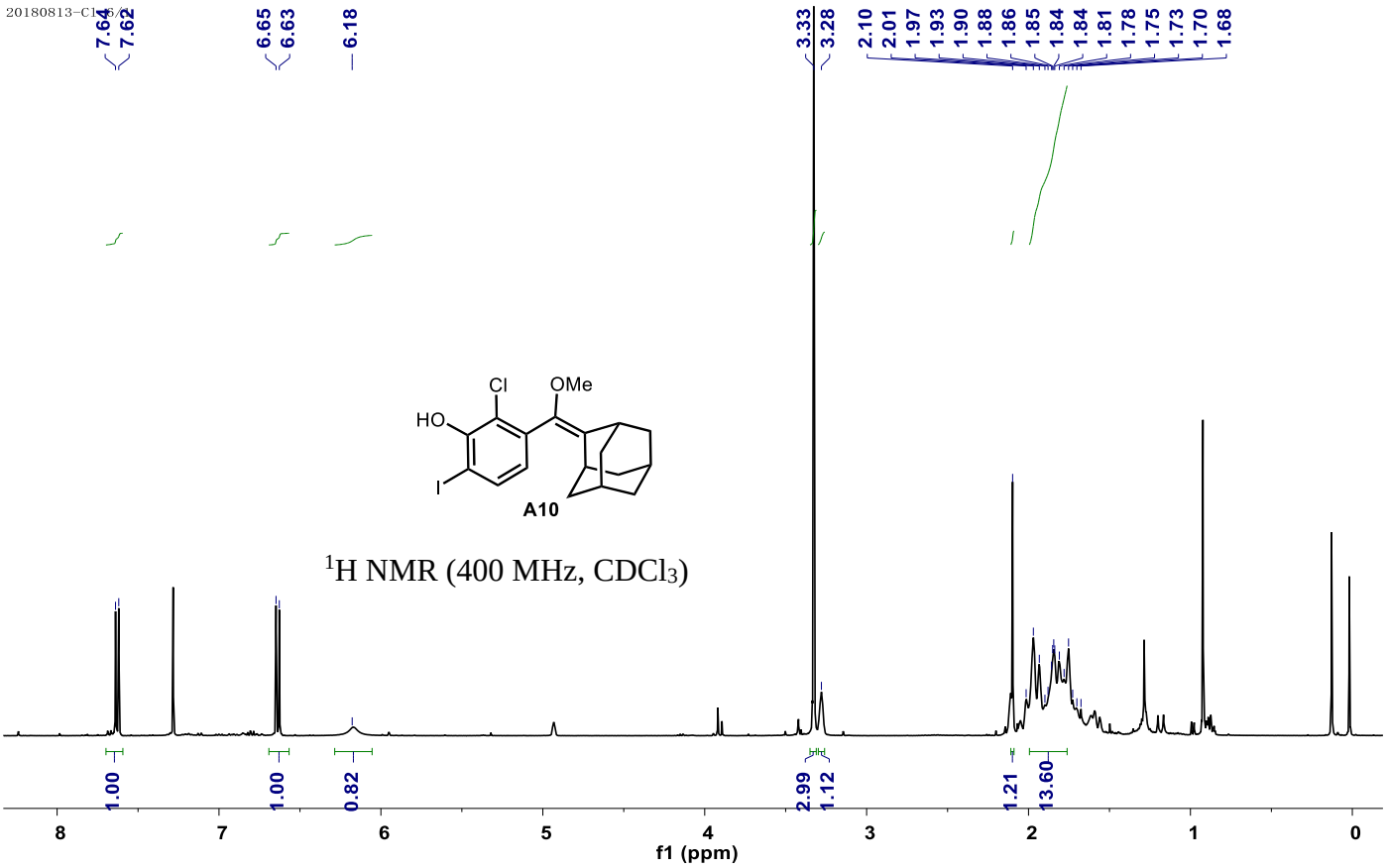
7.64
7.62
6.65
6.63
6.18
3.33
3.28
2.10
2.01
1.97
1.93
1.90
1.88
1.86
1.85
1.84
1.84
1.81
1.78
1.75
1.73
1.70
1.68
Cl
OMe
HO
I
A10
1H NMR (400 MHz, CDCl3)
1.00
1.00
0.82
2.99
1.12
1.21
13.60
8
7
6
5
4
3
2
1
0
f1 (ppm)

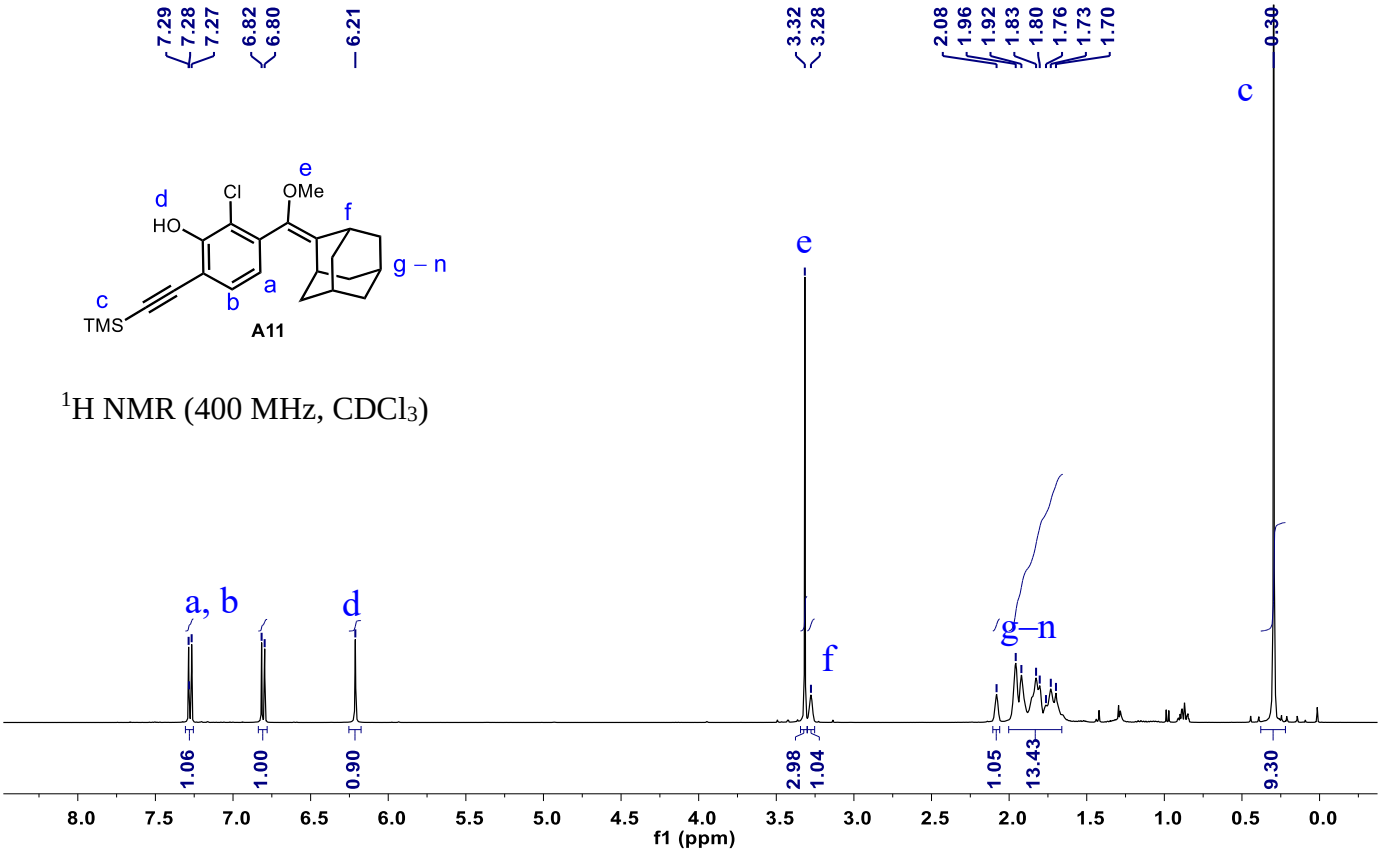

^{1}H NMR (400 MHz, $CDCl_3$)

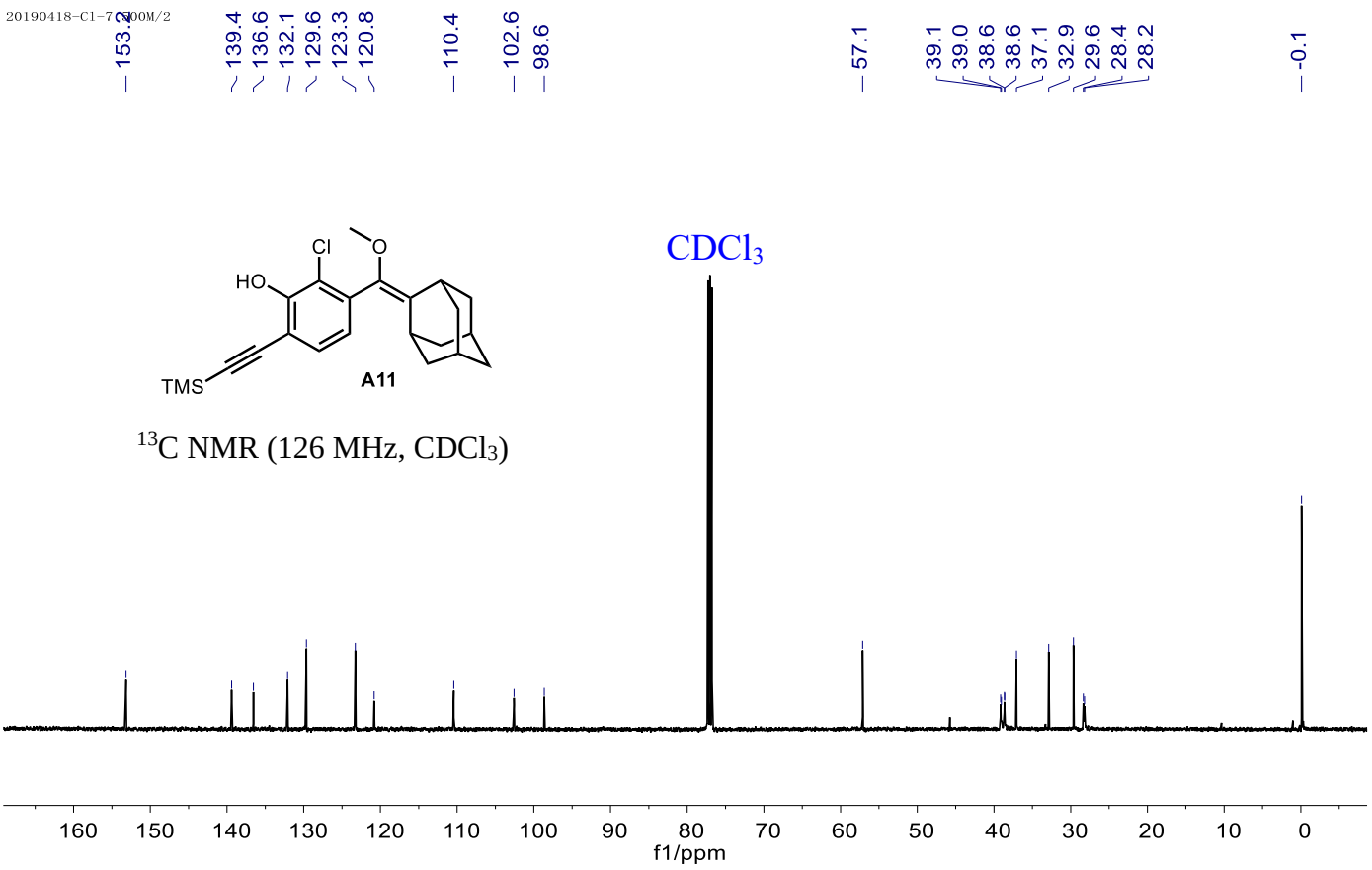

^{13}C NMR (126 MHz, $CDCl_3$)

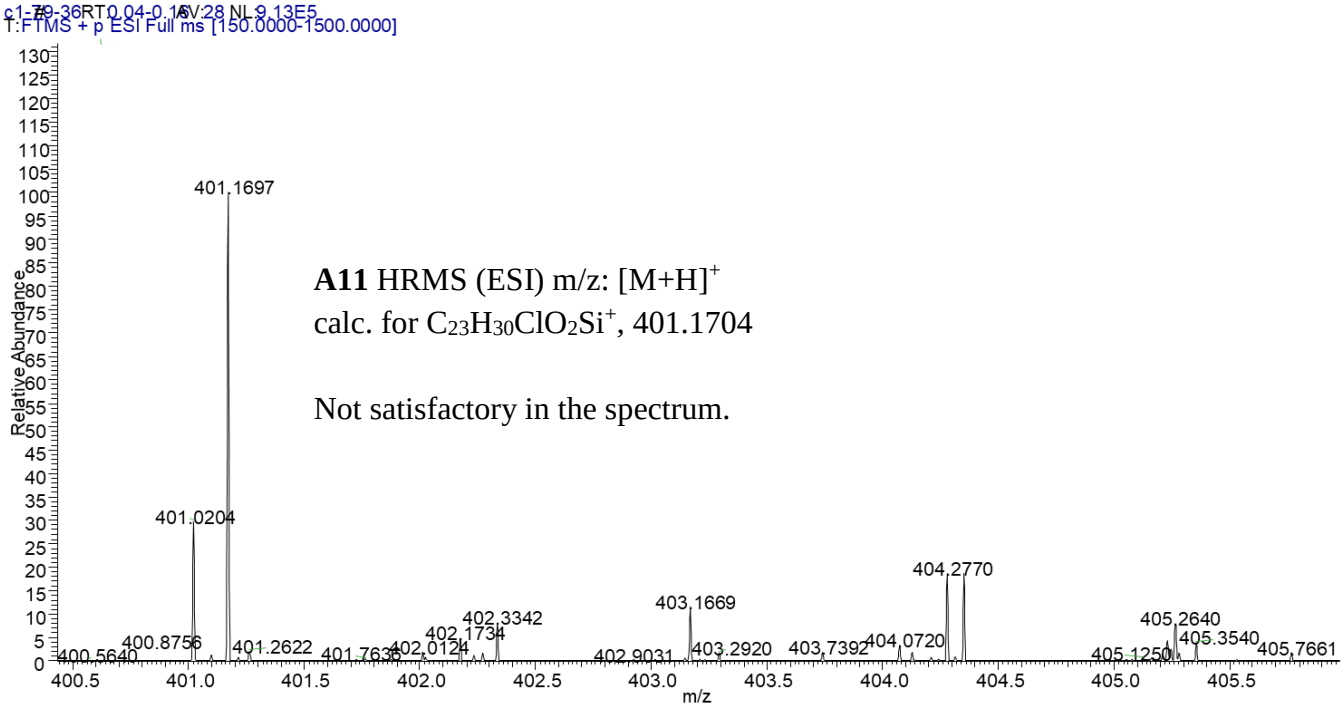

A11 HRMS (ESI) m/z: $[M+H]^+$
calc. for $C_{23}H_{30}ClO_2Si^+$, 401.1704

Not satisfactory in the spectrum.

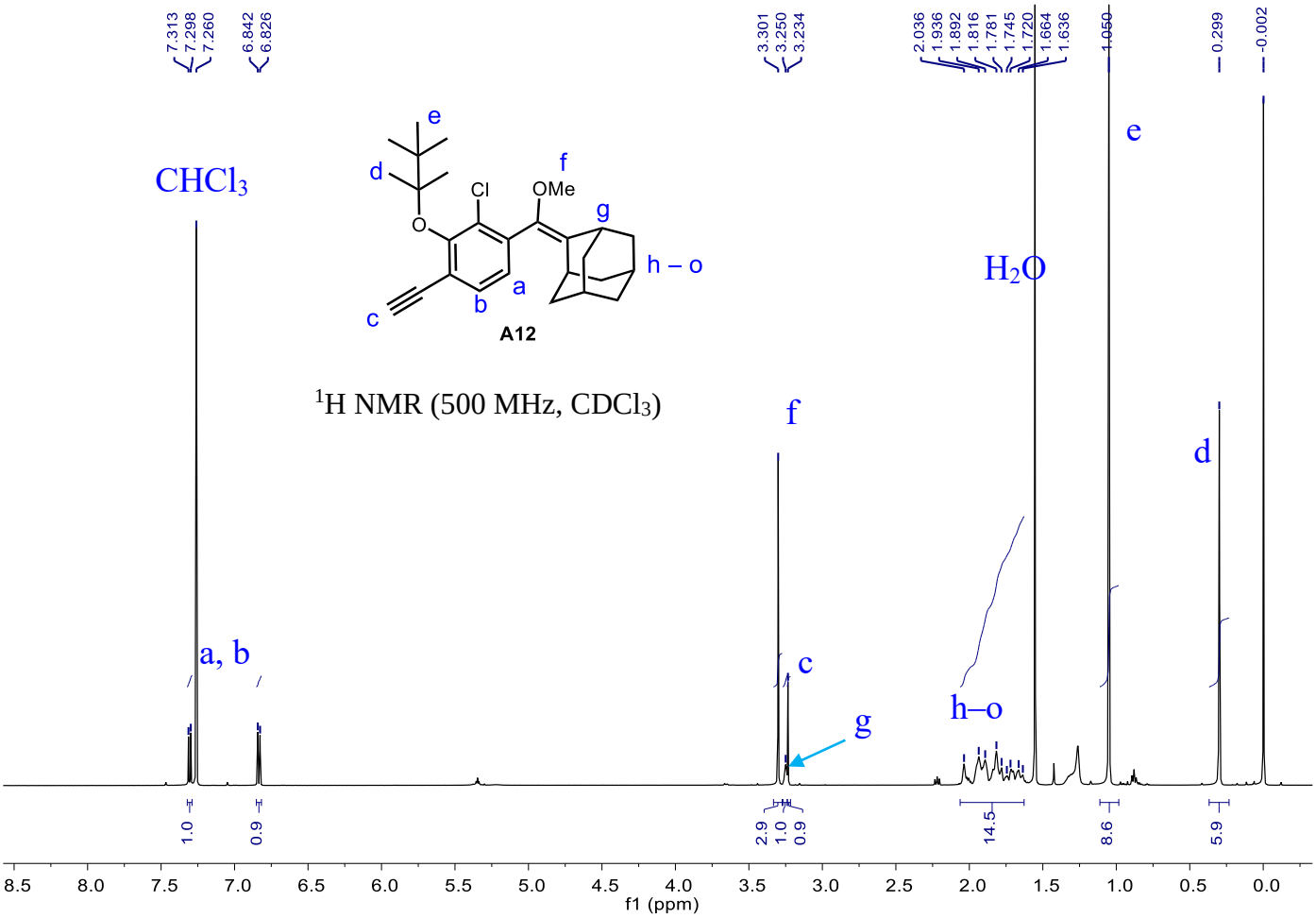

^{1}H NMR (500 MHz, $CDCl_3$)

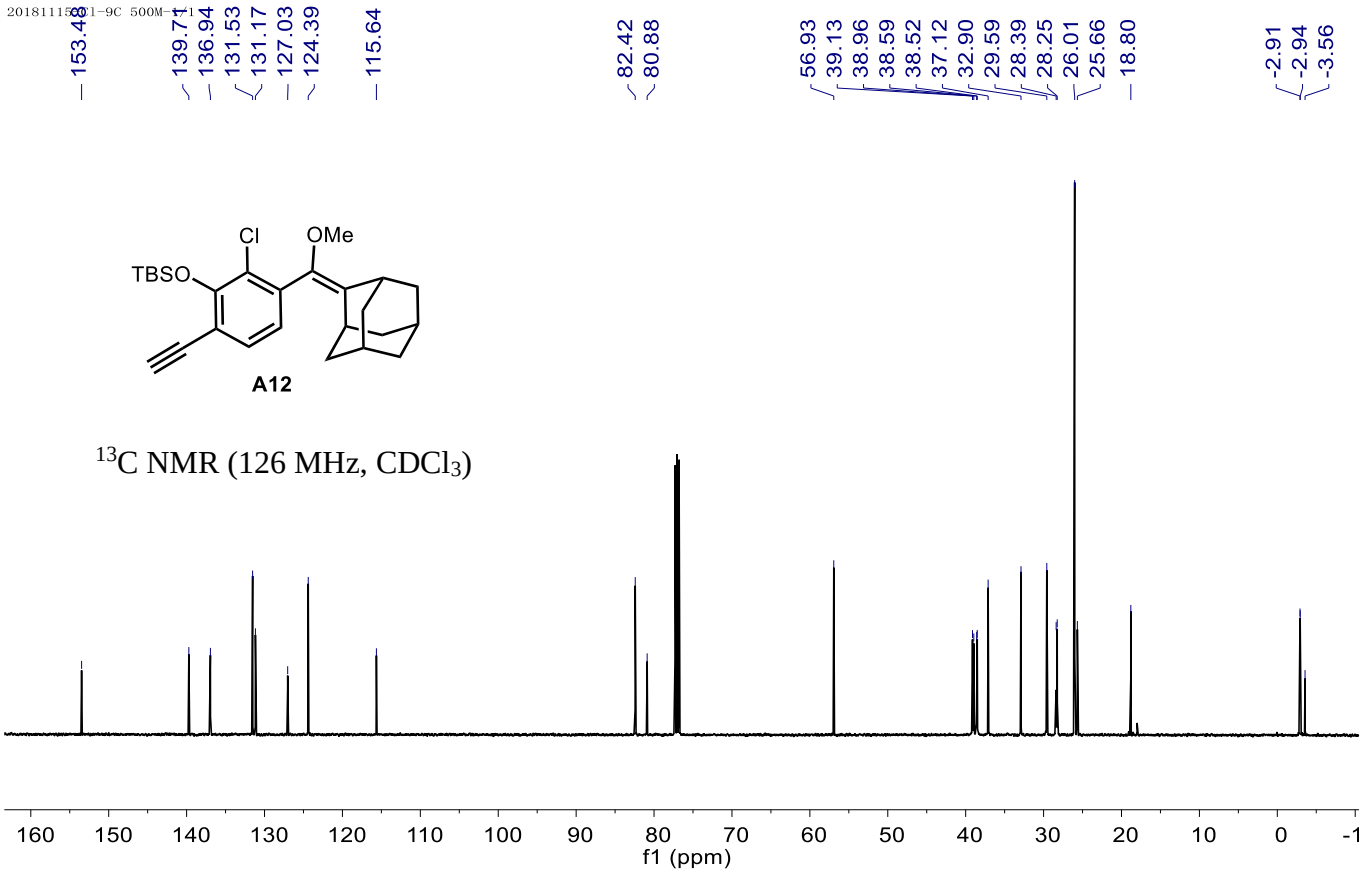

^{13}C NMR (126 MHz, $CDCl_3$)

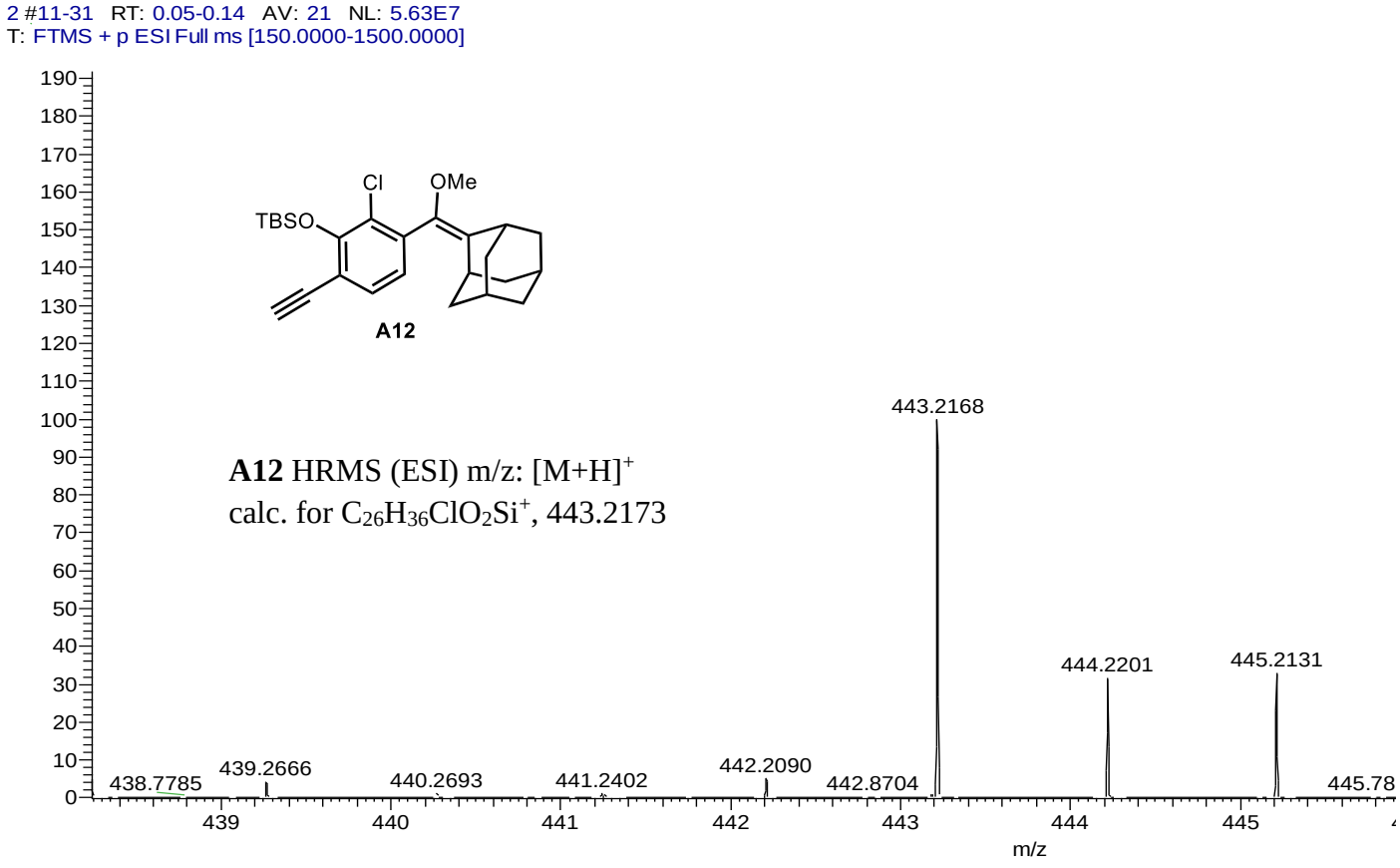

A12 HRMS (ESI) m/z: $[M+H]^+$
calc. for $C_{26}H_{36}ClO_2Si^+$, 443.2173

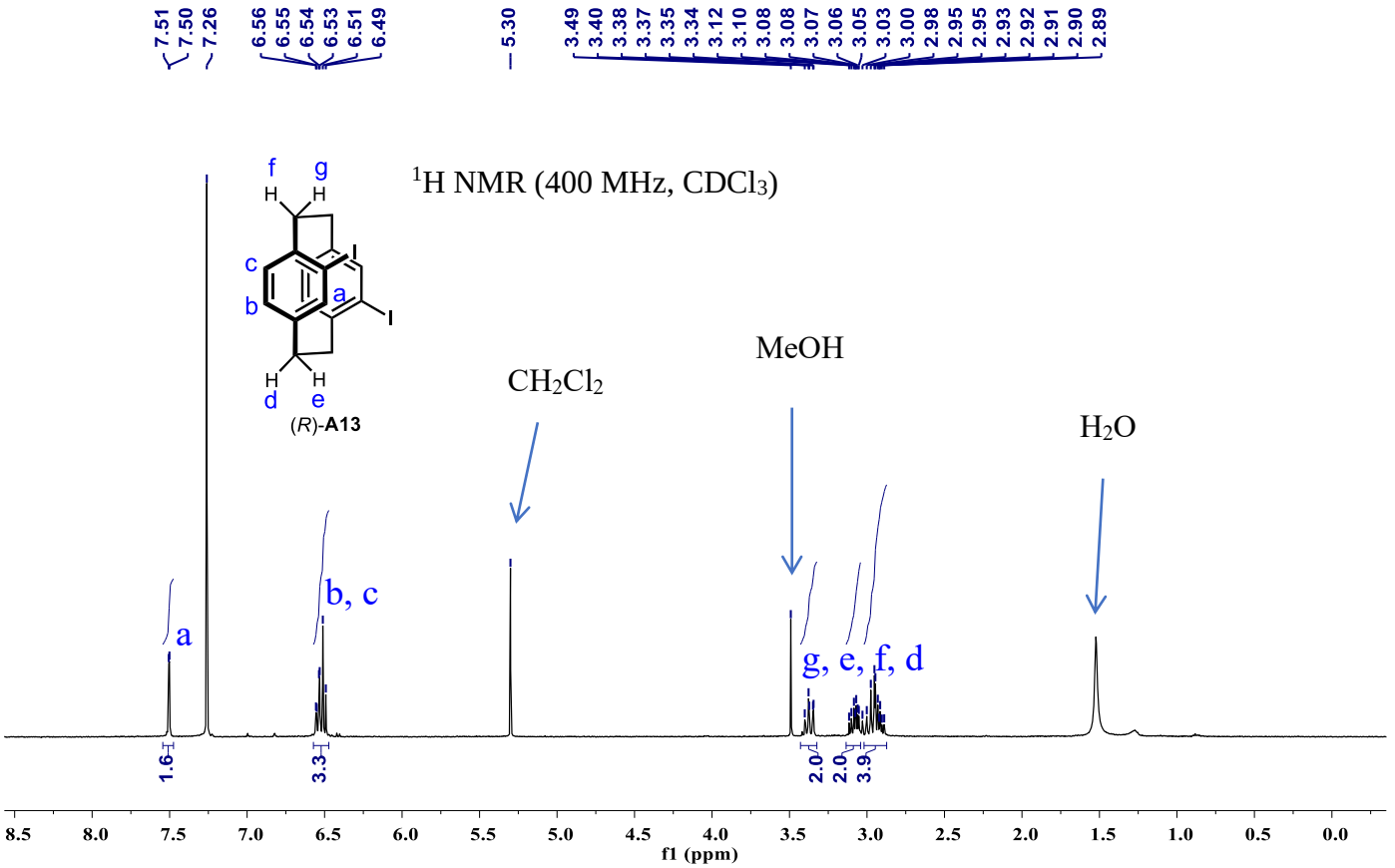

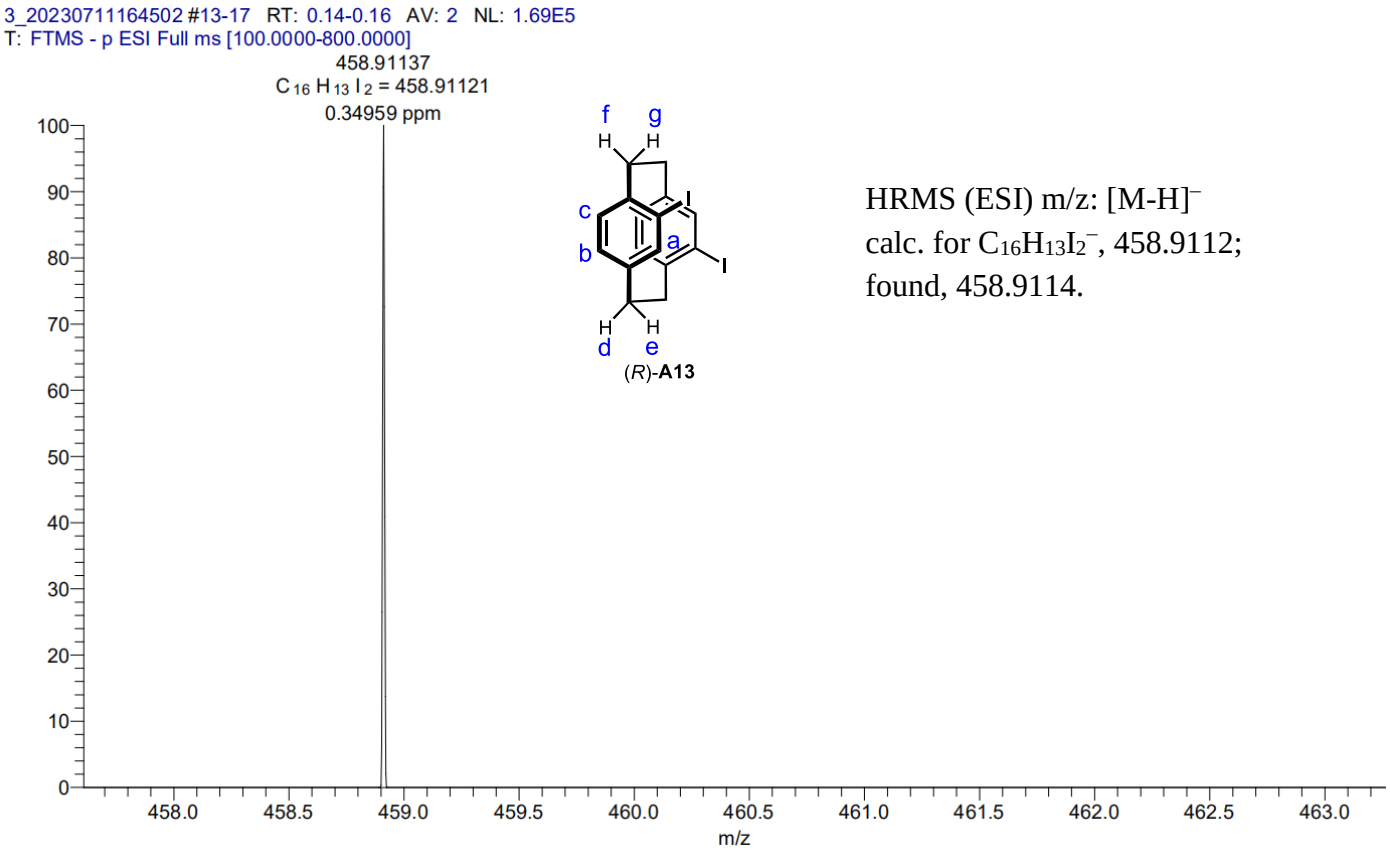

HRMS (ESI) m/z: $[M-H]^-$
calc. for $C_{16}H_{13}I_2^-$, 458.9112;
found, 458.9114.

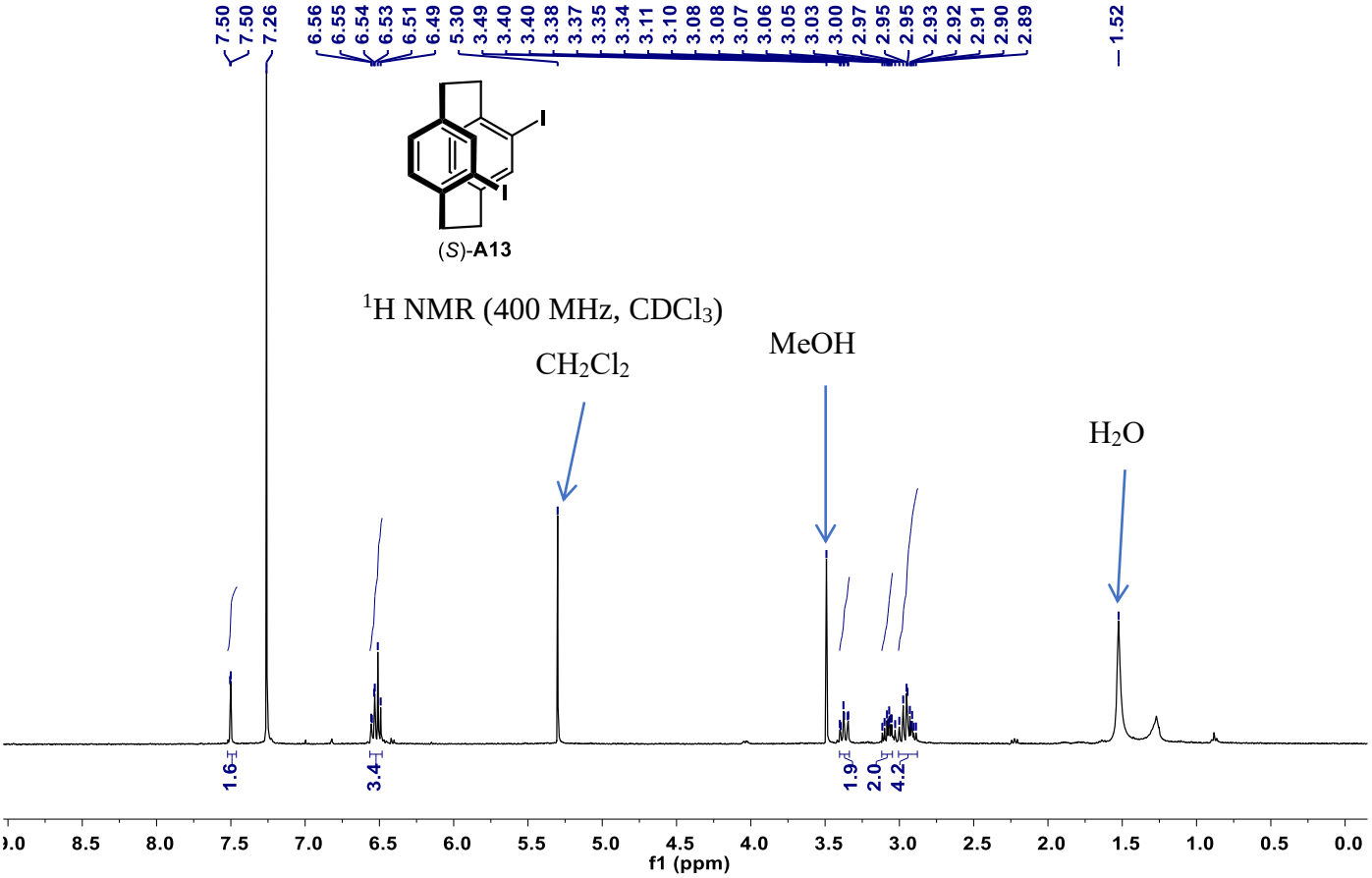

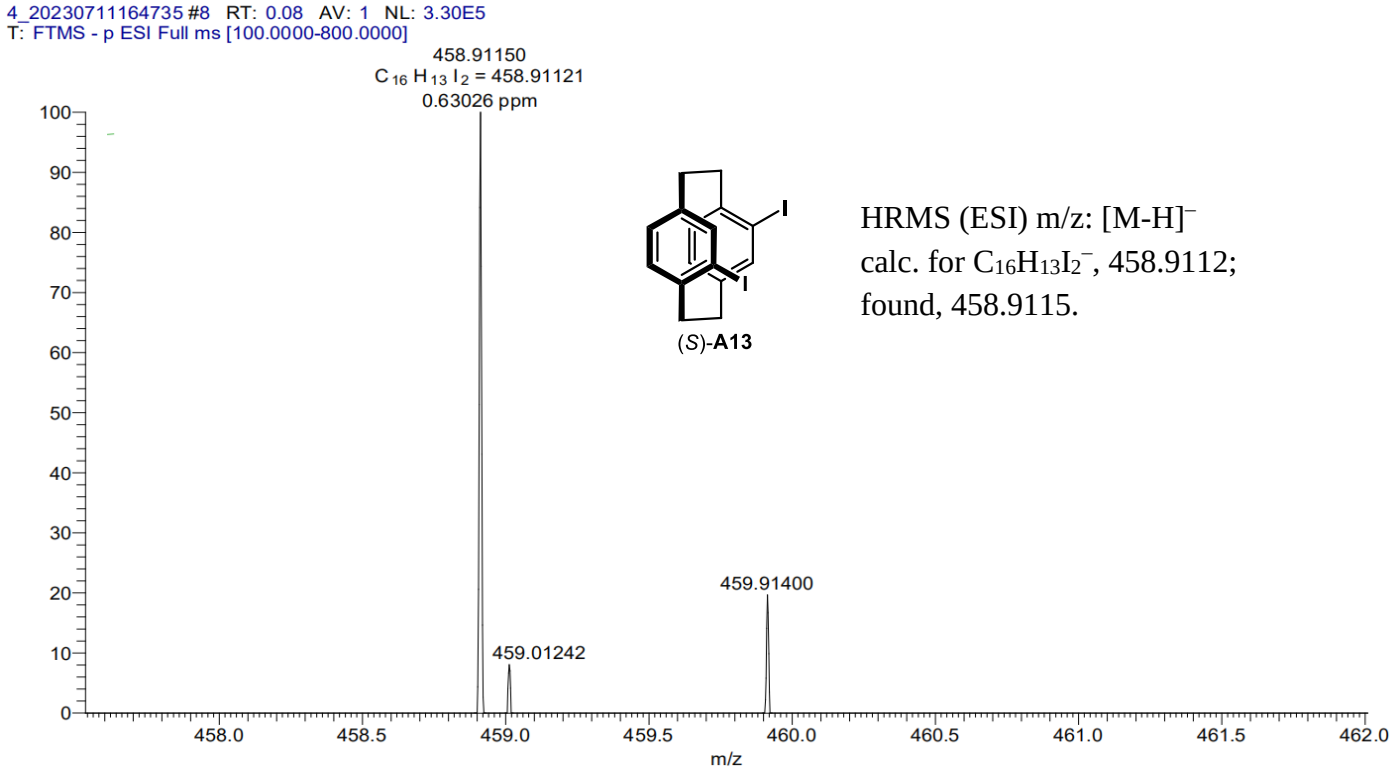

HRMS (ESI) m/z: $[M-H]^-$
calc. for $C_{16}H_{13}I_2^-$, 458.9112;
found, 458.9115.

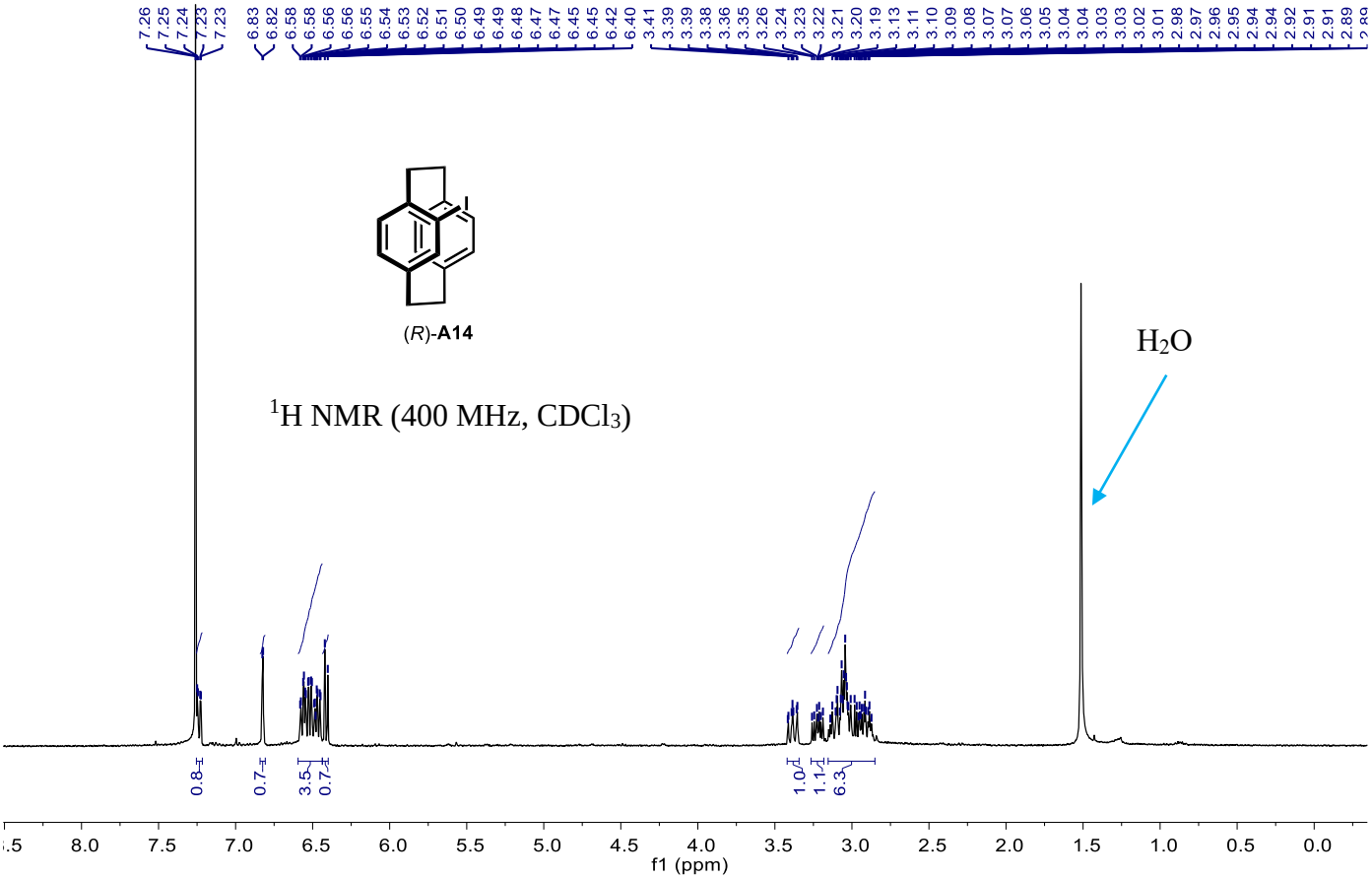

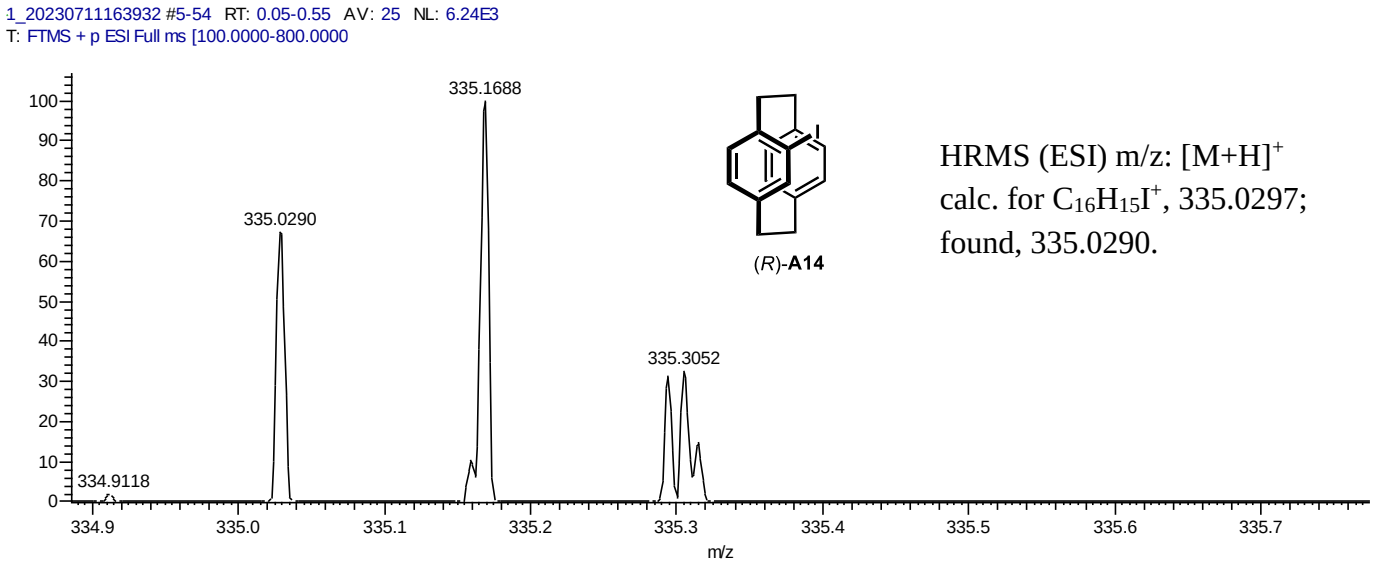

HRMS (ESI) m/z: $[M+H]^+$
calc. for $C_{16}H_{15}I^+$, 335.0297;
found, 335.0290.

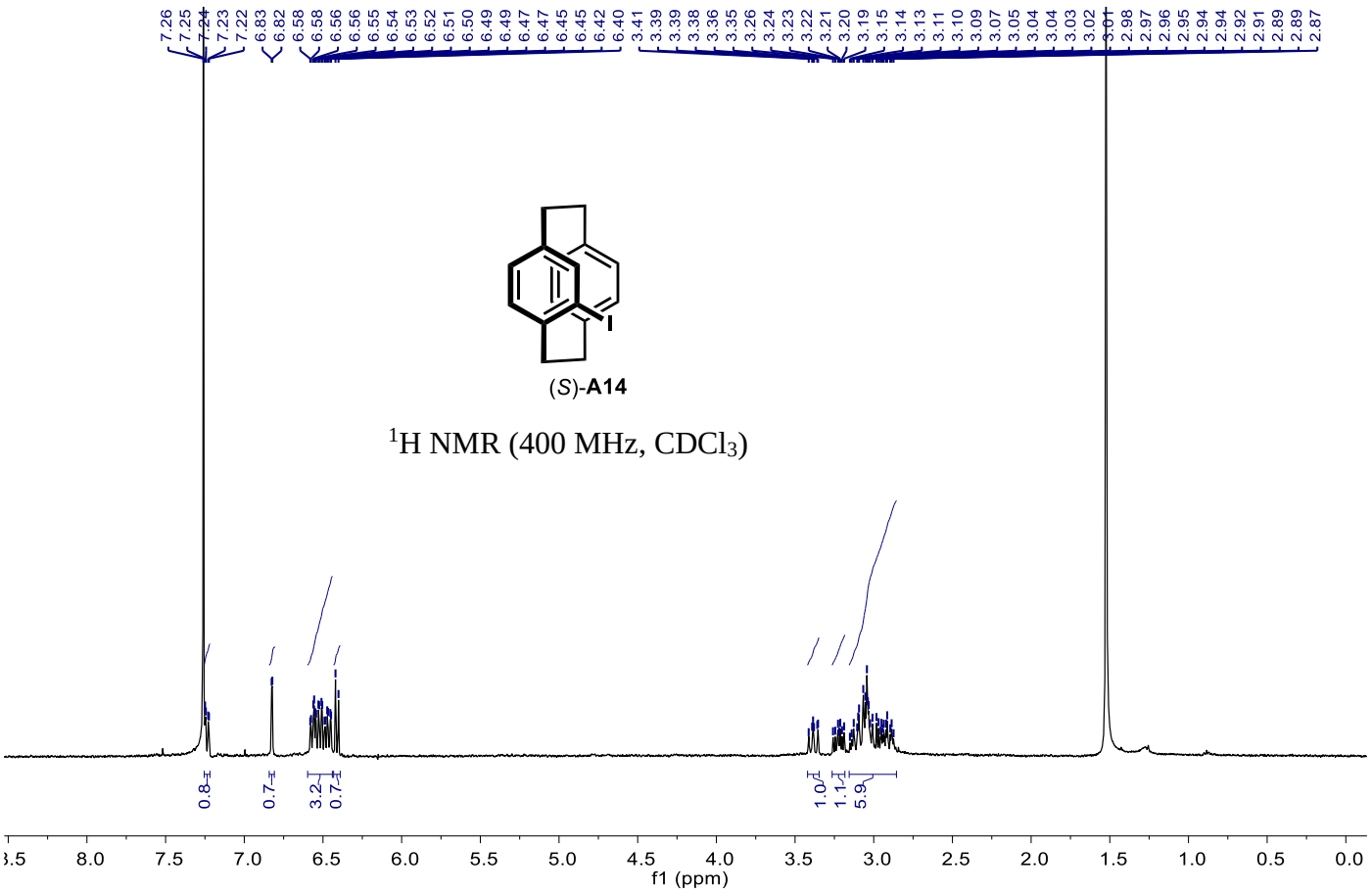

(*S*)-**A14**

^{1}H NMR (400 MHz, $CDCl_3$)

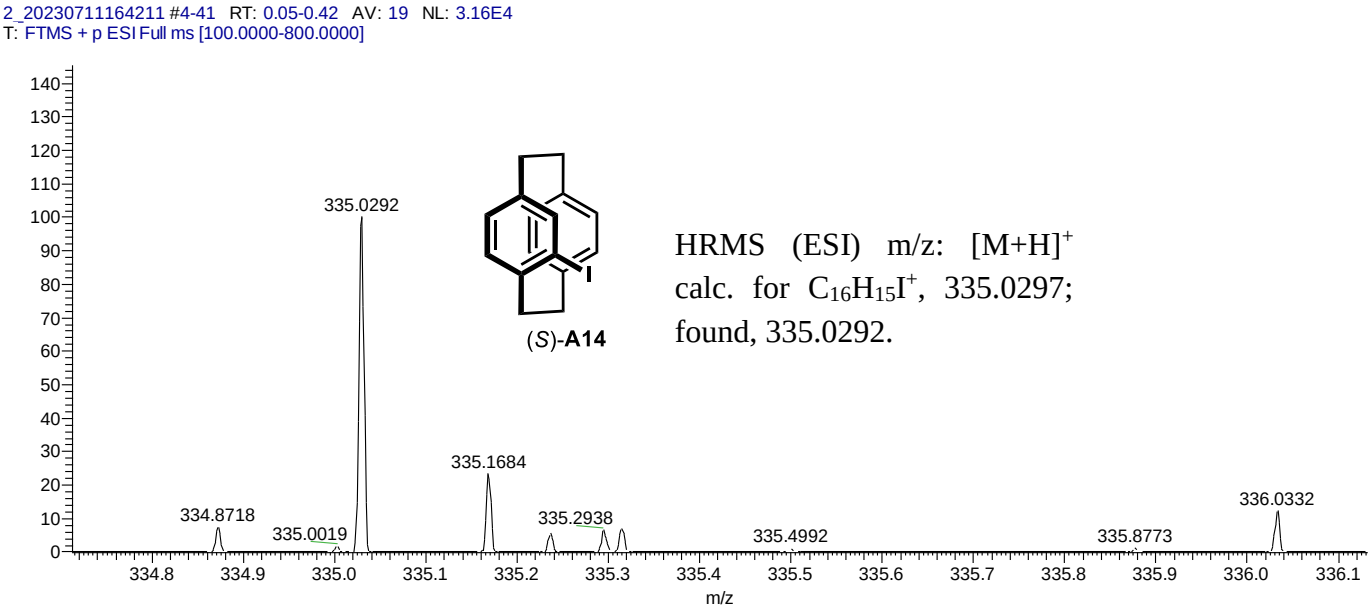

(*S*)-**A14**

HRMS (ESI) m/z: $[M+H]^+$ calc. for $C_{16}H_{15}I^+$, 335.0297; found, 335.0292.

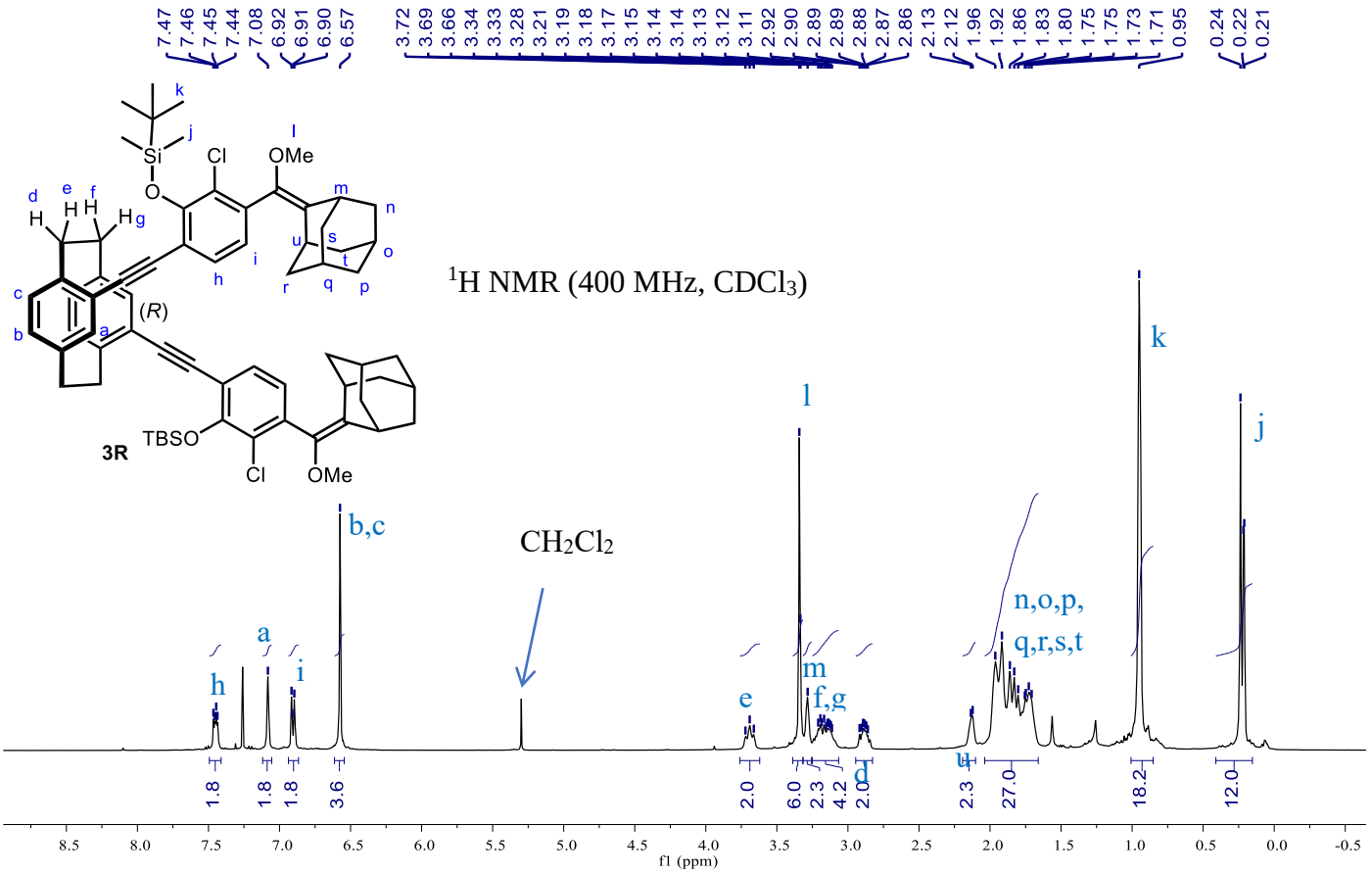
7.47 7.46 7.45 7.44 7.08 6.92 6.91 6.90 6.57
3.72 3.69 3.66 3.34 3.33 3.28 3.21 3.19 3.18 3.17 3.15 3.14 3.14 3.13 3.12 3.11 2.92 2.90 2.89 2.89 2.88 2.87 2.86
2.13 2.12 1.96 1.92 1.86 1.83 1.80 1.75 1.75 1.73 1.71 0.95
0.24 0.22 0.21
3R
TBSO
Cl
OMe
(R)
^{1}H NMR (400 MHz, CDCl$_3$)
CH$_2$Cl$_2$
b,c
a
h
i
l
k
j
m
e
f,g
d
u
n,o,p,
q,r,s,t
1.8 1.8 1.8 3.6 2.0 6.0 2.3 4.2 2.0 2.3 27.0 18.2 12.0
f1 (ppm)

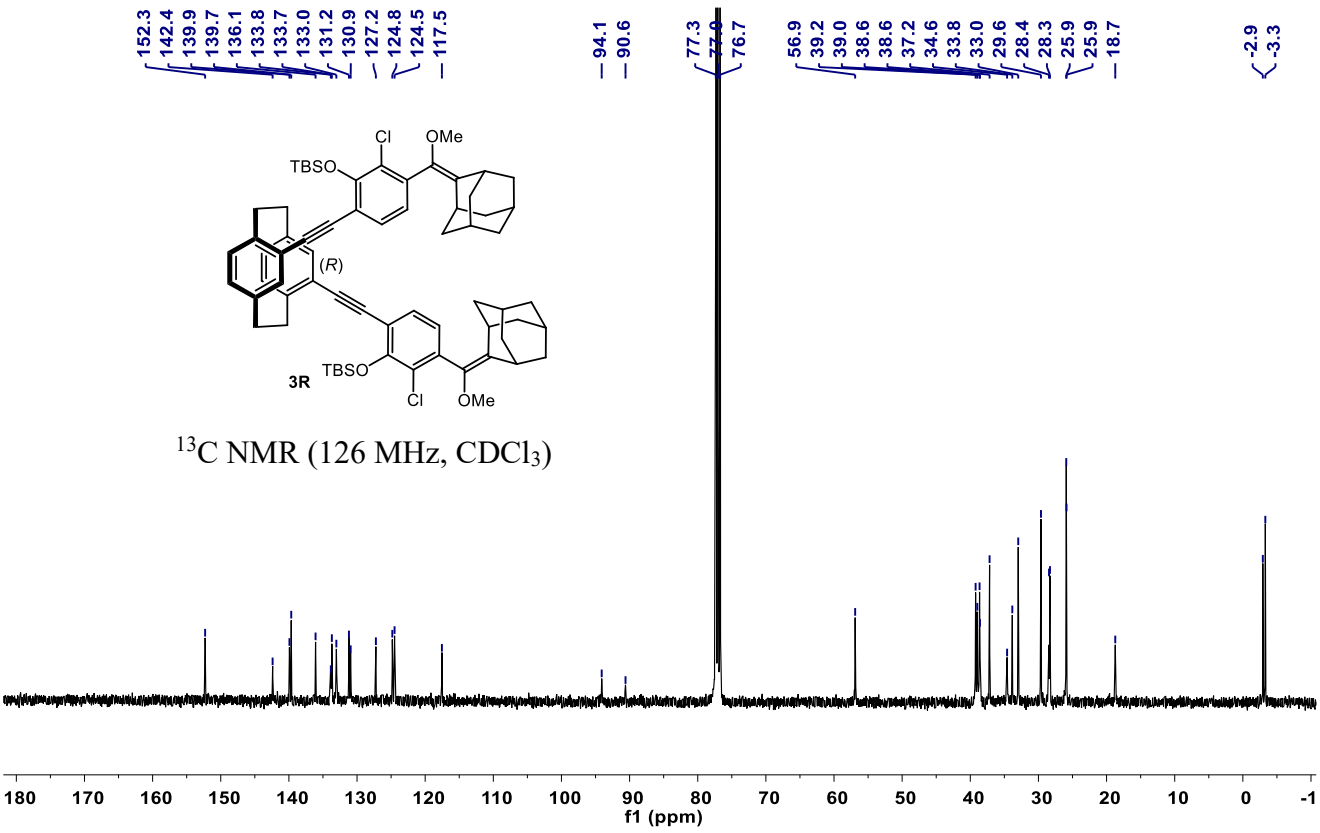
152.3 142.4 139.9 139.7 136.1 133.8 133.7 133.0 131.2 130.9 127.2 124.8 124.5 117.5
94.1 90.6
77.3 77.0 76.7
56.9 39.2 39.0 38.6 38.6 37.2 34.6 33.8 33.0 29.6 28.4 28.3 25.9 25.9 18.7
-2.9 -3.3
3R
TBSO
Cl
OMe
(R)
^{13}C NMR (126 MHz, CDCl$_3$)
f1 (ppm)

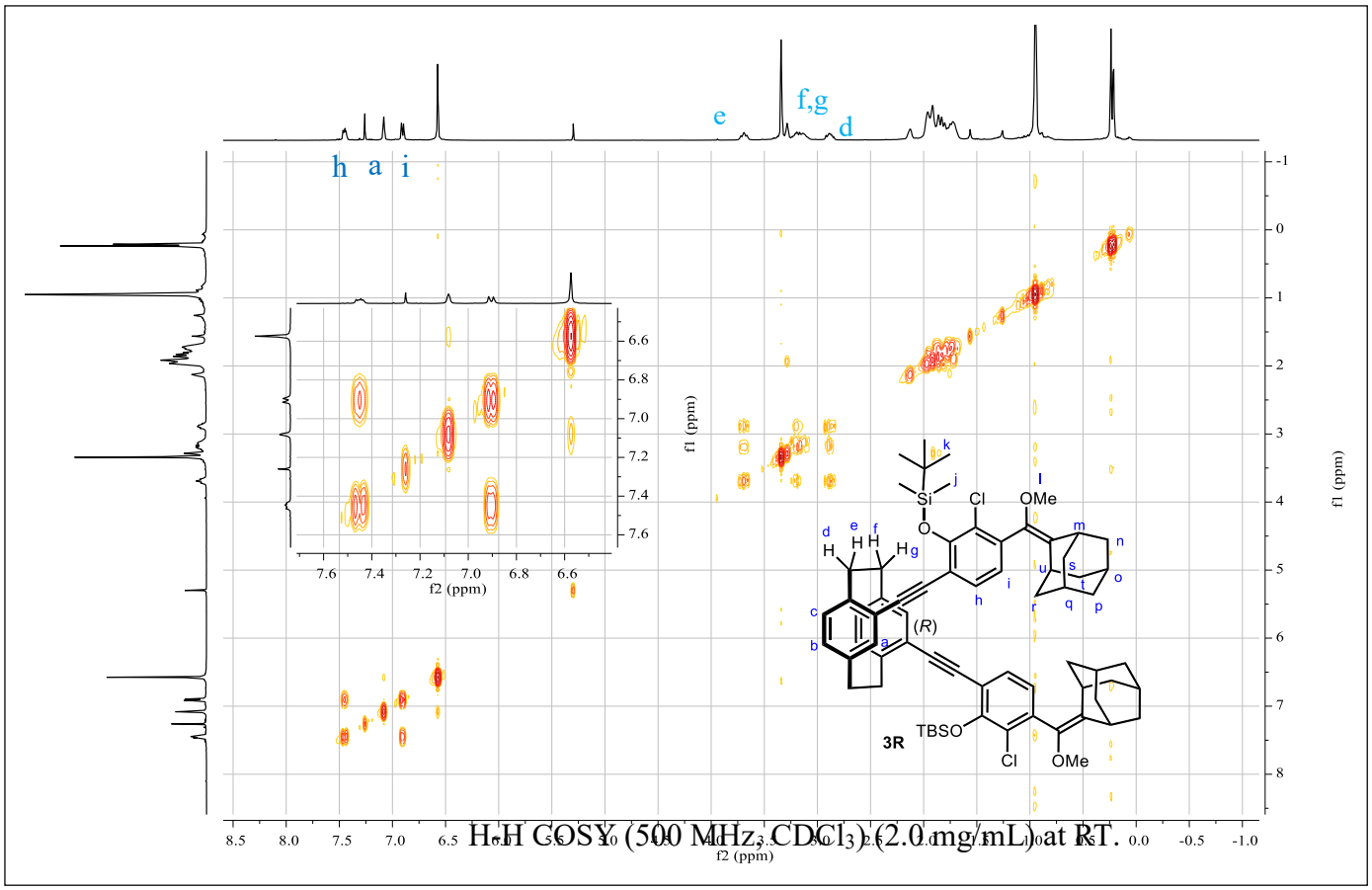

H-H COSY (500 MHz, $CDCl_3$) (2.0 mg/mL) at RT.

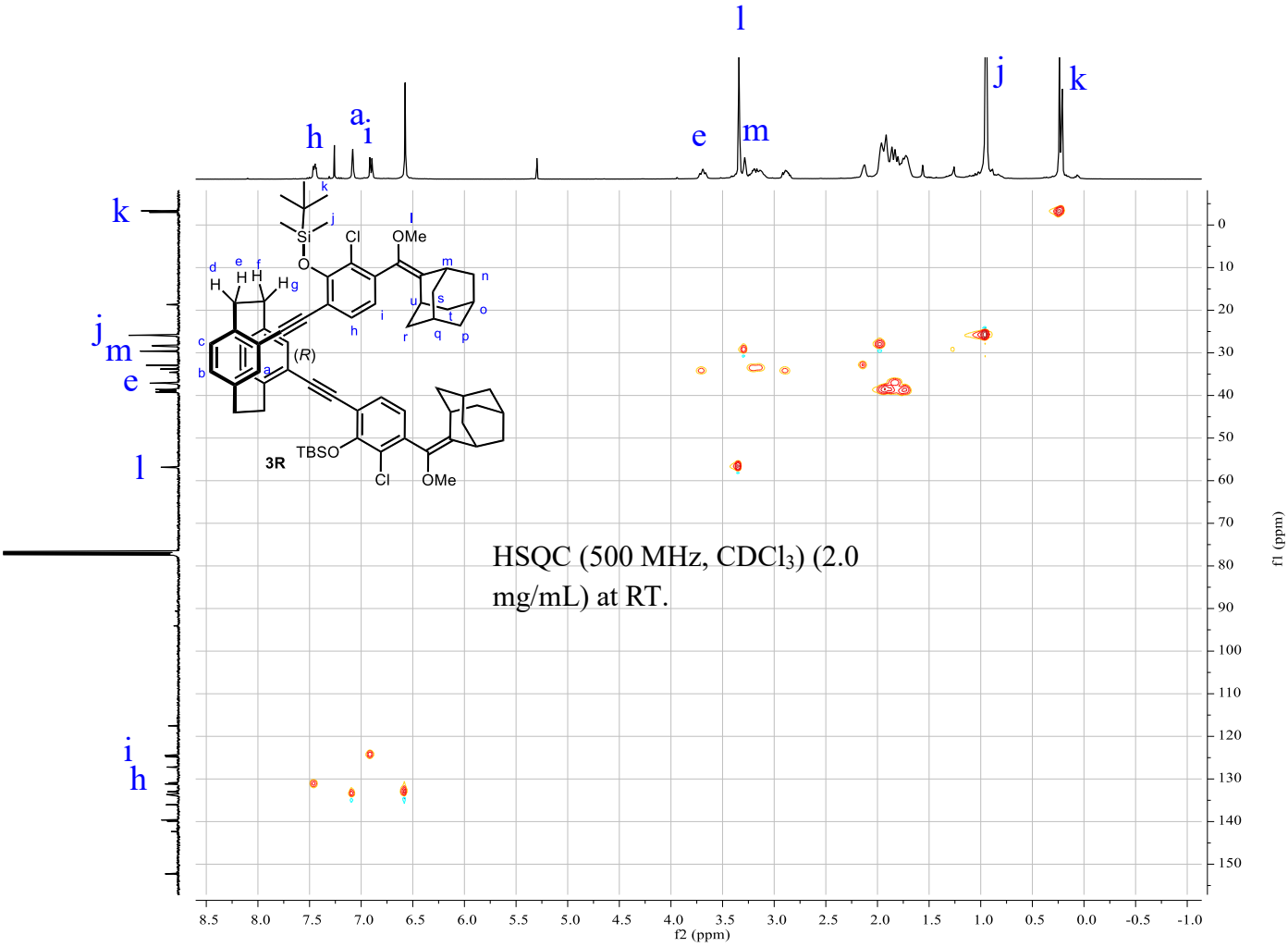

HSQC (500 MHz, $CDCl_3$) (2.0 mg/mL) at RT.

SML-1 #13 RT: 0.12 AV: 1 NL: 6.80E6
T: FTMS + p ESI Full ms [500.0000-2000.0000]

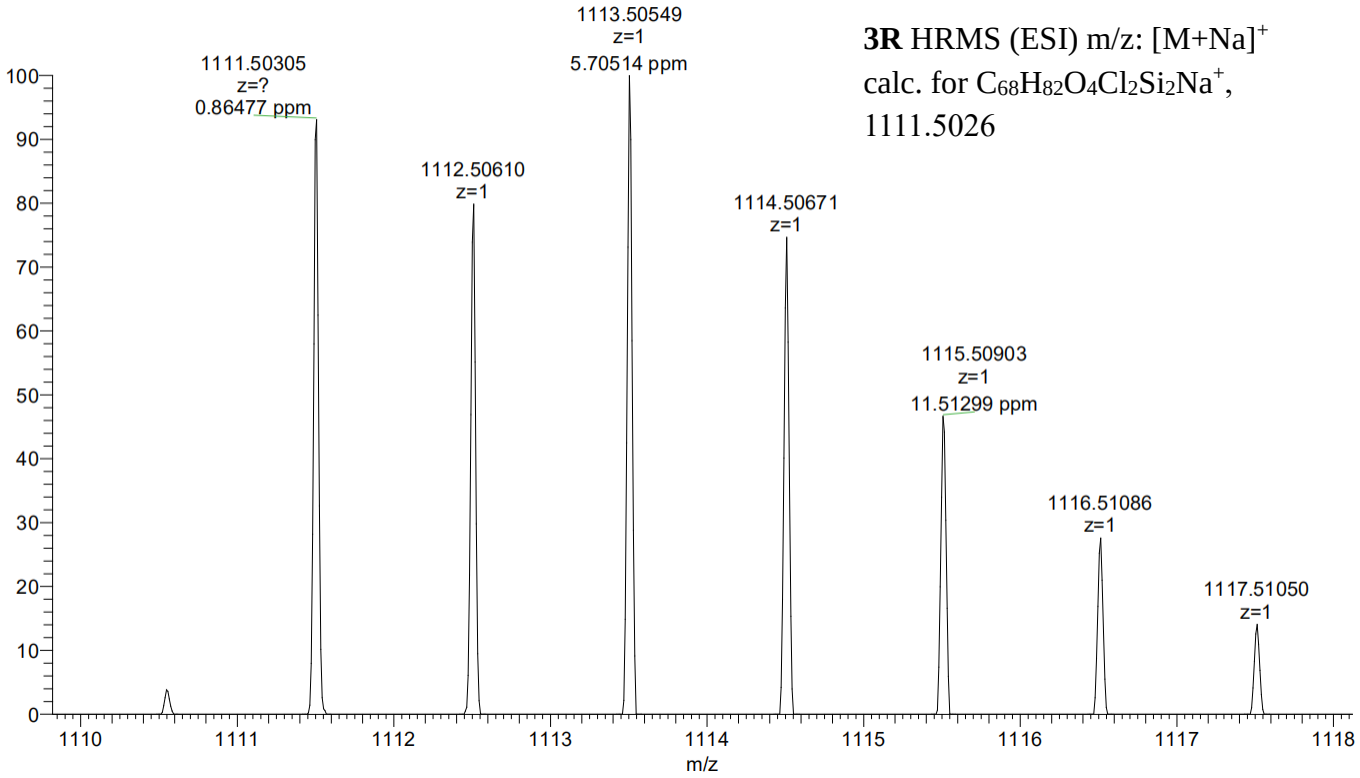

3R HRMS (ESI) m/z: $[M+Na]^+$ calc. for $C_{68}H_{82}O_4Cl_2Si_2Na^+$, 1111.5026

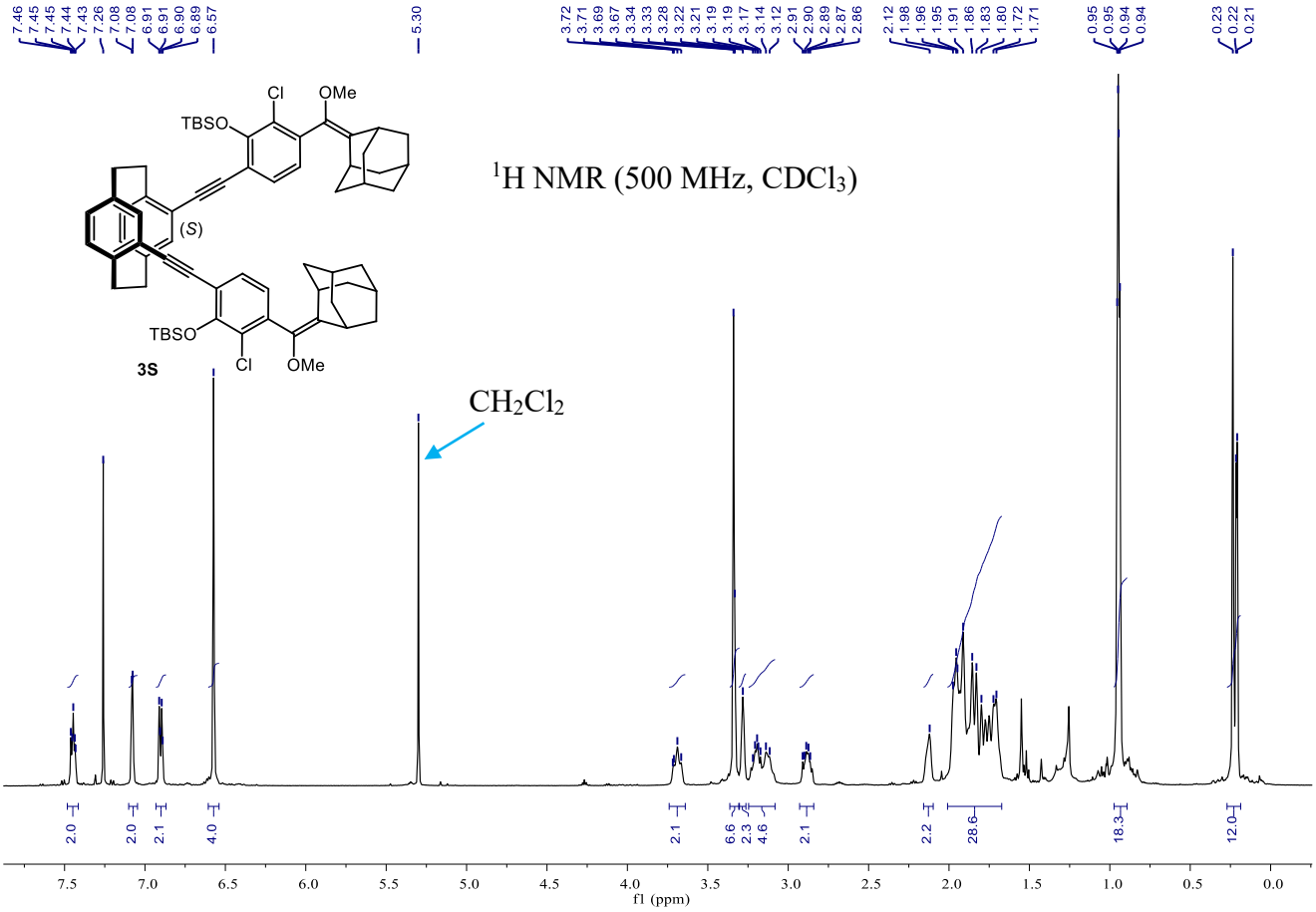

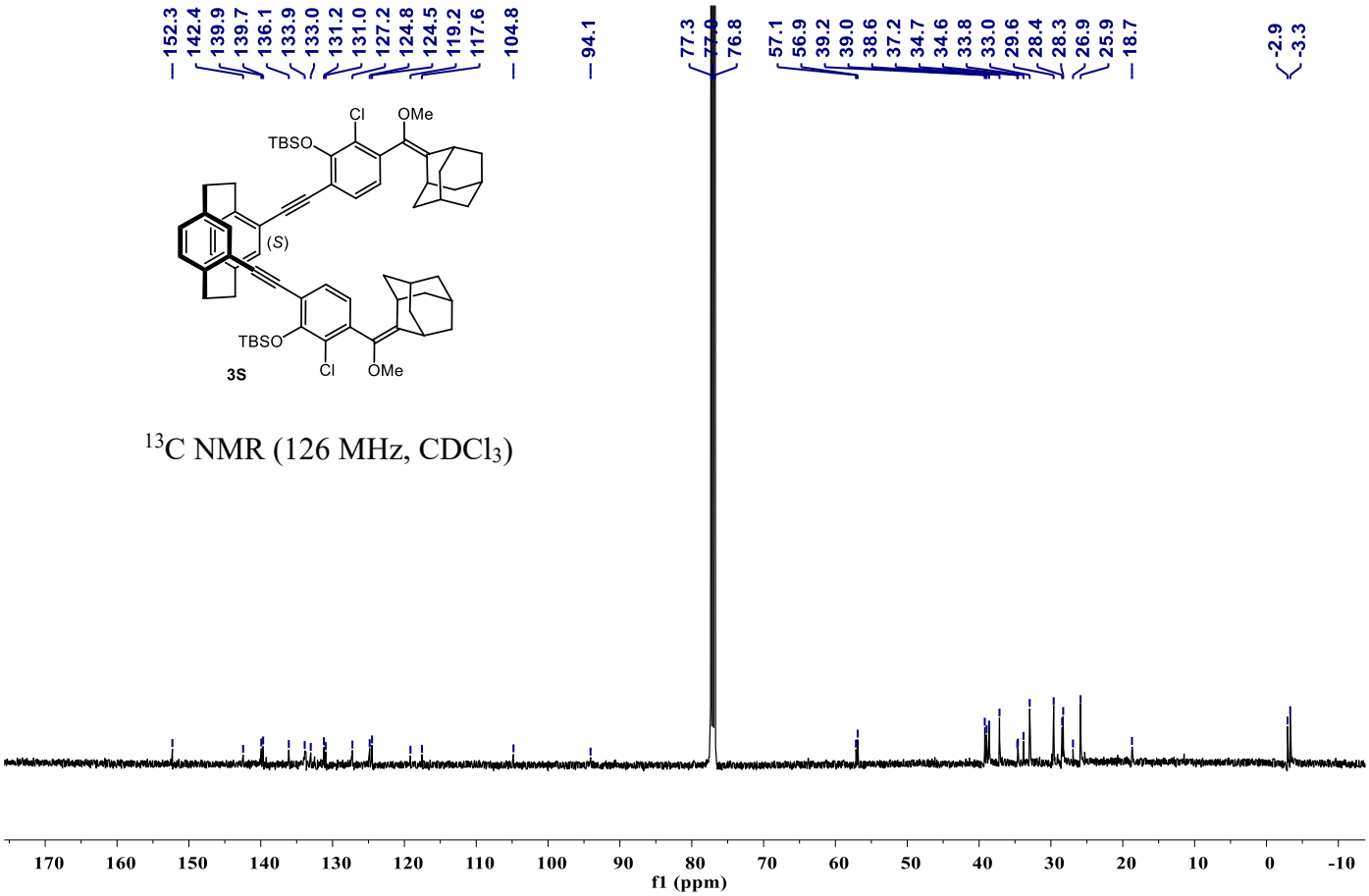

^{13}C NMR (126 MHz, $CDCl_3$)

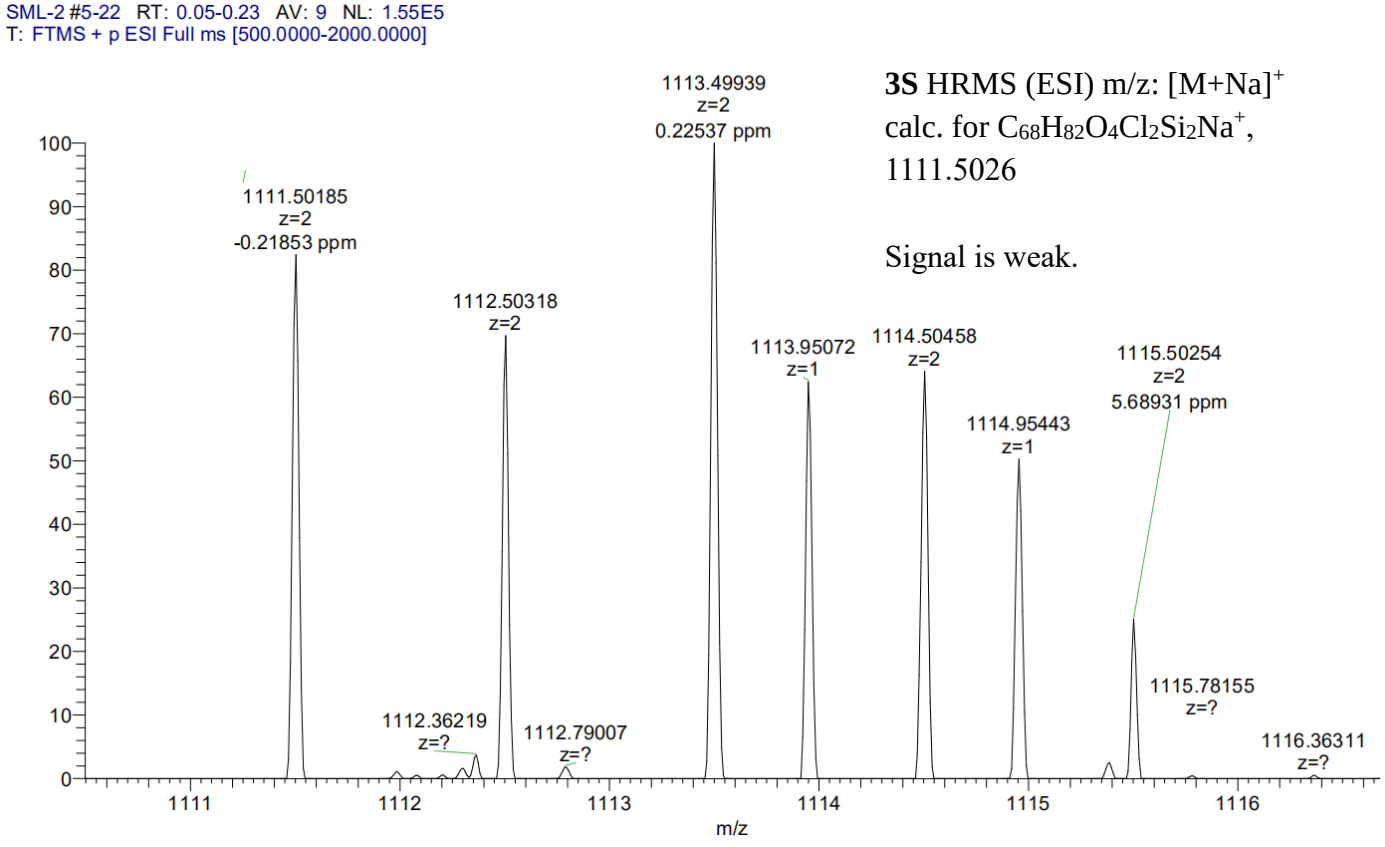

3S HRMS (ESI) m/z: $[M+Na]^+$ calc. for $C_{68}H_{82}O_4Cl_2Si_2Na^+$, 1111.5026

Signal is weak.

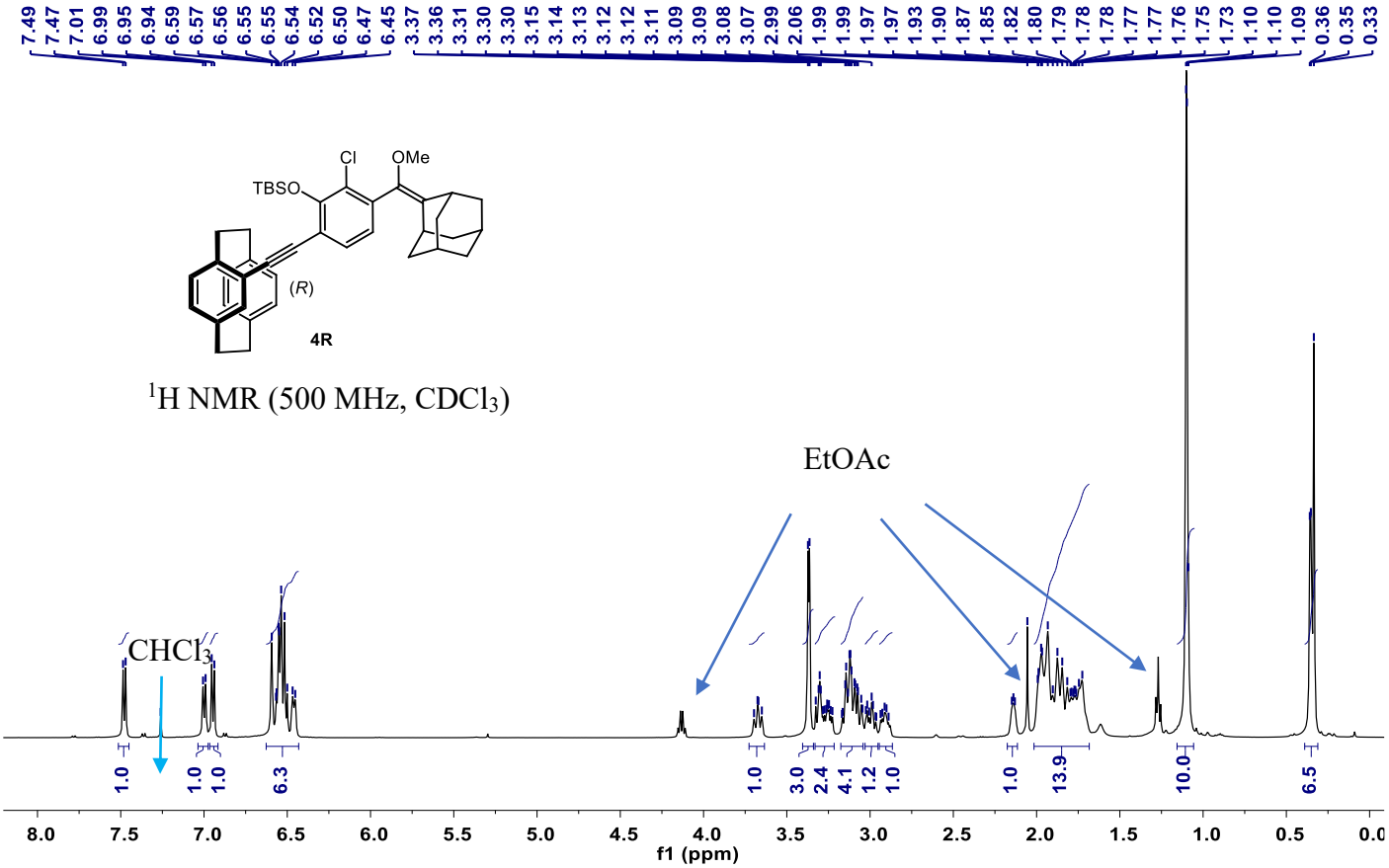
7.49 7.47 7.01 6.99 6.95 6.94 6.59 6.57 6.56 6.55 6.55 6.54 6.52 6.50 6.47 6.45
3.37 3.36 3.31 3.30 3.30 3.15 3.14 3.13 3.12 3.12 3.11 3.09 3.09 3.08 3.07 2.99 2.06 1.99 1.99 1.97 1.97 1.93 1.90 1.87 1.85 1.82 1.80 1.79 1.78 1.78 1.77 1.77 1.76 1.75 1.73 1.10 1.10 1.09 0.36 0.35 0.33
Cl
OMe
TBSO
(R)
4R
1H NMR (500 MHz, CDCl3)
EtOAc
CHCl3
1.0 1.0 1.0 6.3 1.0 3.0 2.4 4.1 1.2 1.0 1.0 13.9 10.0 6.5
8.0 7.5 7.0 6.5 6.0 5.5 5.0 4.5 4.0 3.5 3.0 2.5 2.0 1.5 1.0 0.5 0.0
f1 (ppm)

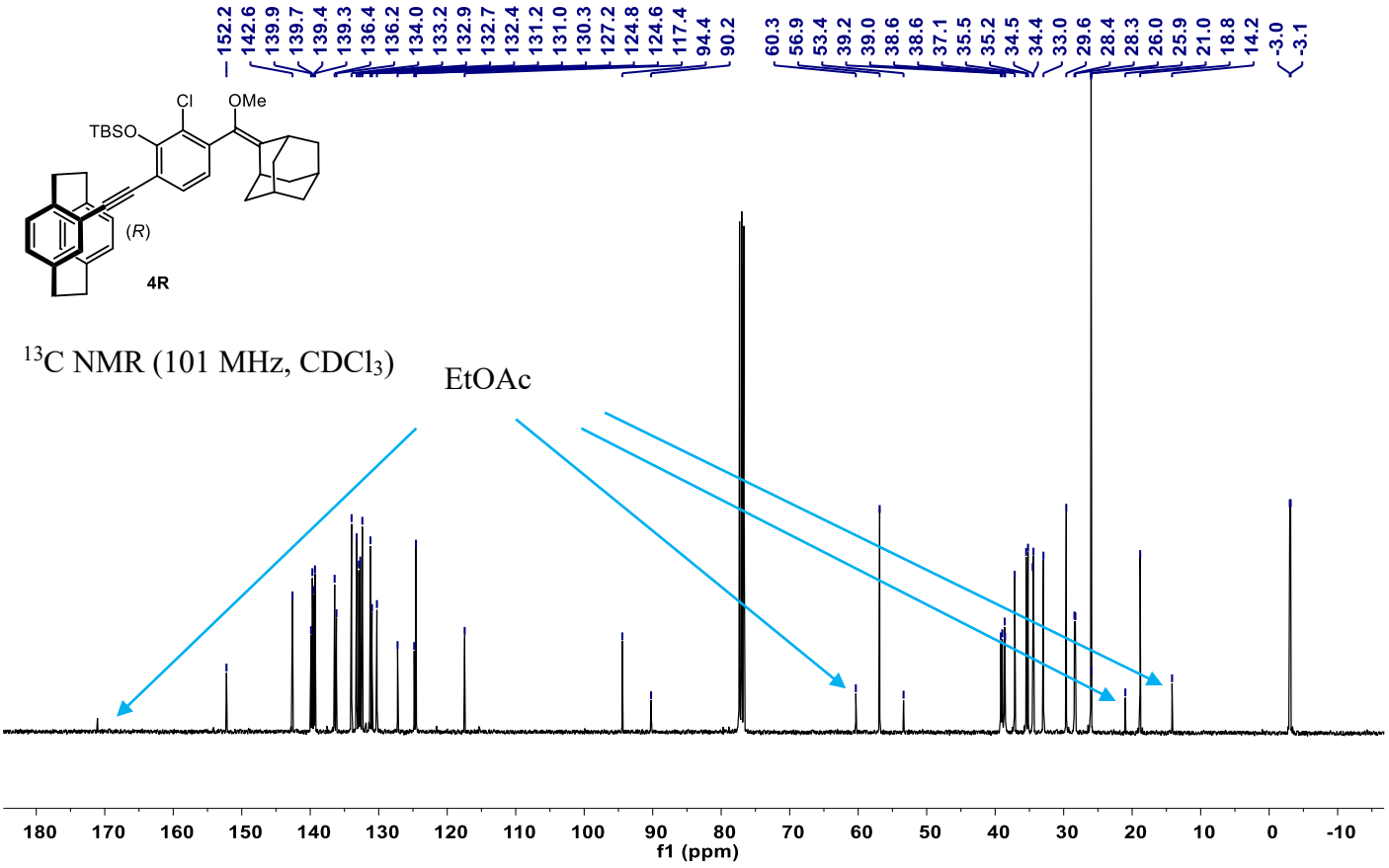
152.2 142.6 139.9 139.7 139.4 139.3 136.4 136.2 134.0 133.2 132.9 132.7 132.4 131.2 131.0 130.3 127.2 124.8 124.6 117.4 94.4 90.2
60.3 56.9 53.4 39.2 39.0 38.6 38.6 37.1 35.5 35.2 34.5 34.4 33.0 29.6 28.4 28.3 26.0 25.9 21.0 18.8 14.2 -3.0 -3.1
Cl
OMe
TBSO
(R)
4R
13C NMR (101 MHz, CDCl3)
EtOAc
180 170 160 150 140 130 120 110 100 90 80 70 60 50 40 30 20 10 0 -10
f1 (ppm)

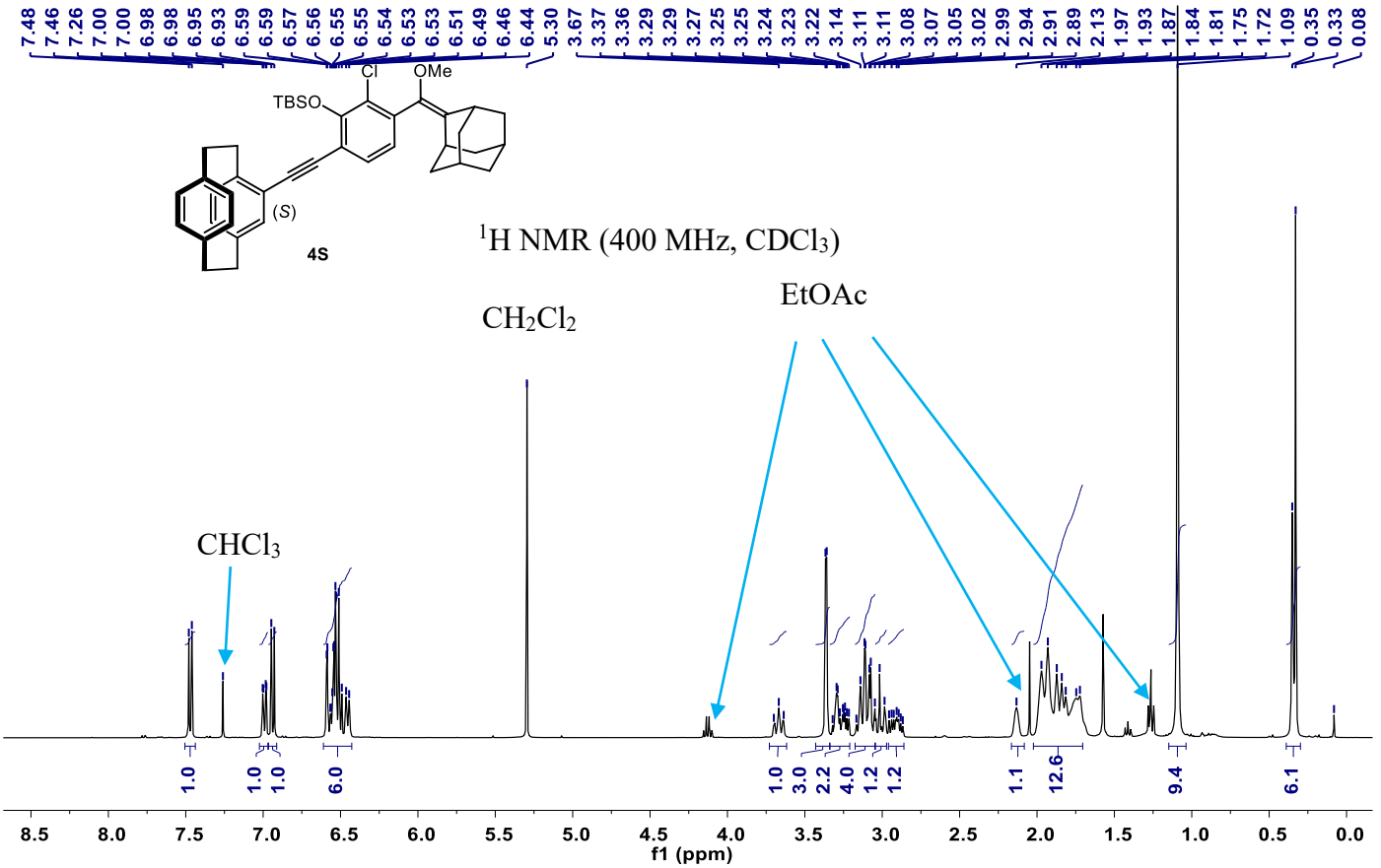
Cl
OMe
TBSO
(S)
4S
^{1}H NMR (400 MHz, $CDCl_3$)
CH_2Cl_2
EtOAc
$CHCl_3$
f1 (ppm)

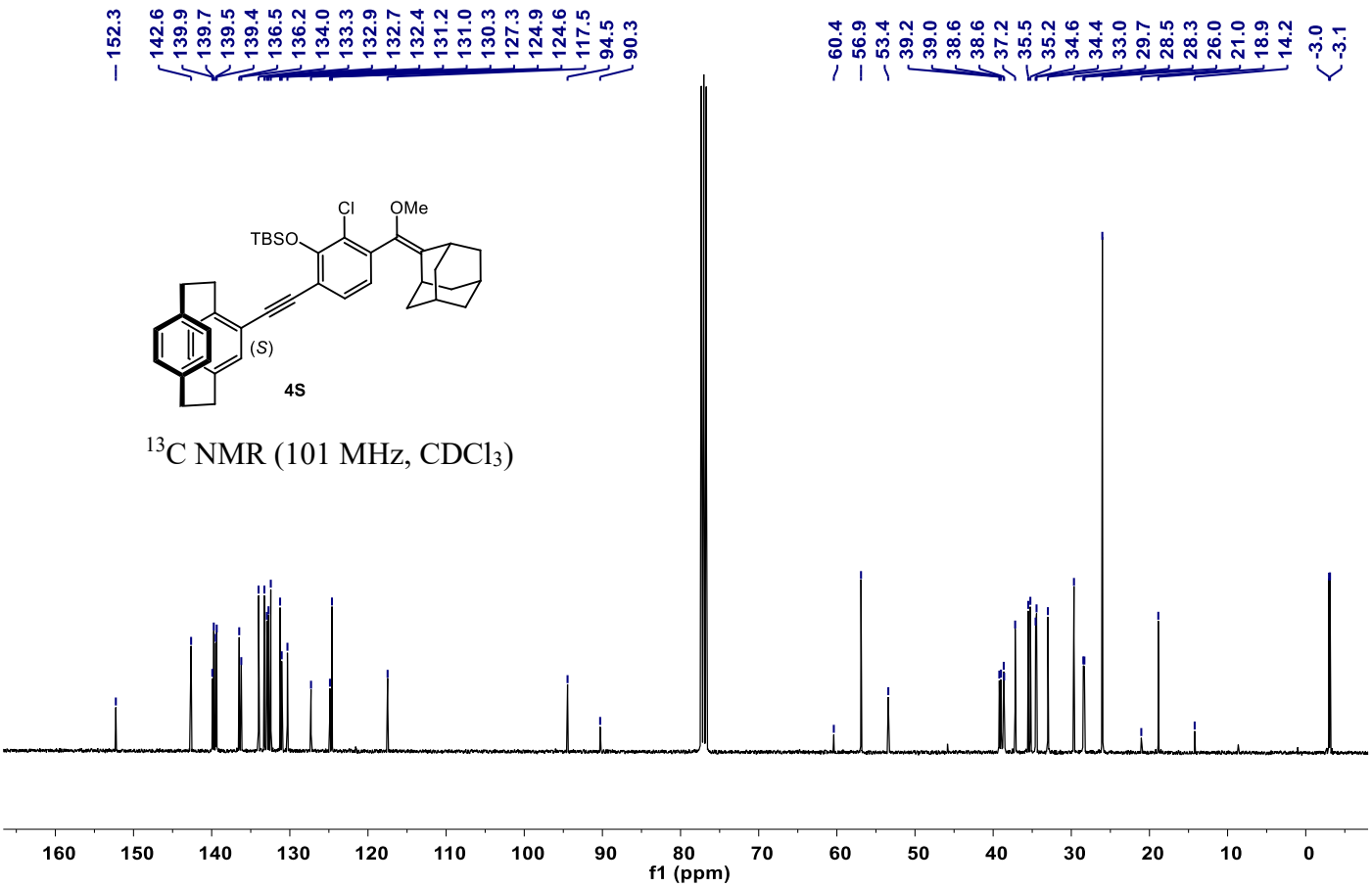
Cl
OMe
TBSO
(S)
4S
^{13}C NMR (101 MHz, $CDCl_3$)
f1 (ppm)

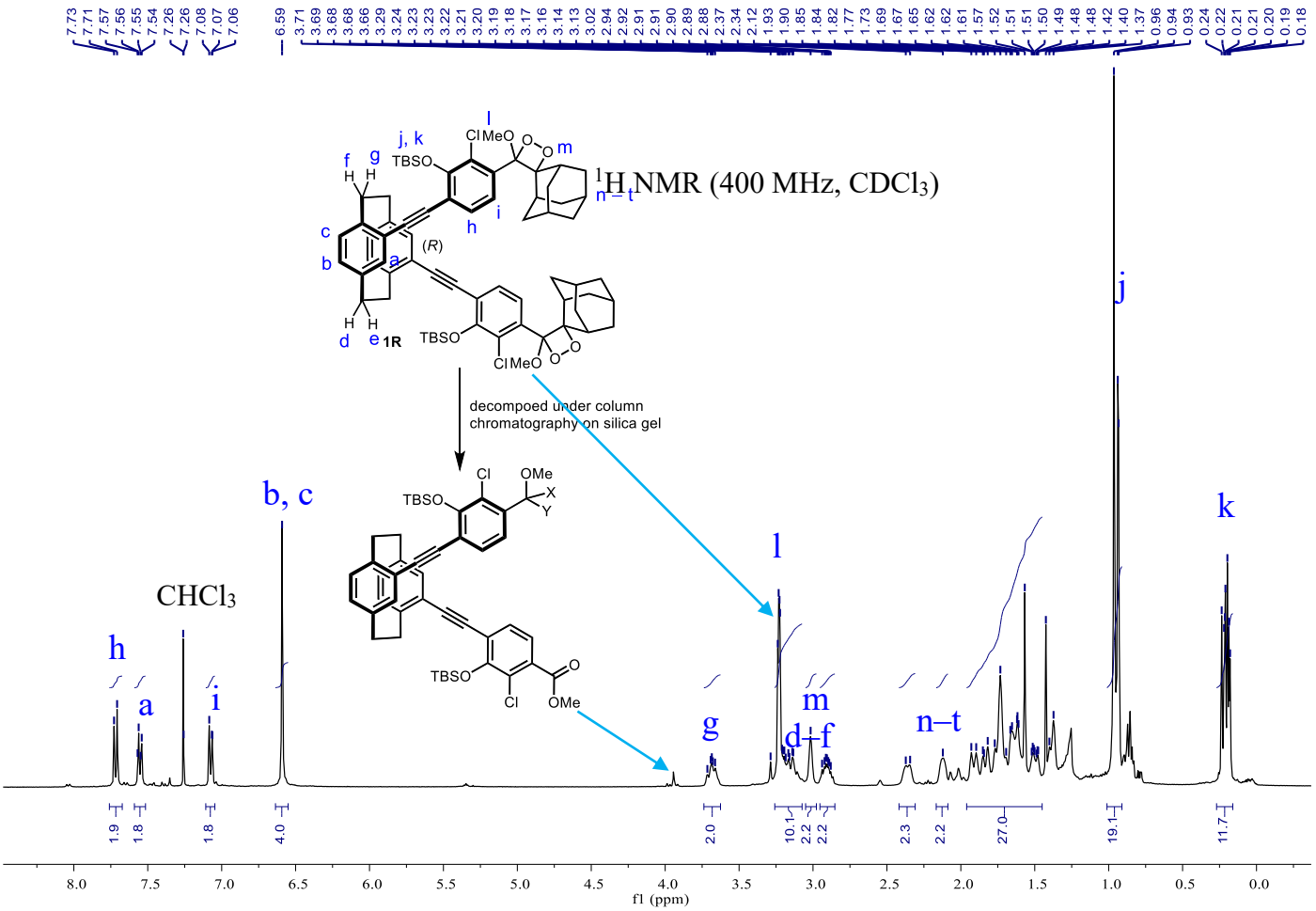
^{1}H NMR (400 MHz, CDCl$_3$)
1R
decompoed under column chromatography on silica gel
CHCl$_3$
h
a
i
b, c
l
g
m
d–f
n–t
j
k
f1 (ppm)

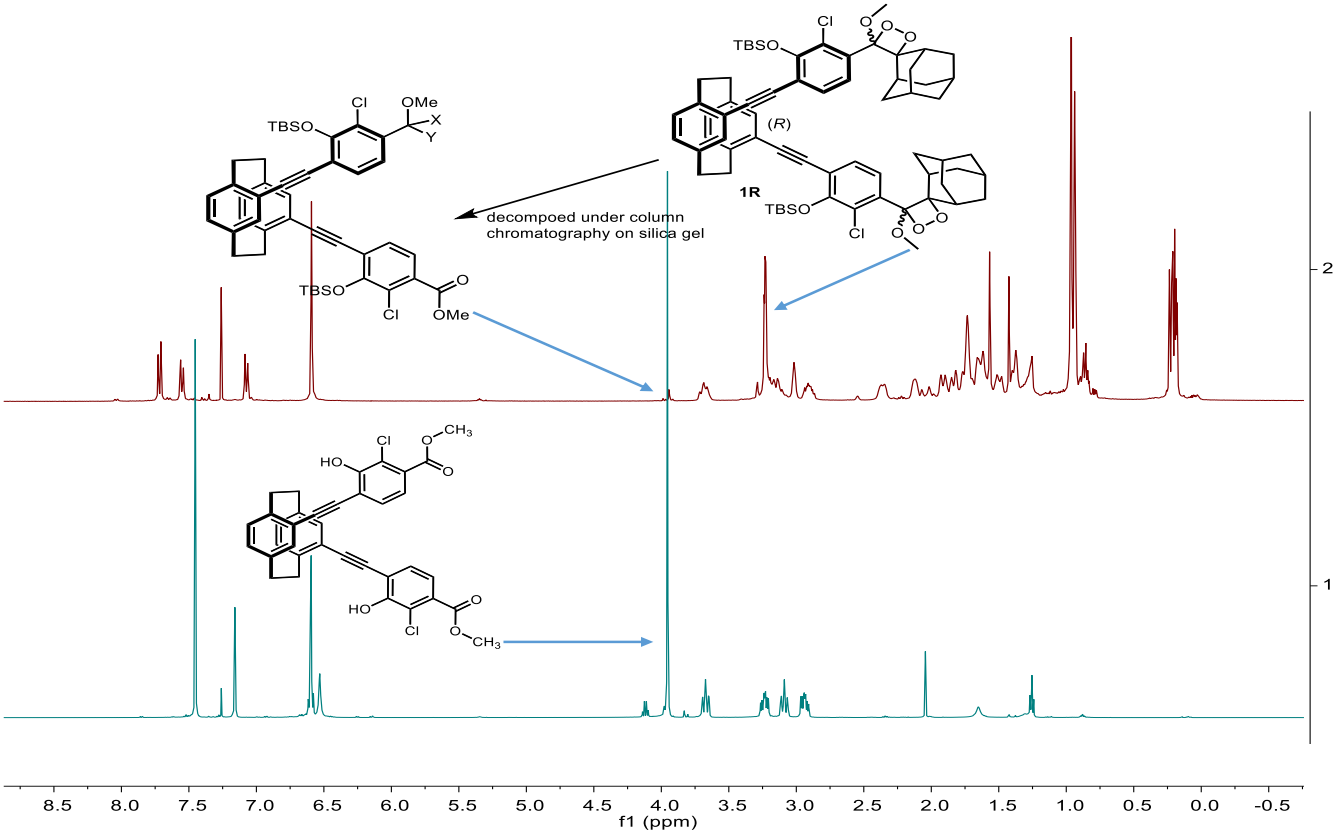
1R
decompoed under column chromatography on silica gel
f1 (ppm)

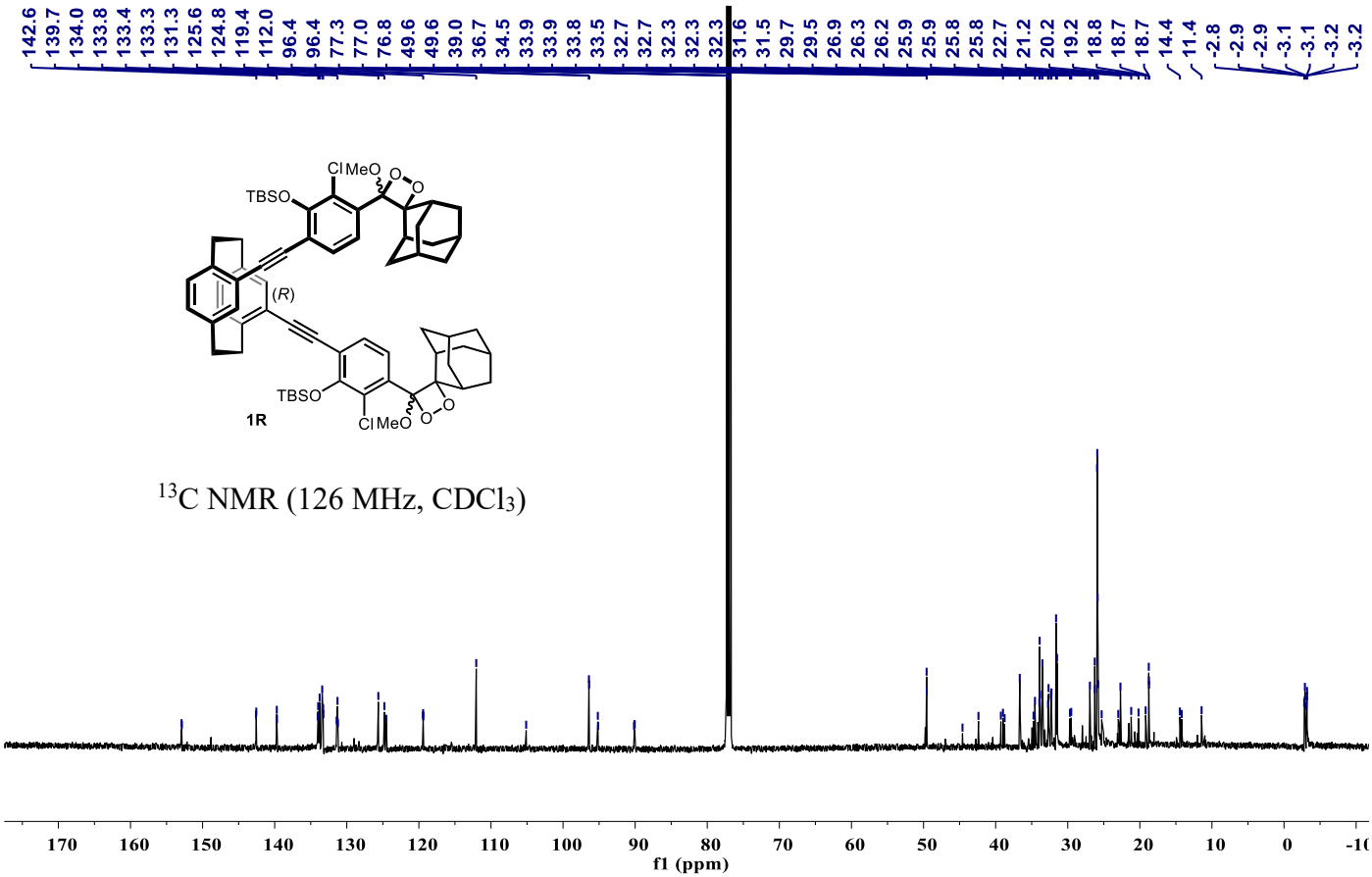

^{13}C NMR (126 MHz, $CDCl_3$)

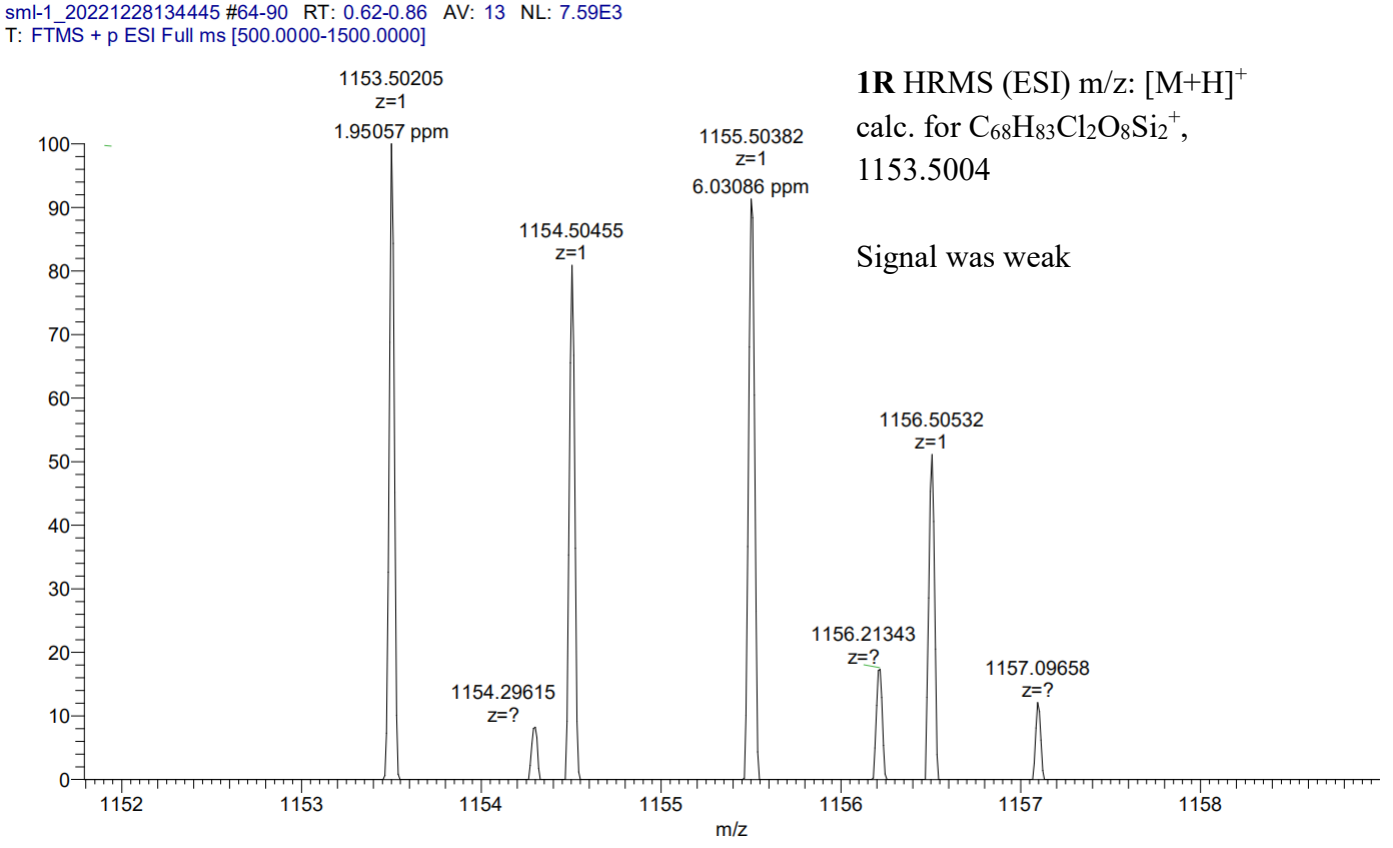

1R HRMS (ESI) m/z: $[M+H]^+$ calc. for $C_{68}H_{83}Cl_2O_8Si_2^+$, 1153.5004

Signal was weak

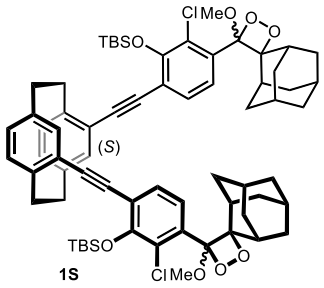

^{1}H NMR (400 MHz, $CDCl_3$)

$CHCl_3$

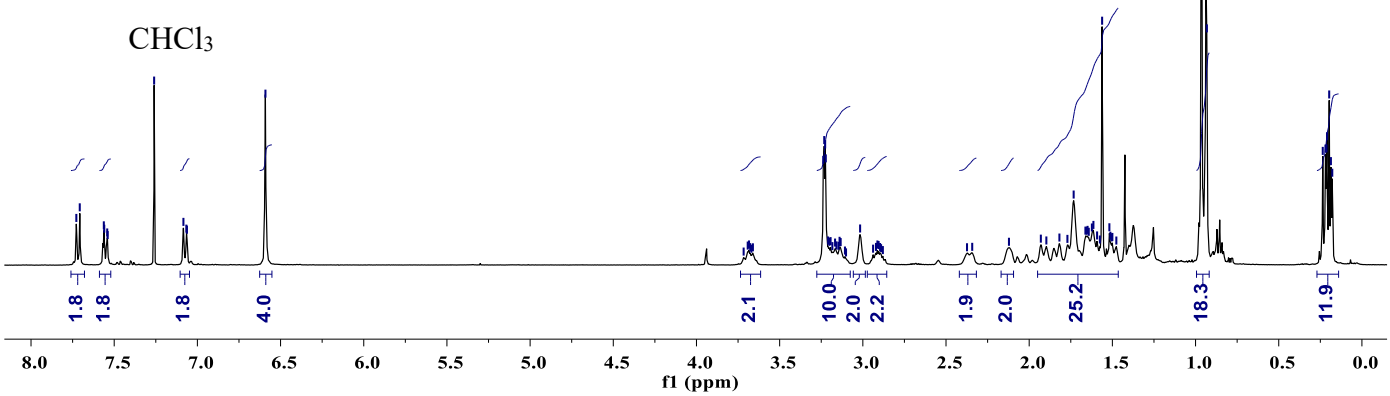

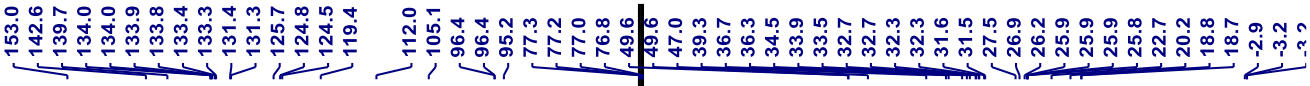

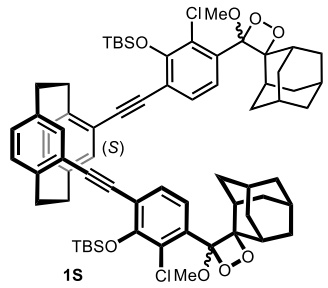

^{13}C NMR (126 MHz, $CDCl_3$)

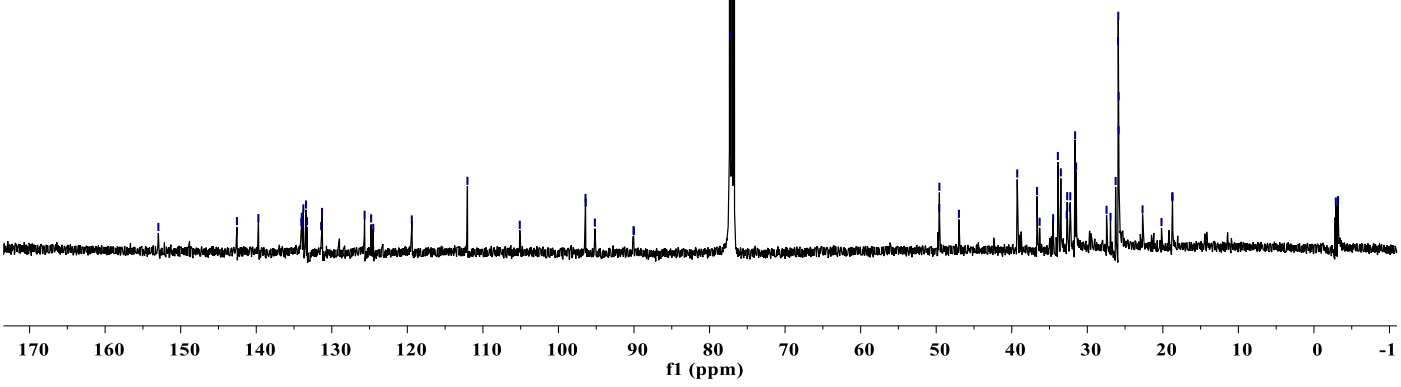

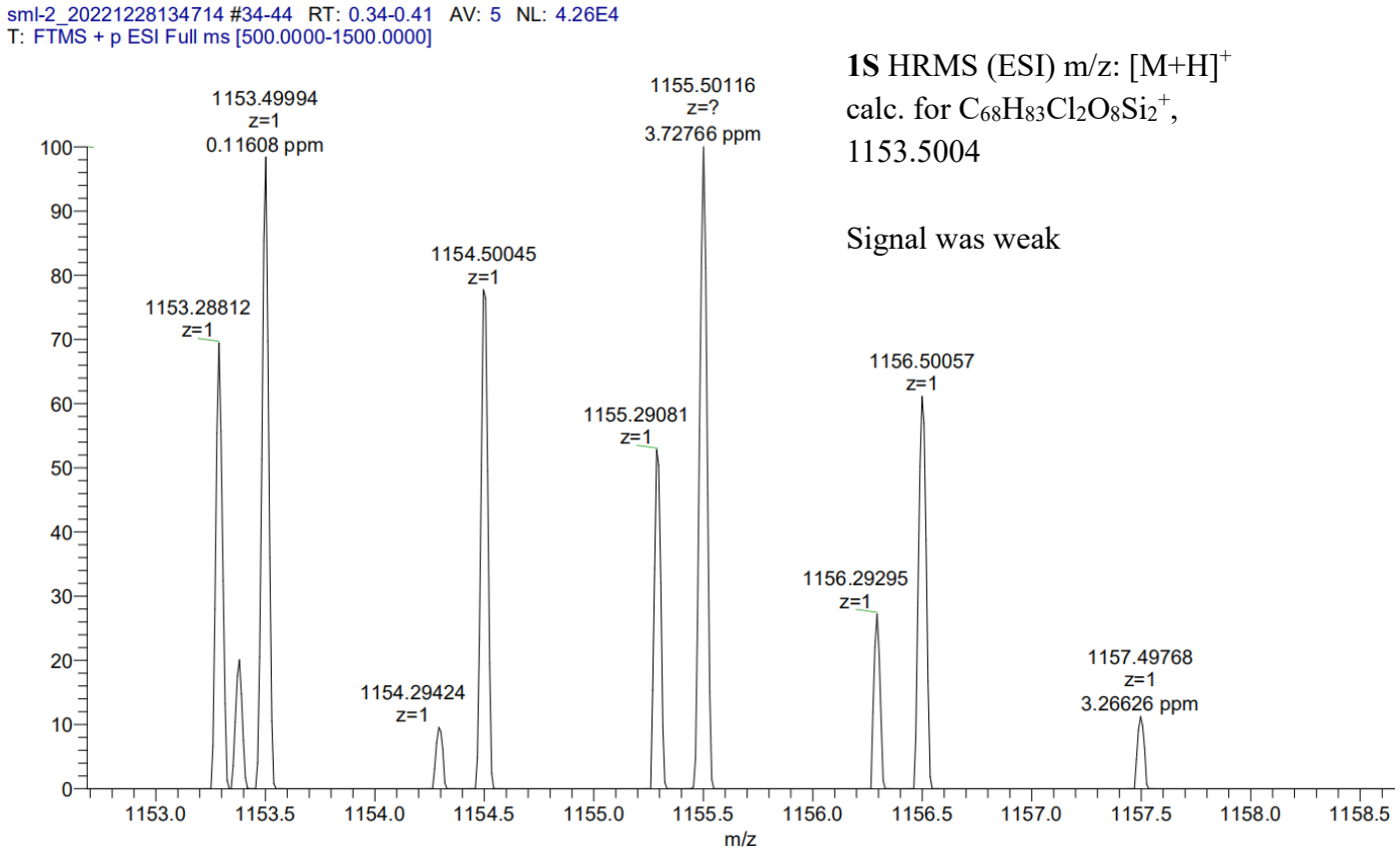

1S HRMS (ESI) m/z: $[M+H]^+$ calc. for $C_{68}H_{83}Cl_2O_8Si_2^+$, 1153.5004

Signal was weak

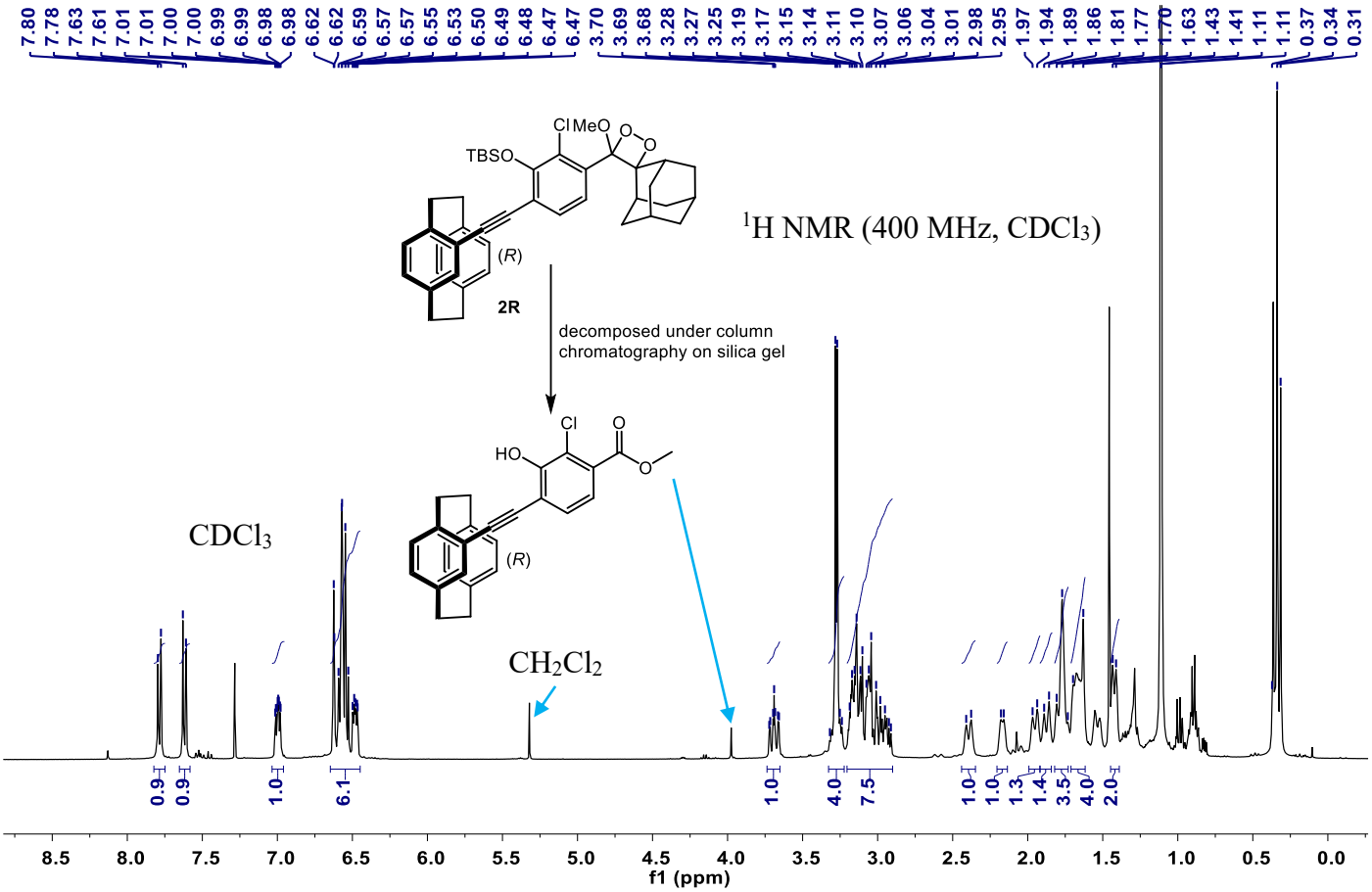

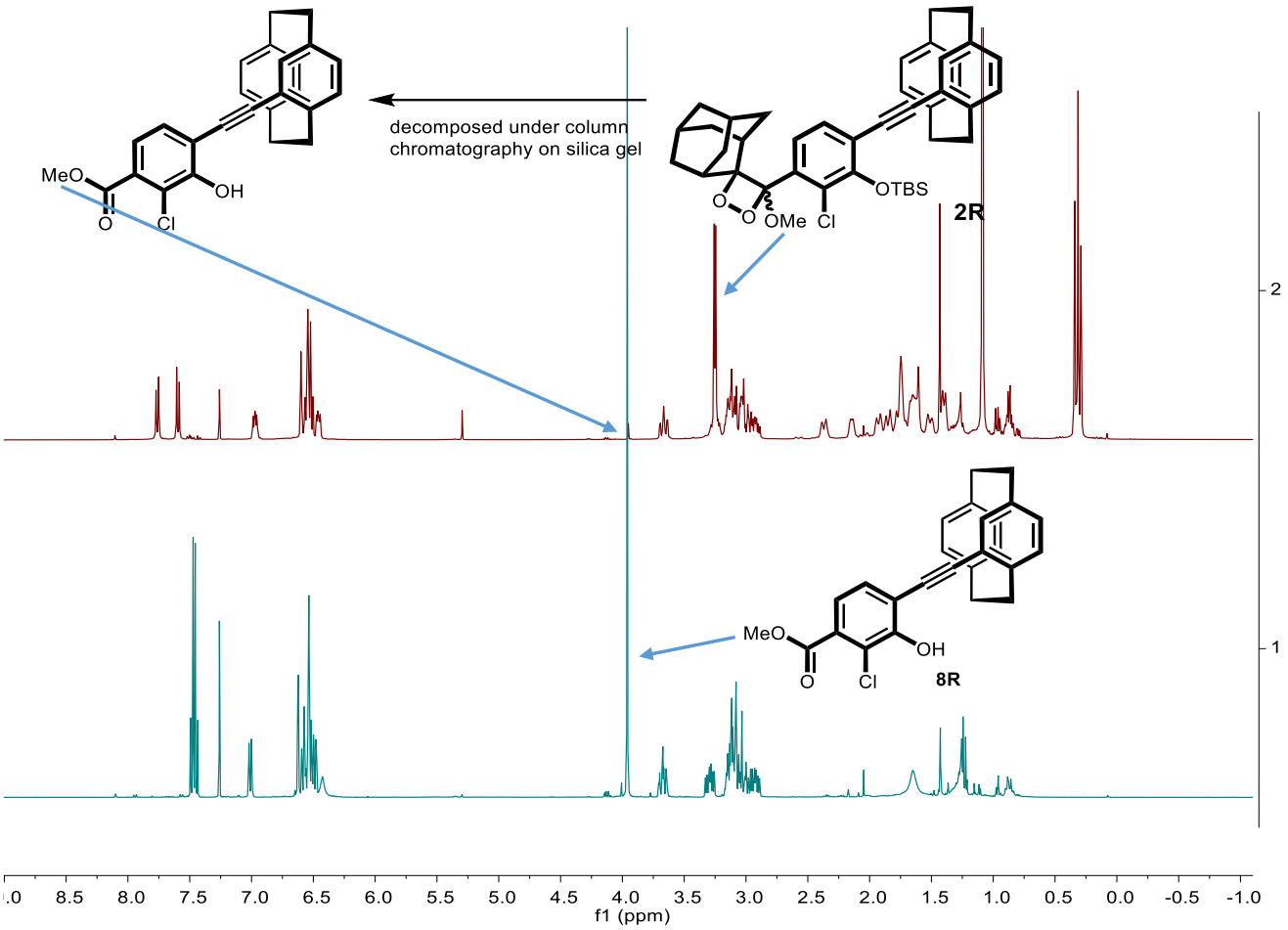

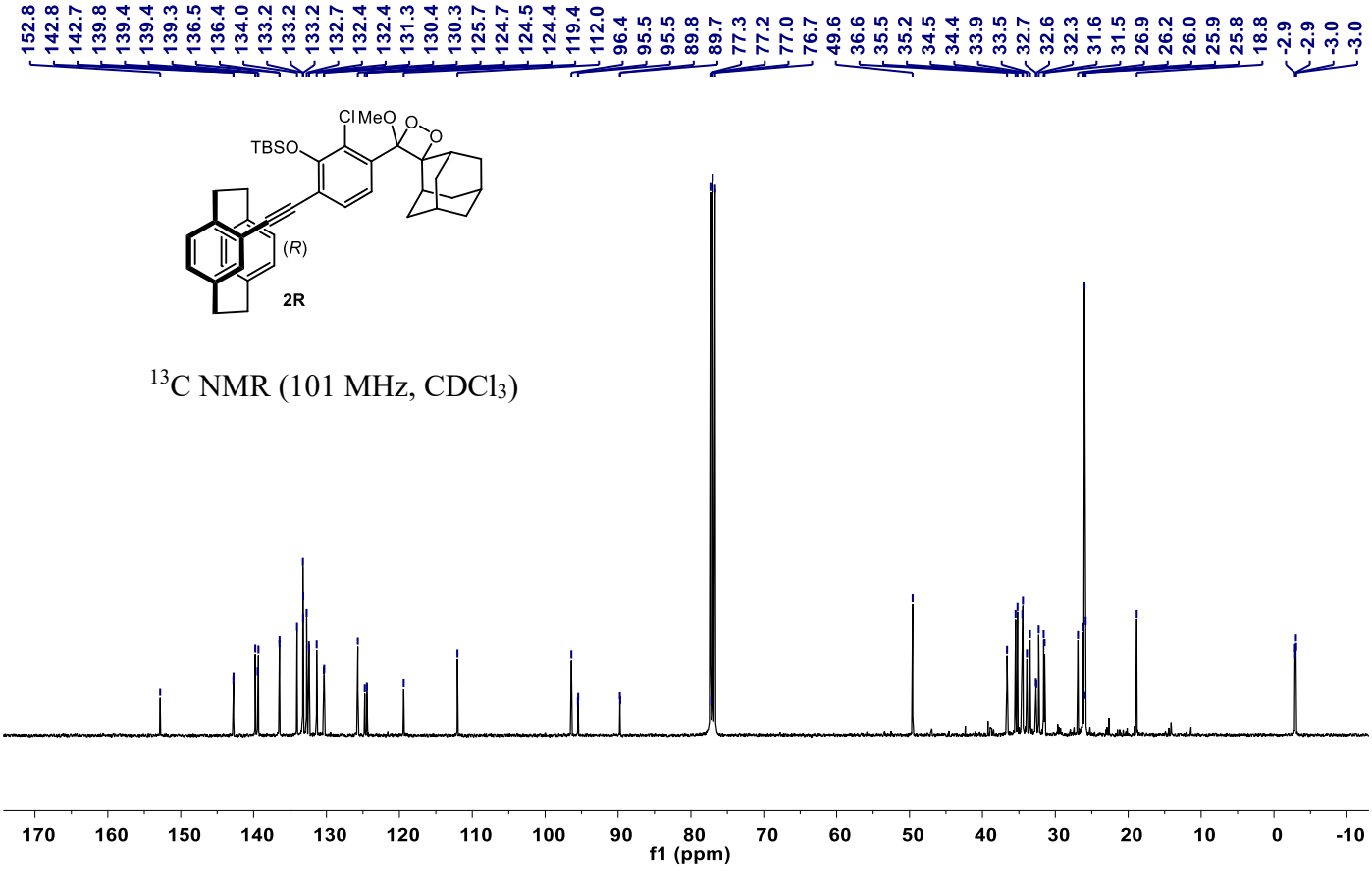

^{13}C NMR (101 MHz, $CDCl_3$)

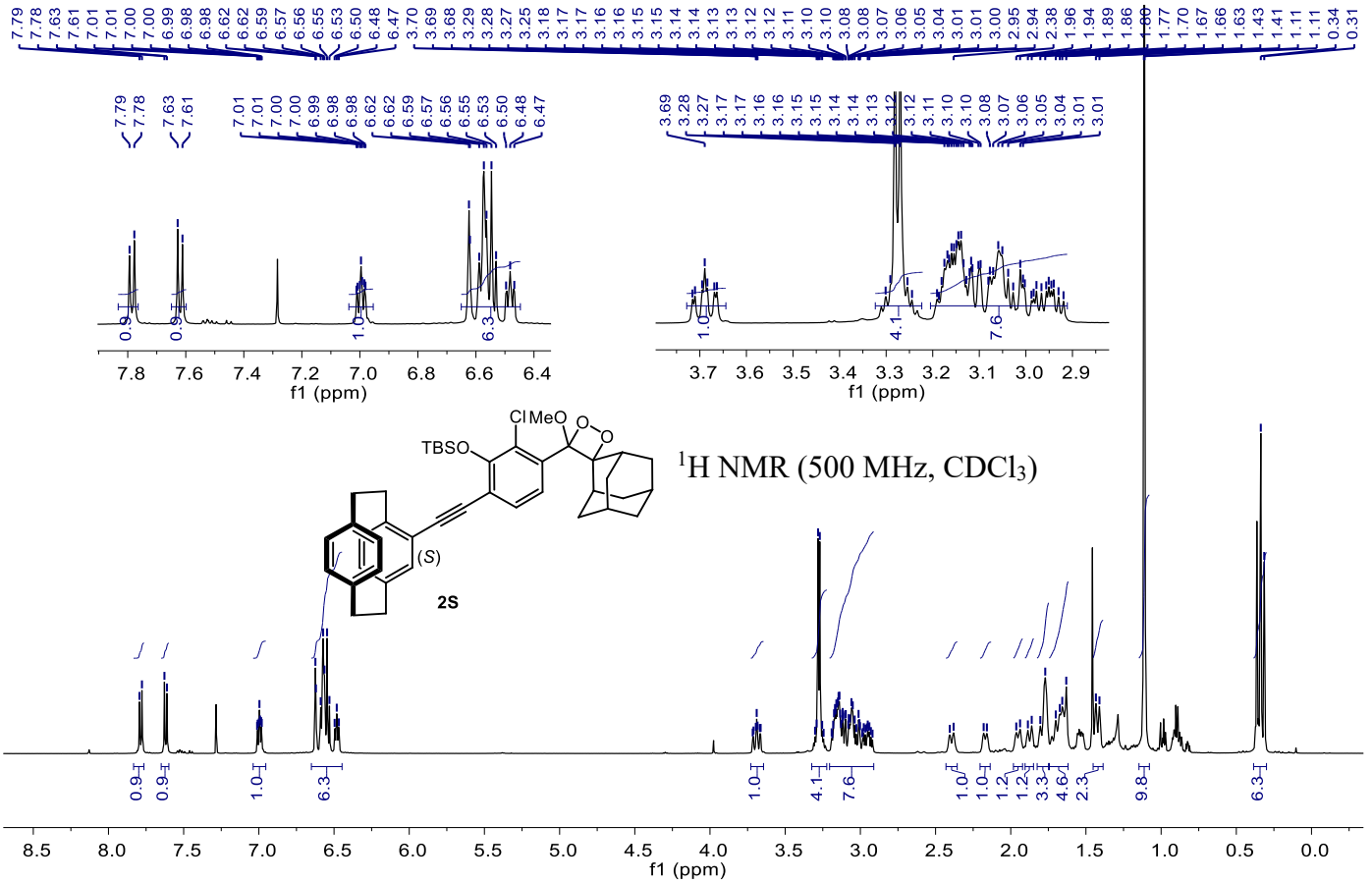

^{1}H NMR (500 MHz, $CDCl_3$)

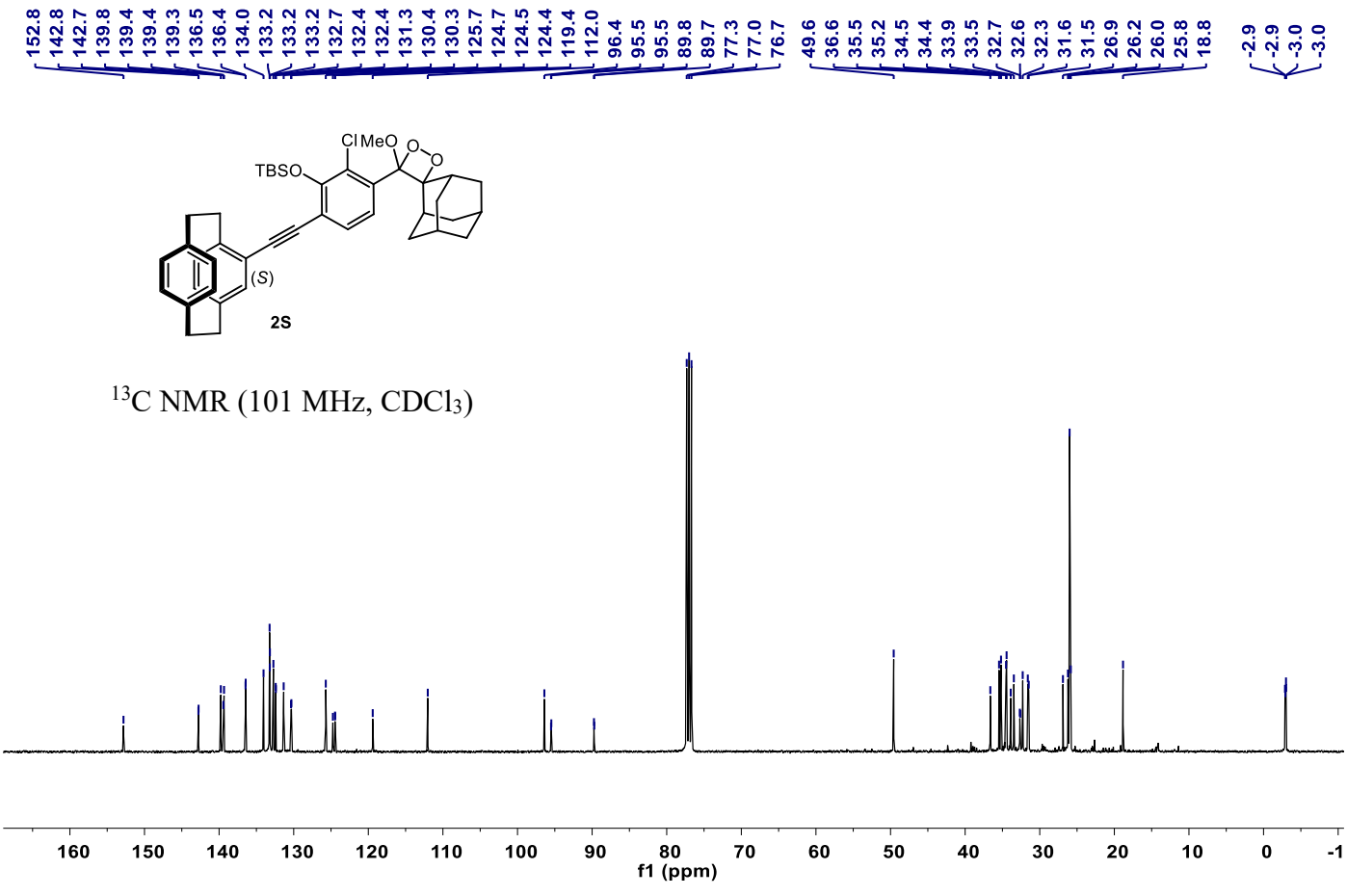

^{13}C NMR (101 MHz, $CDCl_3$)

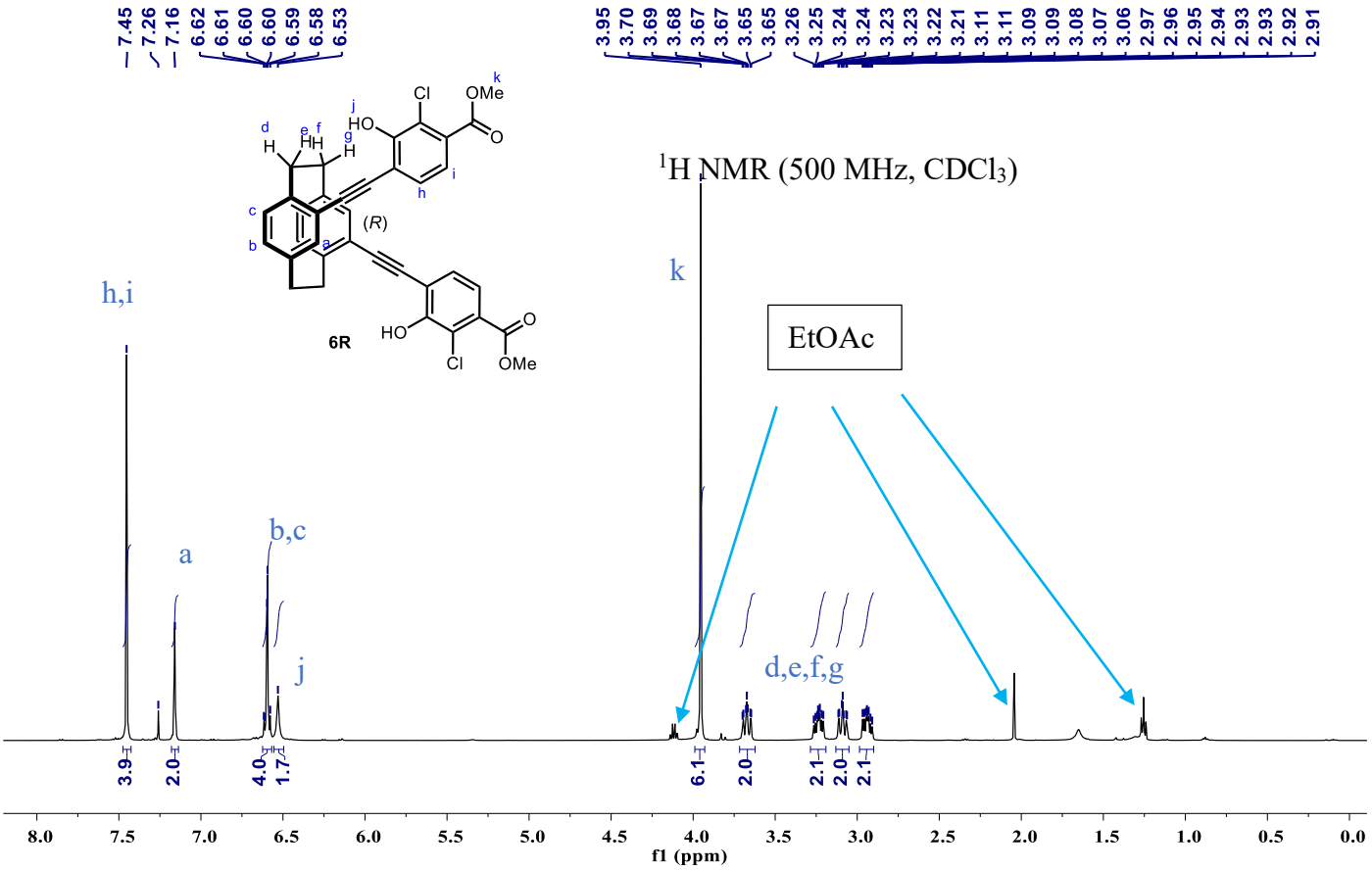
7.45
7.26
7.16
6.62
6.61
6.60
6.60
6.59
6.58
6.53
3.95
3.70
3.69
3.68
3.67
3.67
3.65
3.65
3.26
3.25
3.24
3.24
3.23
3.23
3.22
3.21
3.11
3.11
3.09
3.09
3.08
3.07
3.06
2.97
2.96
2.95
2.94
2.93
2.93
2.92
2.91
6R
(R)
1H NMR (500 MHz, CDCl3)
h,i
a
b,c
j
k
EtOAc
d,e,f,g
3.9
2.0
4.0
1.7
6.1
2.0
2.1
2.0
2.1
f1 (ppm)

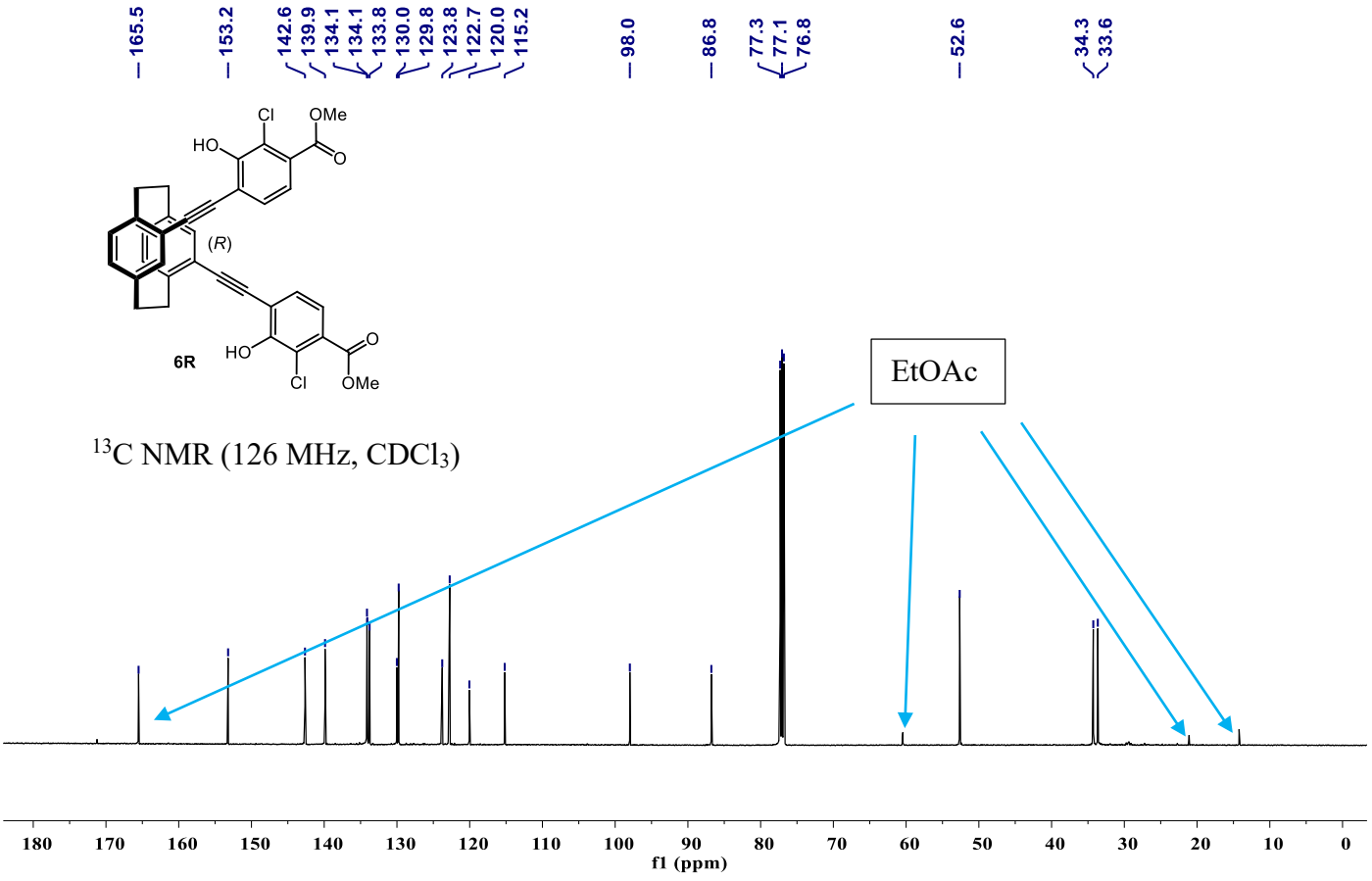
165.5
153.2
142.6
139.9
134.1
134.1
133.8
130.0
129.8
123.8
122.7
120.0
115.2
98.0
86.8
77.3
77.1
76.8
52.6
34.3
33.6
6R
(R)
13C NMR (126 MHz, CDCl3)
EtOAc
f1 (ppm)

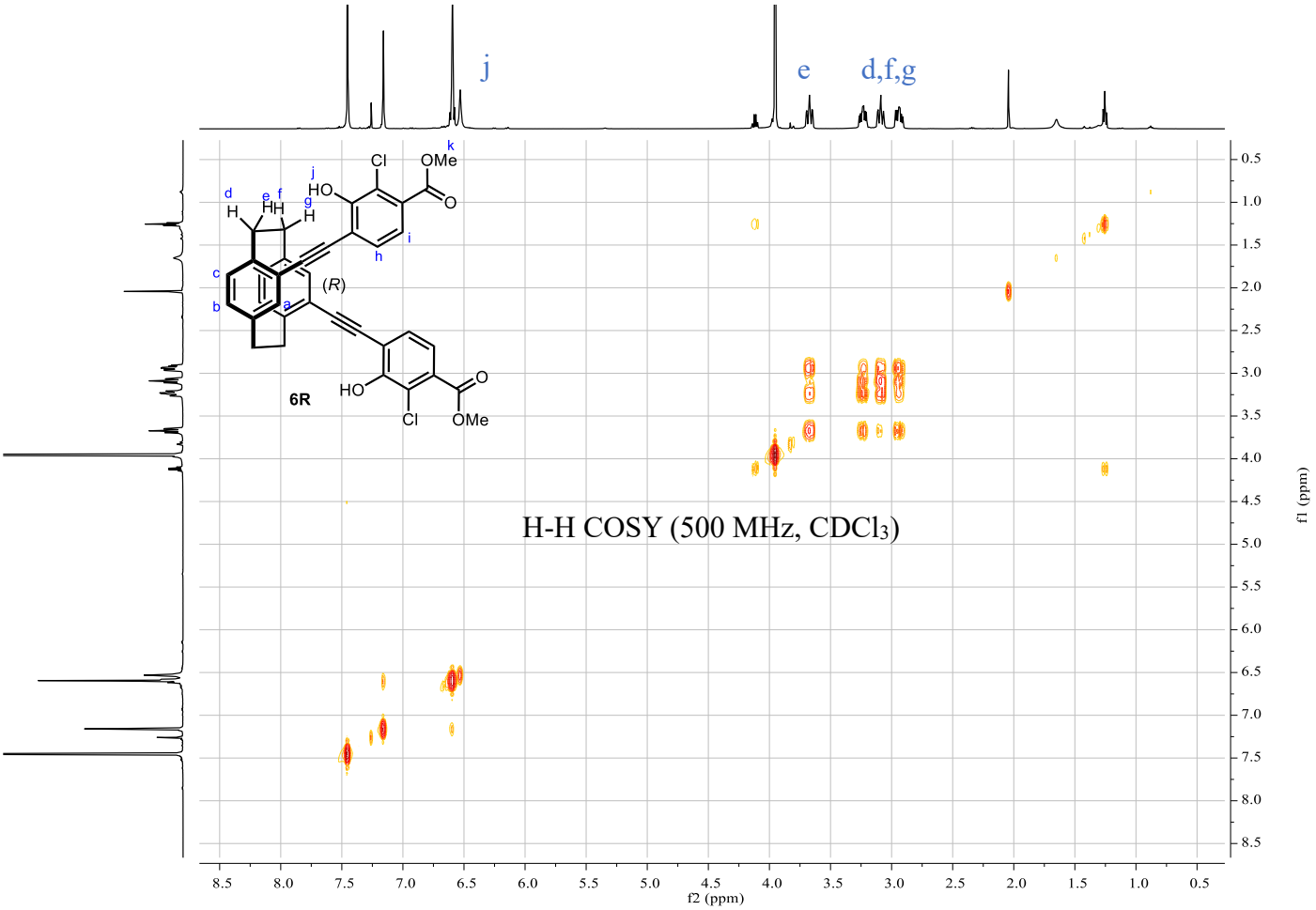
j
e
d,f,g
Cl
OMe
HO
O
(R)
HO
Cl
OMe
6R
H-H COSY (500 MHz, CDCl3)
f2 (ppm)
f1 (ppm)

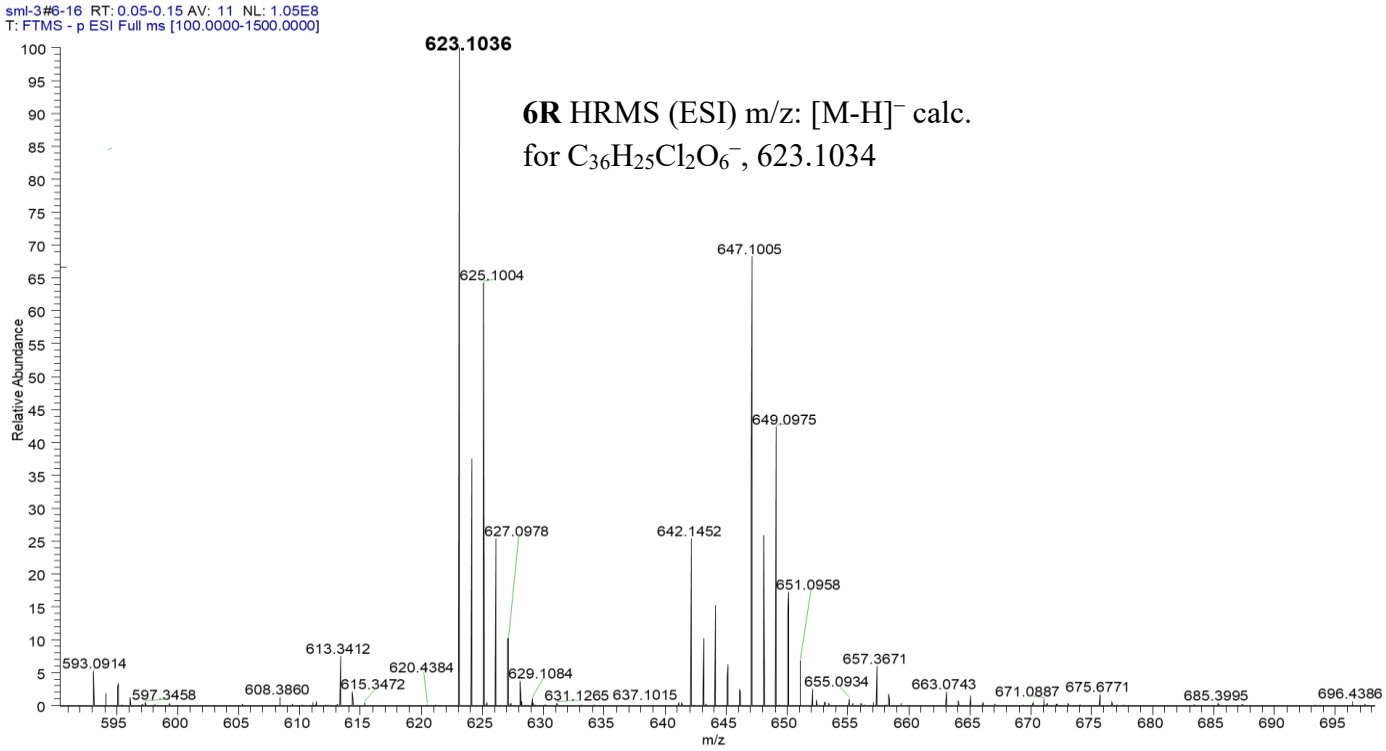
sml-3#6-16 RT: 0.05-0.15 AV: 11 NL: 1.05E8
T: FTMS - p ESI Full ms [100.0000-1500.0000]
623.1036
6R HRMS (ESI) m/z: [M-H]⁻ calc. for C36H25Cl2O6⁻, 623.1034
647.1005
625.1004
649.0975
627.0978
642.1452
651.0958
593.0914
613.3412
620.4384
597.3458
608.3860
615.3472
629.1084
631.1265
637.1015
655.0934
657.3671
663.0743
671.0887
675.6771
685.3995
696.4386
Relative Abundance
m/z

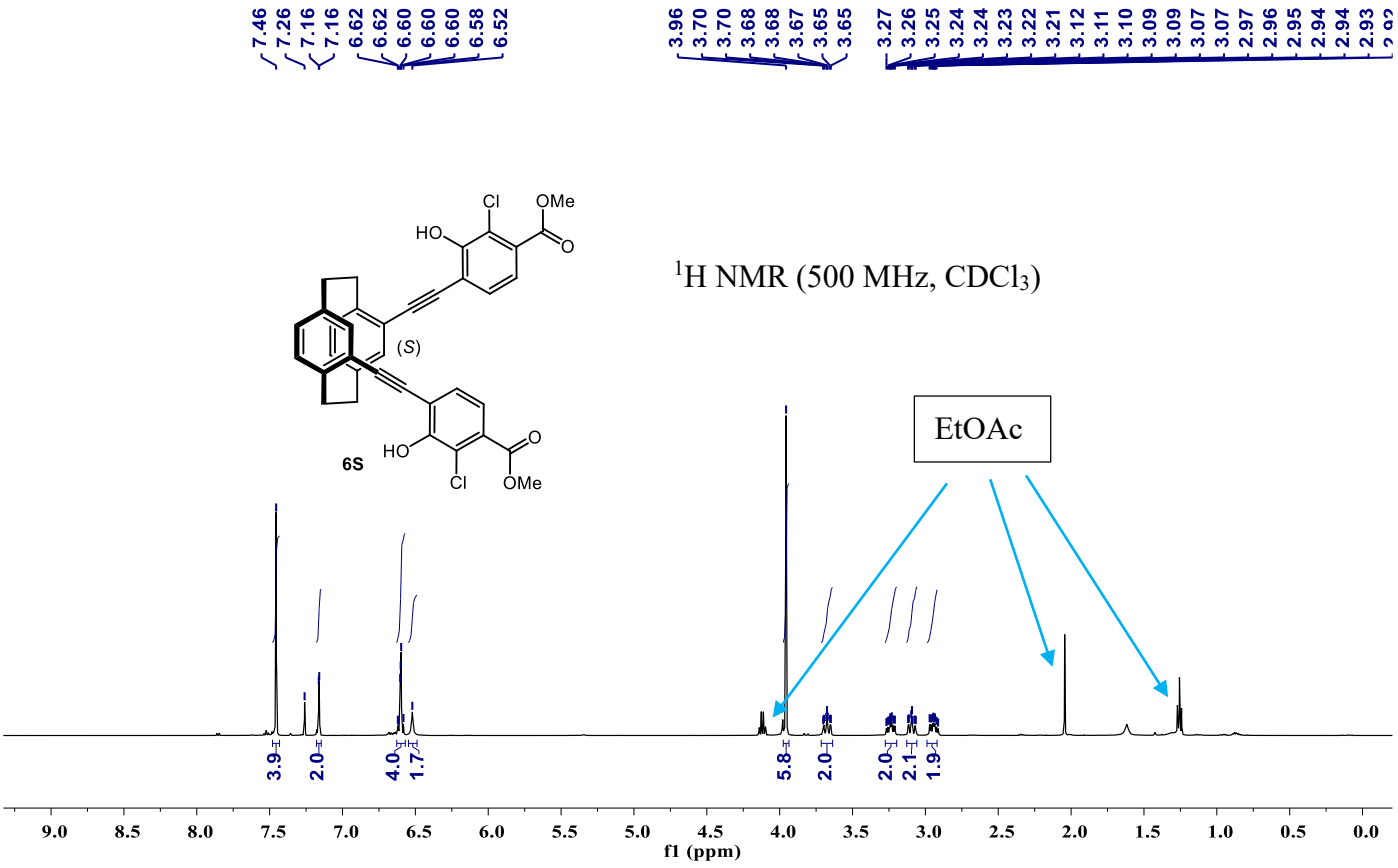
7.46
7.26
7.16
7.16
6.62
6.62
6.60
6.60
6.60
6.58
6.52
3.96
3.70
3.70
3.68
3.68
3.67
3.65
3.65
3.27
3.26
3.25
3.24
3.24
3.23
3.22
3.21
3.12
3.11
3.10
3.09
3.09
3.07
3.07
2.97
2.96
2.95
2.94
2.94
2.93
Cl
OMe
HO
O
(S)
HO
O
6S
Cl
OMe
1H NMR (500 MHz, CDCl3)
EtOAc
3.9
2.0
4.0
1.7
5.8
2.0
2.0
2.1
1.9
9.0
8.5
8.0
7.5
7.0
6.5
6.0
5.5
5.0
4.5
4.0
3.5
3.0
2.5
2.0
1.5
1.0
0.5
0.0
f1 (ppm)

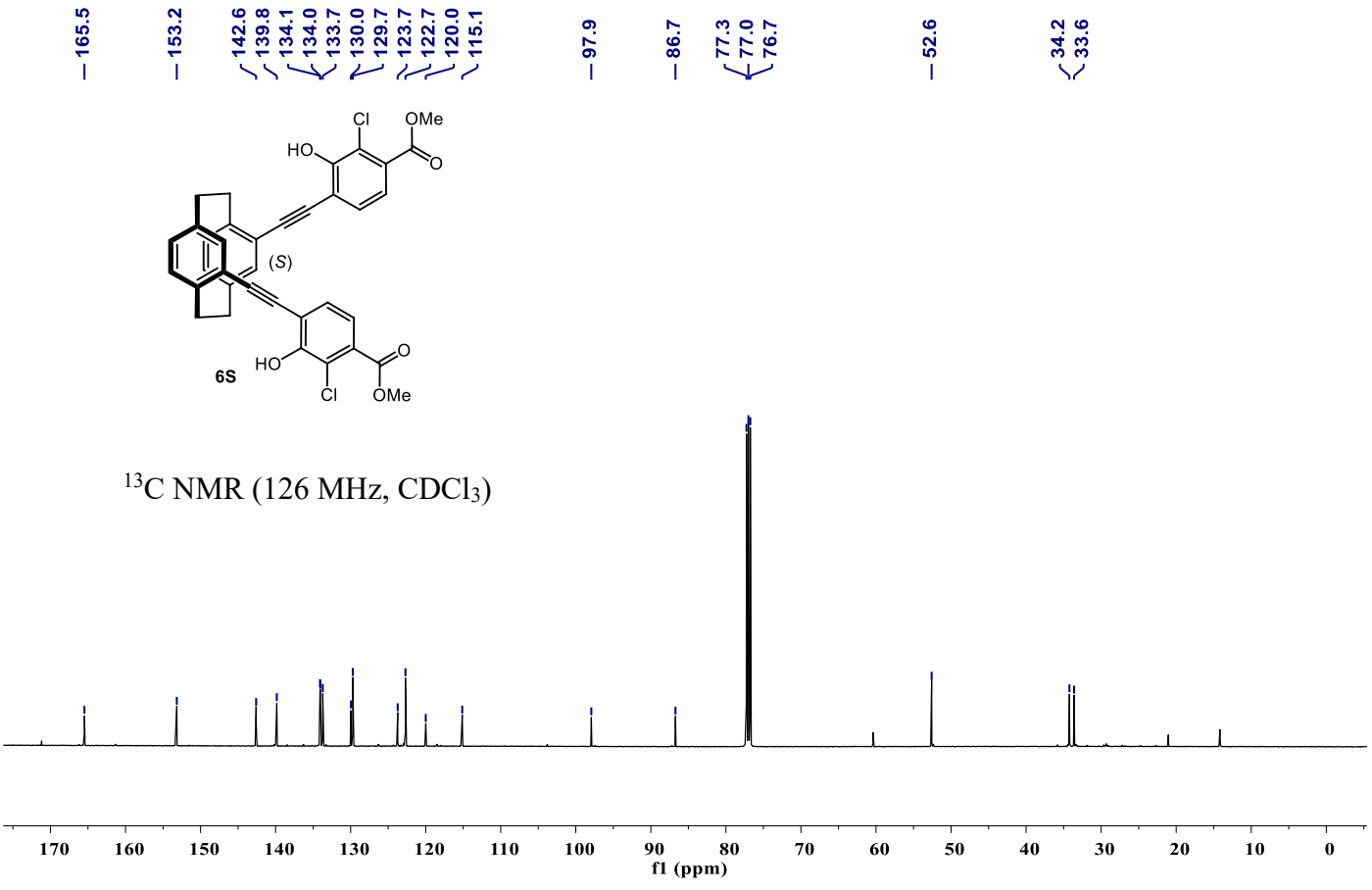
165.5
153.2
142.6
139.8
134.1
134.0
133.7
130.0
129.7
123.7
122.7
120.0
115.1
97.9
86.7
77.3
77.0
76.7
52.6
34.2
33.6
Cl
OMe
HO
O
(S)
HO
O
6S
Cl
OMe
13C NMR (126 MHz, CDCl3)
170
160
150
140
130
120
110
100
90
80
70
60
50
40
30
20
10
0
f1 (ppm)

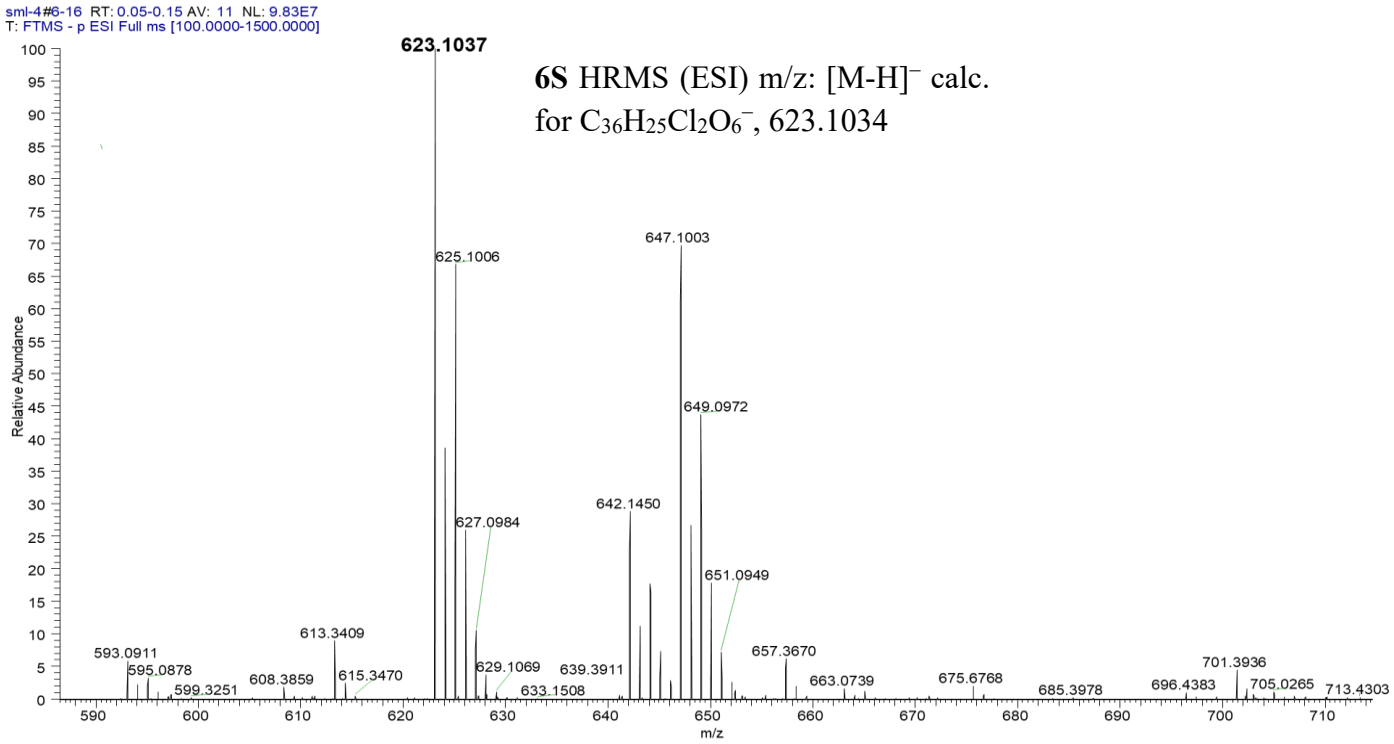

6S HRMS (ESI) m/z: $[M-H]^-$ calc. for $C_{36}H_{25}Cl_2O_6^-$, 623.1034

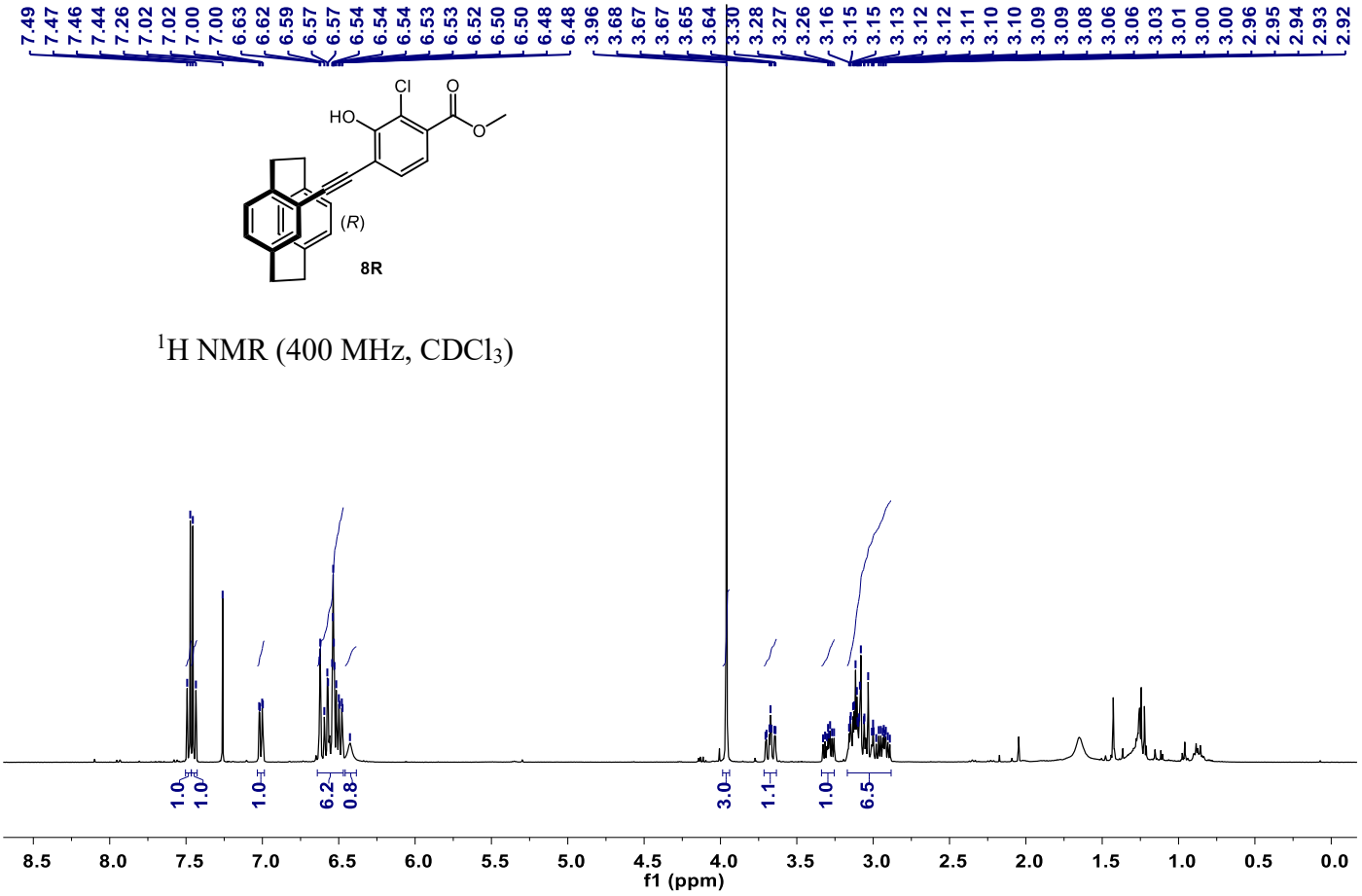

^{1}H NMR (400 MHz, $CDCl_3$)

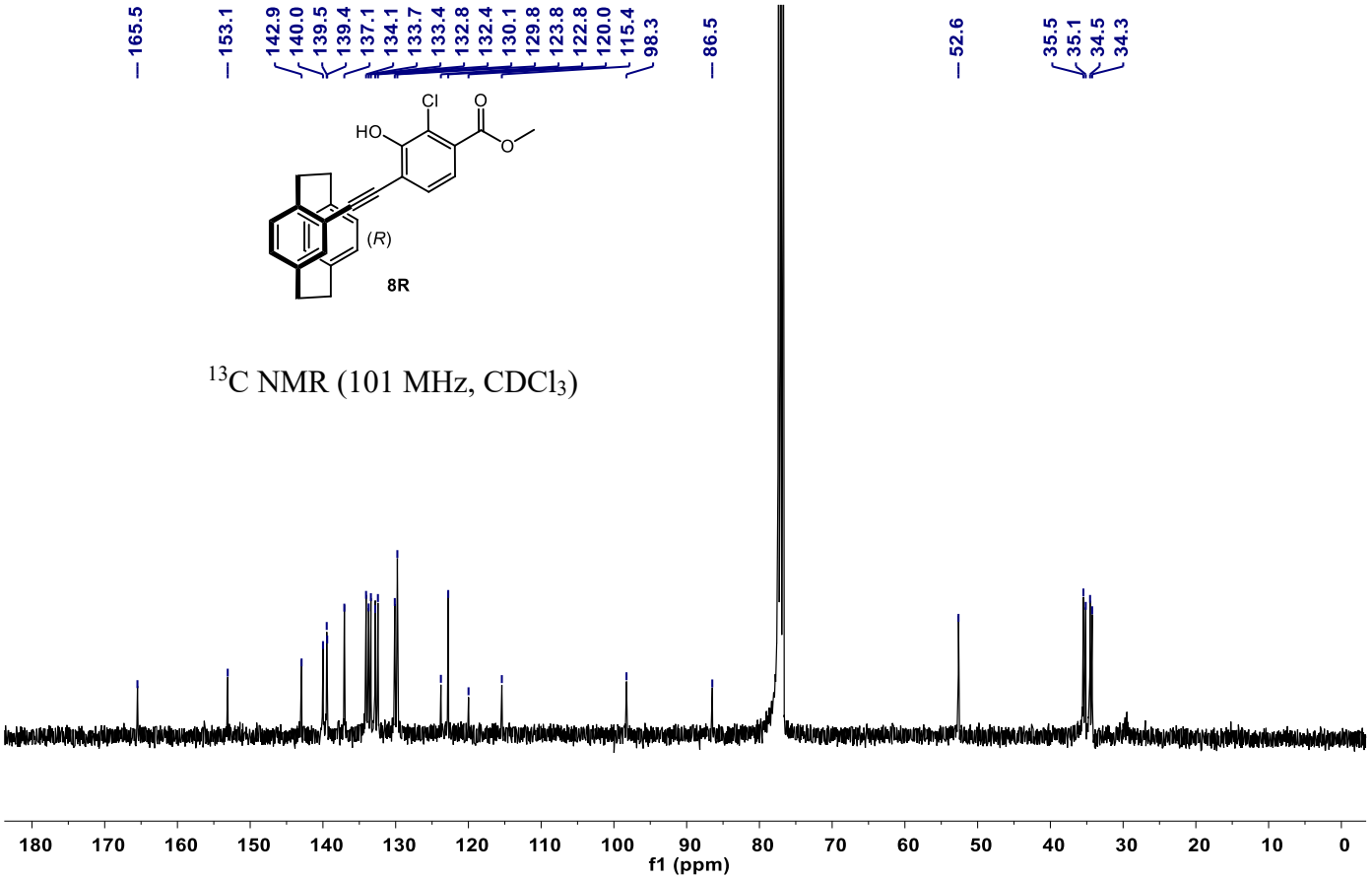

^{13}C NMR (101 MHz, $CDCl_3$)

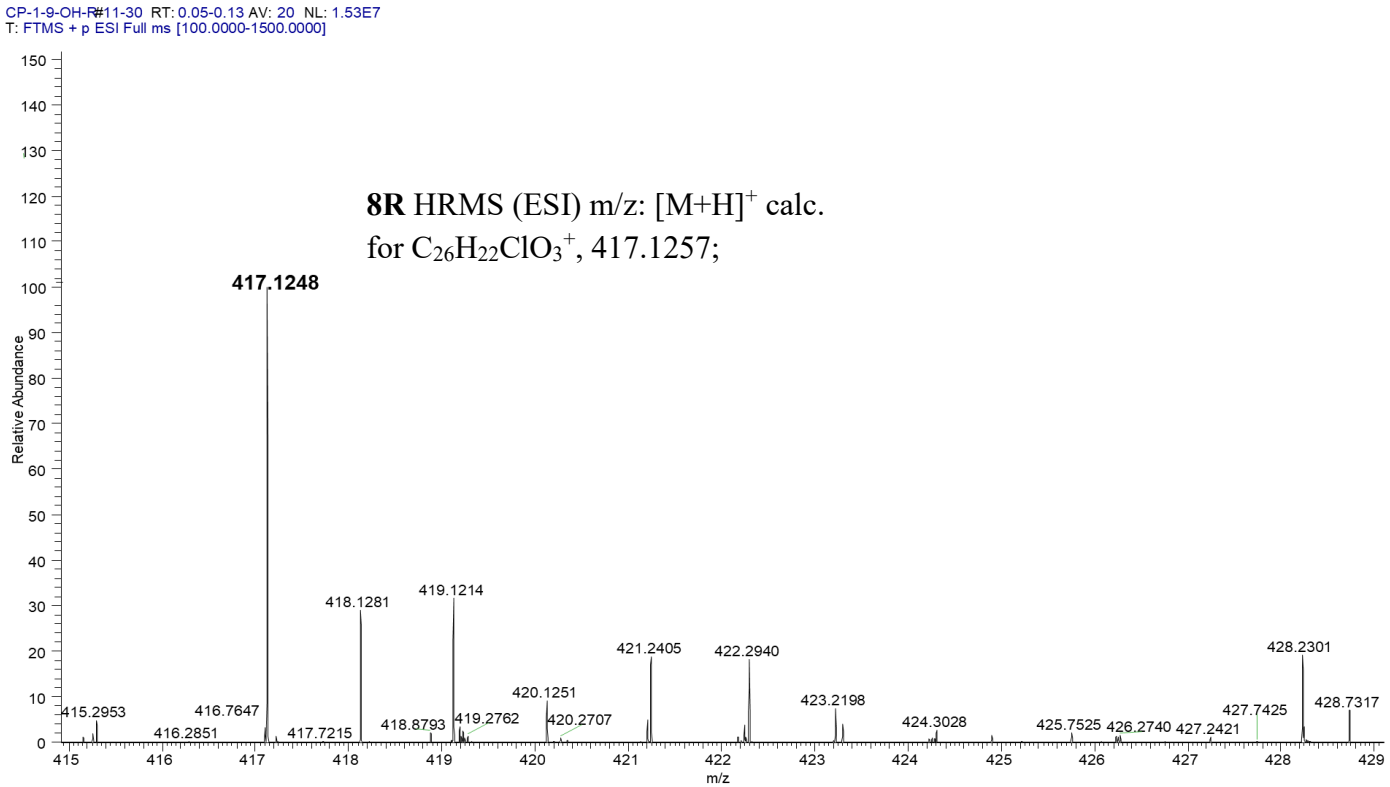

8R HRMS (ESI) m/z: $[M+H]^+$ calc. for $C_{26}H_{22}ClO_3^+$, 417.1257;

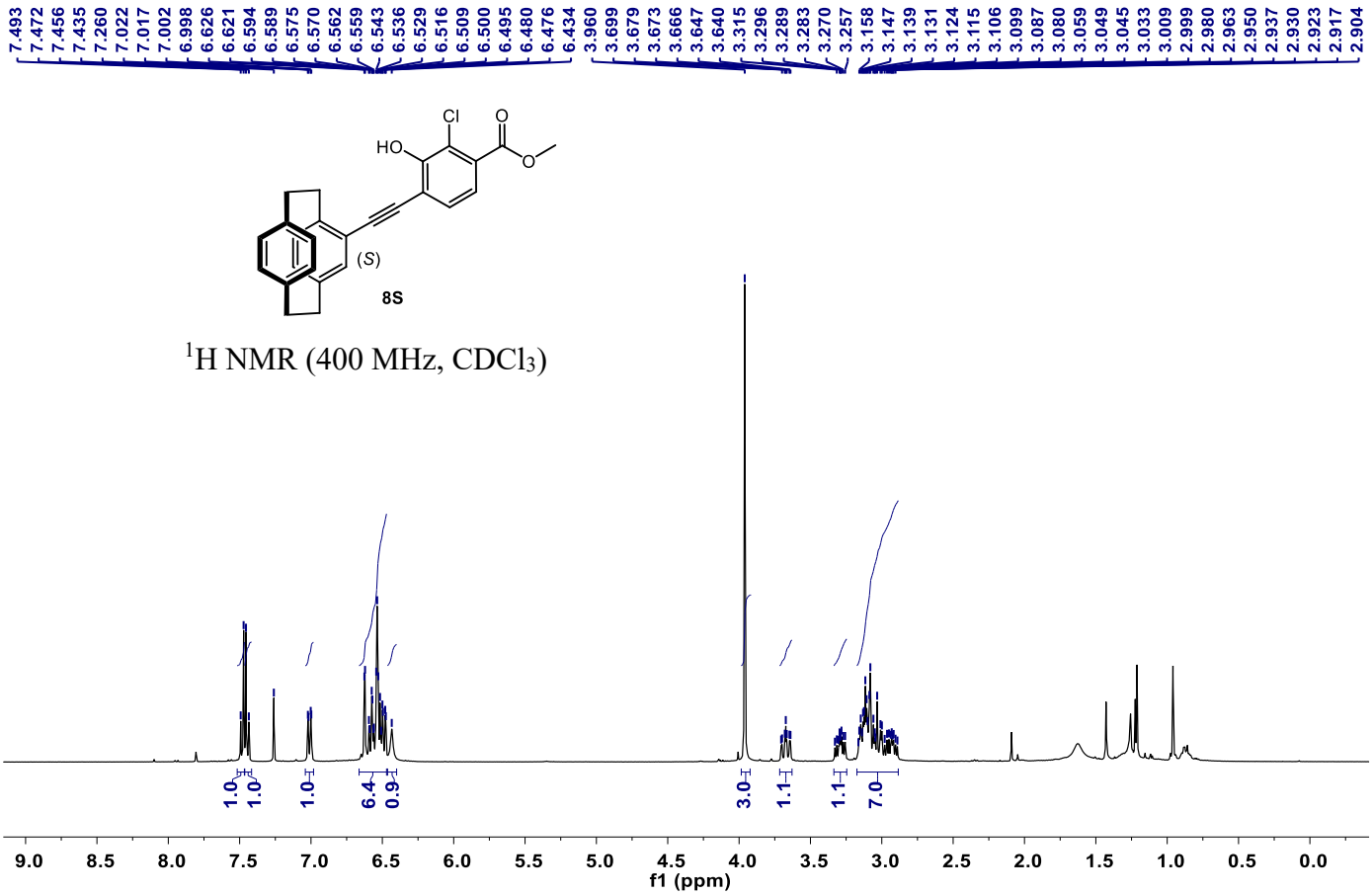

^{1}H NMR (400 MHz, $CDCl_3$)

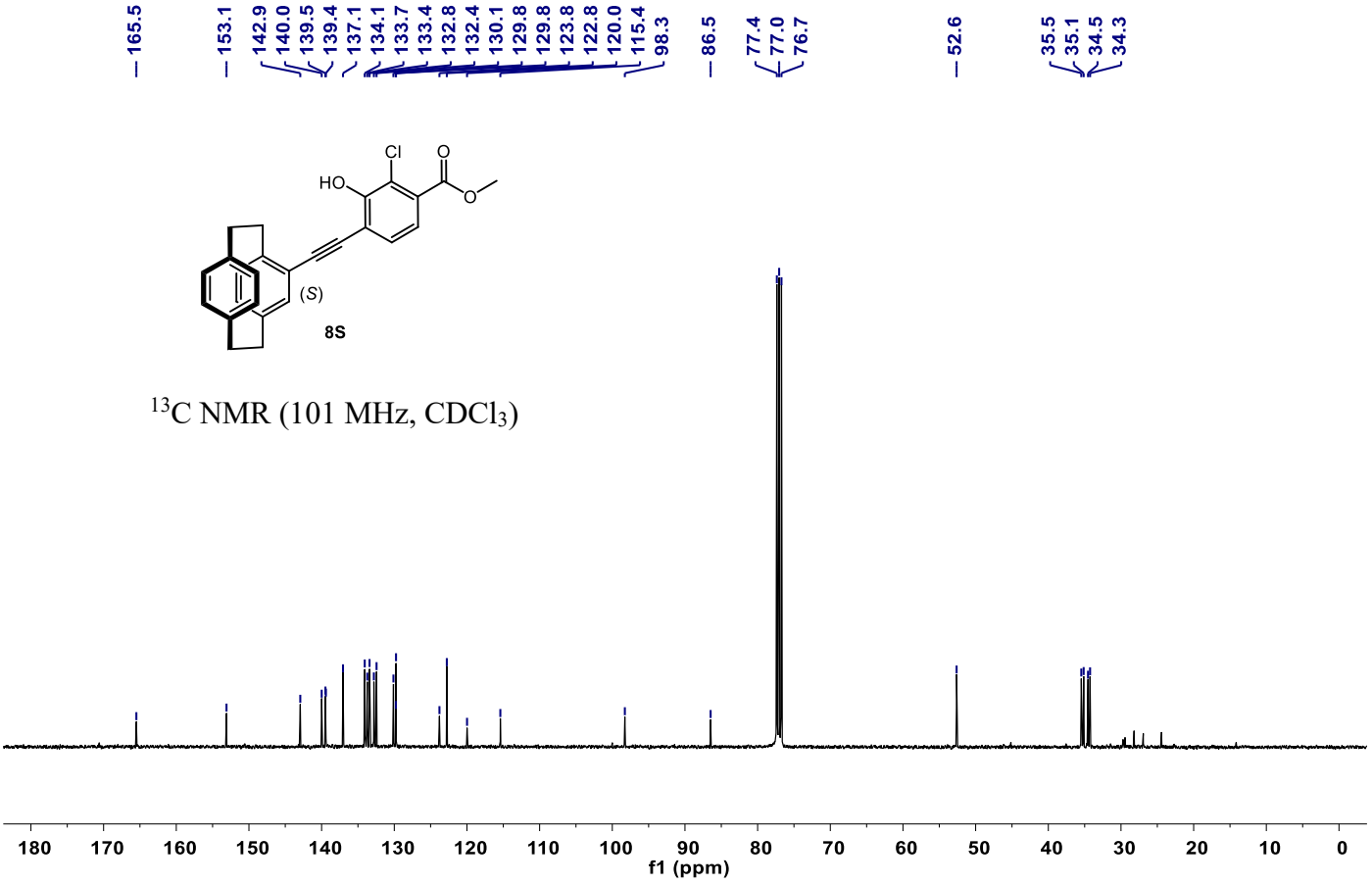

^{13}C NMR (101 MHz, $CDCl_3$)

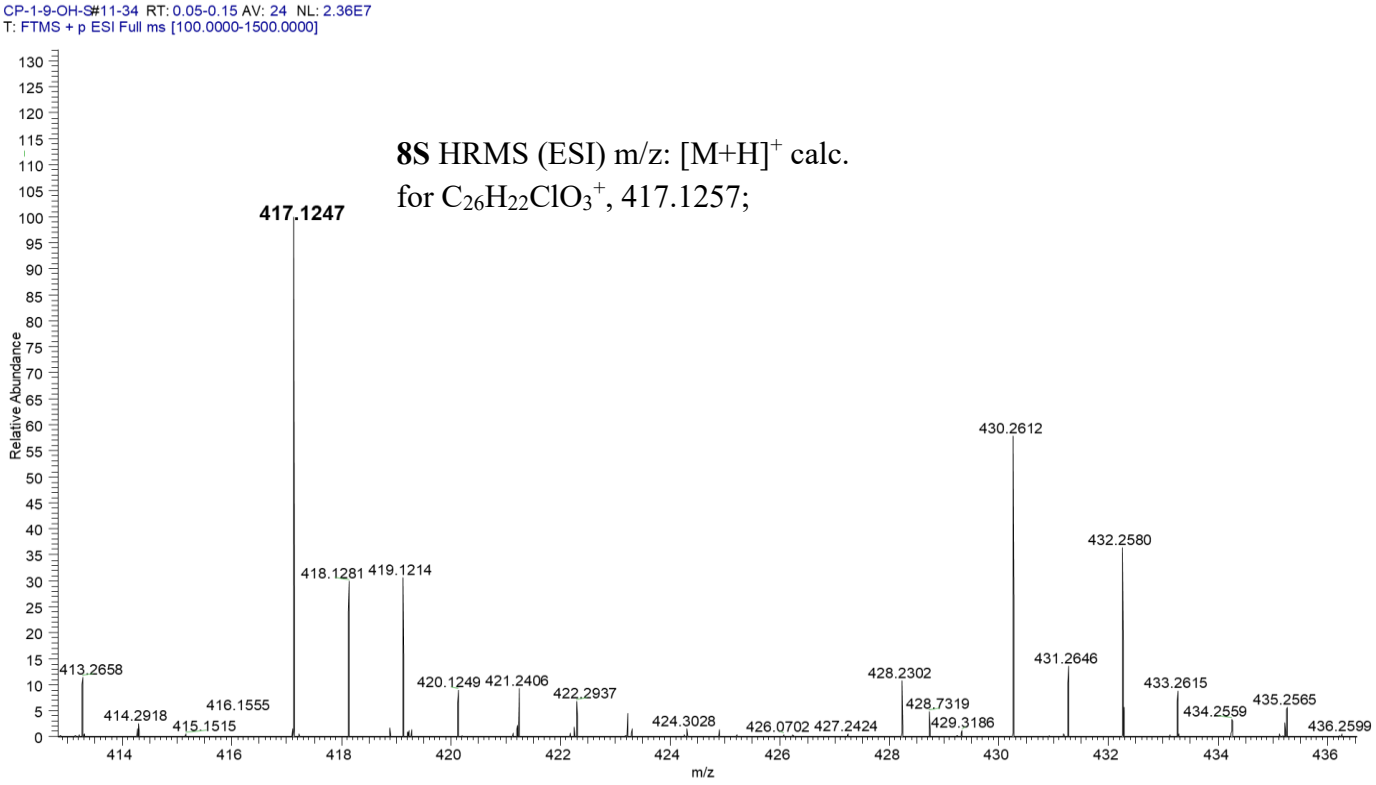

8S HRMS (ESI) m/z: $[M+H]^+$ calc. for $C_{26}H_{22}ClO_3^+$, 417.1257;

Table S1. Crystal Data of **6R**

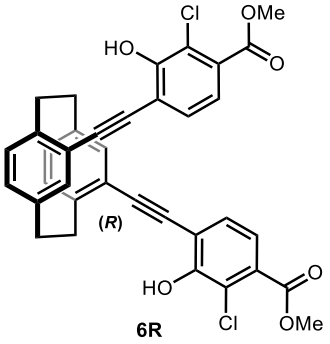

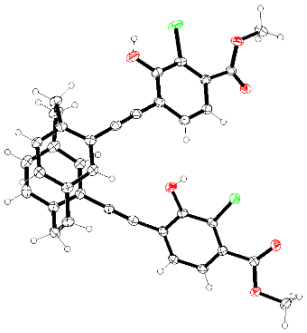

Identification code	cxy3235_0m
Empirical formula	$C_{36}H_{26}Cl_2O_6$
Formula weight	625.47
Temperature/K	100.0
Crystal system	orthorhombic
Space group	$P2_12_12_1$
a/Å	7.2696(4)
b/Å	19.8223(11)
c/Å	20.3510(11)
α/°	90
β/°	90
γ/°	90
Volume/Å^3	2932.6(3)
Z	4
ρ_{calc} g/cm^3	1.417
μ/mm^{-1}	2.395
F(000)	1296.0
Crystal size/mm^3	0.35 × 0.28 × 0.22
Radiation	CuKα (λ = 1.54178)
2*Θ* range for data collection/°	6.224 to 136.768
Index ranges	-8 ≤ h ≤ 8, -23 ≤ k ≤ 23, -24 ≤ l ≤ 24
Reflections collected	26930
Independent reflections	5386 [R_{int} = 0.0477, R_{sigma} = 0.0307]
Data/restraints/parameters	5386/0/401
Goodness-of-fit on F^2	1.029
Final *R* indexes [I>=2σ (I)]	R_1 = 0.0281, wR_2 = 0.0728
Final *R* indexes [all data]	R_1 = 0.0287, wR_2 = 0.0732
Largest diff. peak/hole / e Å^{-3}	0.23/-0.17
Flack parameter	-0.001(6)

Chemiluminescent and Photophysical Parameters

Table S2. Chemiluminescent Parameters.

	$t_{1/2}^{abs}$ (1 eq. TBAF)	CL^{max} (nm)	$t_{1/2}^{CL}$ (1 eq. TBAF)	$t_{1/2}^{CL}$ (2 eq. TBAF)	g_{CL}	Φ_{CL} (%)	Φ_S (%)
1R	30 s	497	28 min	18 min	+0.0011	7	9.5
1S					-0.0010		
2R	25 s	497	18 min	7 min	N. D.	9	10.2
2S					N. D.		

Table S3. Photophysical Parameters.

	λ_{abs}^{max} (nm)	g_{abs} / $\times 10^{-3}$ (λ / nm)	PL^{max} (nm)	$g_{PL}(10^{-3})$	Φ_{PL} (%)
1R	325	+2.1(295), -0.9(339), +4.0 (365)	418	+3.3	66
1S		-2.2(295), +1.0(339), -3.9 (365)		-3.0	
2R	324	+3.3(266), -1.3(318), +0.4(357)	435	+0.6	10
2S		-3.3(266), +1.2(318), -0.5(357)		-0.5	
6R	332	+1.1(290), -0.5(337), +2.1(374)	417	+1.2	3
6S		-1.1(290), +0.5(337), -2.1(374)		-1.2	
8R	338	+2.5(268), -1.1(314)	428	+0.3	7
8S		-2.5(268), +1.1(314)		-0.3	

Table S4. Comparison of Photophysical Data of Mixtures with Different Sources.

Mixtures	λ_{abs} (nm)	g_{abs} / $\times 10^{-3}$ (λ / nm)	PL^{max} (nm)	$g_{PL}(10^{-3})$	Φ_{PL} (%)
1R+TBAF (**5R**)	314, 422	-0.7(333), +0.9(380), +1.0(451)	497	+1.1	73
6R+TBAF	314, 422	-0.6(334), +0.9(380), +1.0(451)	497	+1.1	74
1S+TBAF (**5S**)	314, 422	+0.6(333), -0.9(380), -1.1(452)	497	-1.1	73
6S+TBAF	314, 422	+0.6(334), -0.8(378), -0.8(450)	497	-1.1	73
2R+TBAF (**7R**)	314, 423	-1.6(314)	497	+0.07	88
8R+TBAF	314, 423	-1.6(314)	497	+0.07	87
2S+TBAF (**7S**)	314, 423	+1.6(314)	497	-0.07	88
8S+TBAF	314, 423	+1.6(314)	497	-0.07	89

Chemiluminescent Spectra

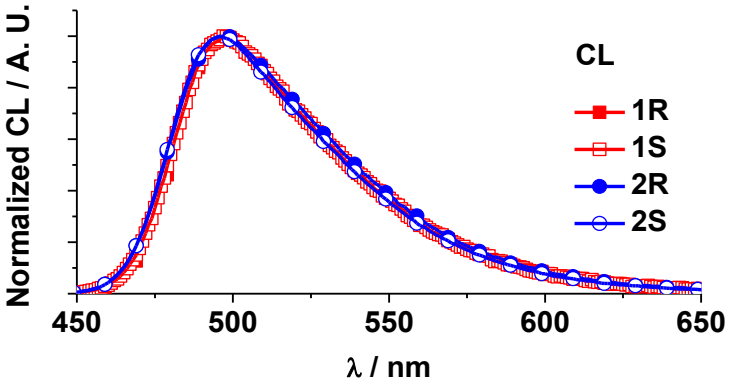

Figure S9 Chemiluminescent Spectra of dioxetanes **1R**/**1S** and **2R**/**2S**. The scan was started 60 s after 2 mL the dioxetane **1R**/**1S** or **2R**/**2S** in DMSO (0.1 mM) was added 0.2 mL TBAF in DMSO (1 mM for **2** or 2 mM for **1**).

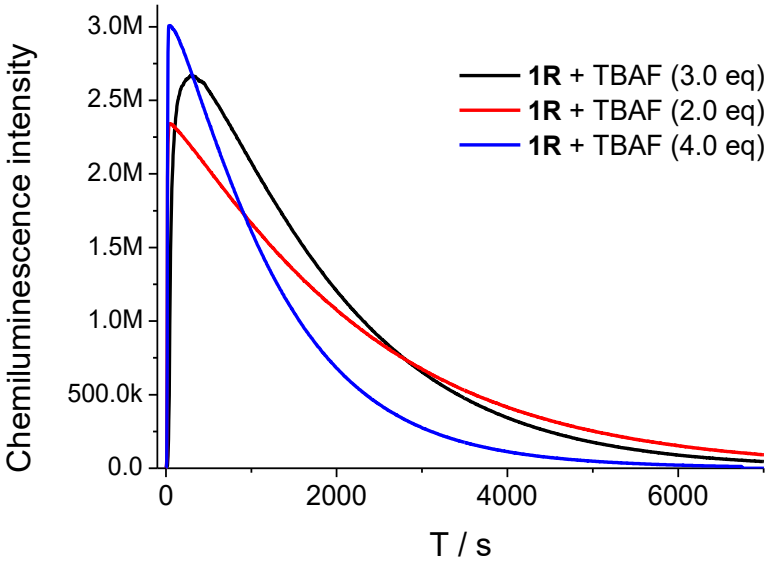

Figure S10 The chemiluminescent kinetic profile (monitored at 500 nm) of **1R** in 2 mL DMSO solution (0.1 mM) with the addition of different TBAF (2 mM in DMSO) (0.2 mL for 2.0 eq.; 0.3 mL for 3.0 eq.; 0.4 mL for 4.0 eq.) with stirring at 293 K.

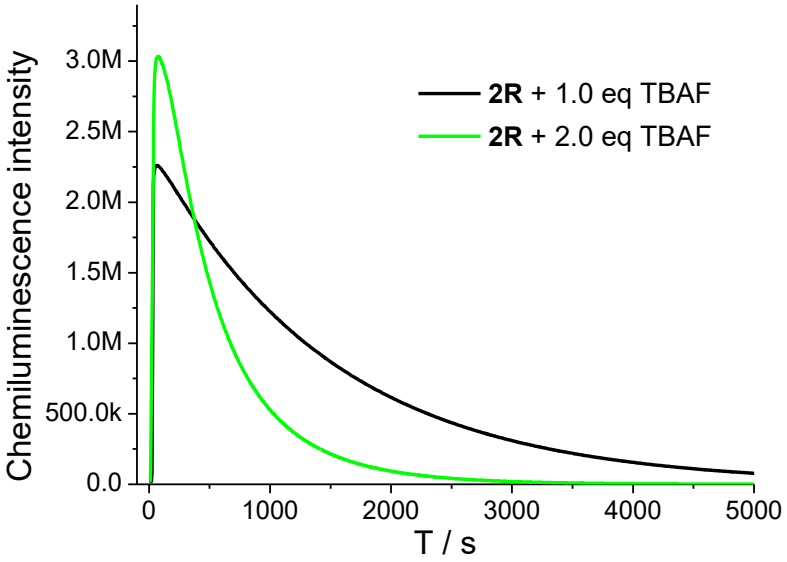

Figure S11 The chemiluminescent kinetic profile (monitored at 500 nm) of **2R** in 2 mL DMSO solution (0.1 mM) with the addition of different TBAF (1 mM in DMSO) (0.2 mL for 1 eq.; 0.4 mL for 2 eq.) with stirring at 293 K.

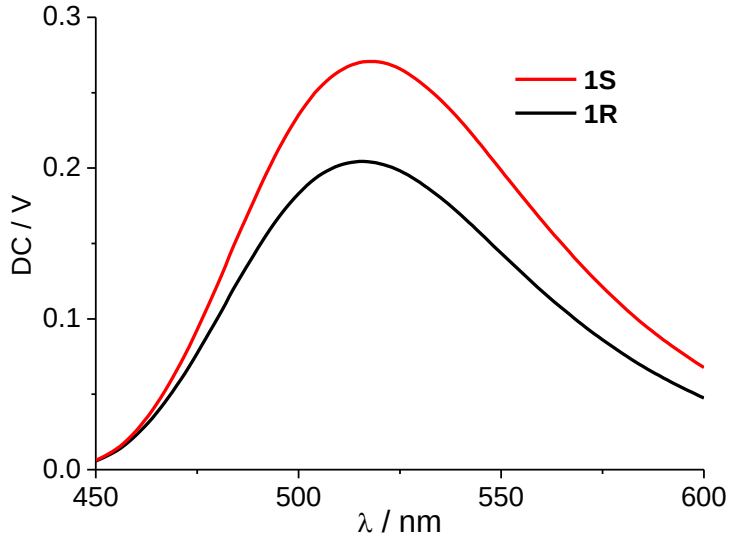

Figure S12 CP-CL DC value spectra of **1R**/**1S** in DMSO (5.0×10^{-4} M) after the addition of TBAF (2.0 equiv. per dioxetane group).

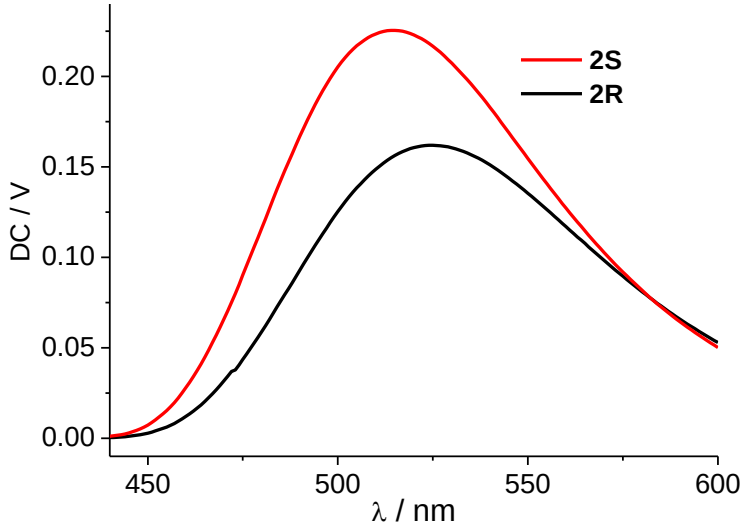

Figure S13 CP-CL DC value spectra of **2R**/**2S** in DMSO (5.0×10^{-4} M) after the addition of TBAF (2.0 equiv. per dioxetane group).

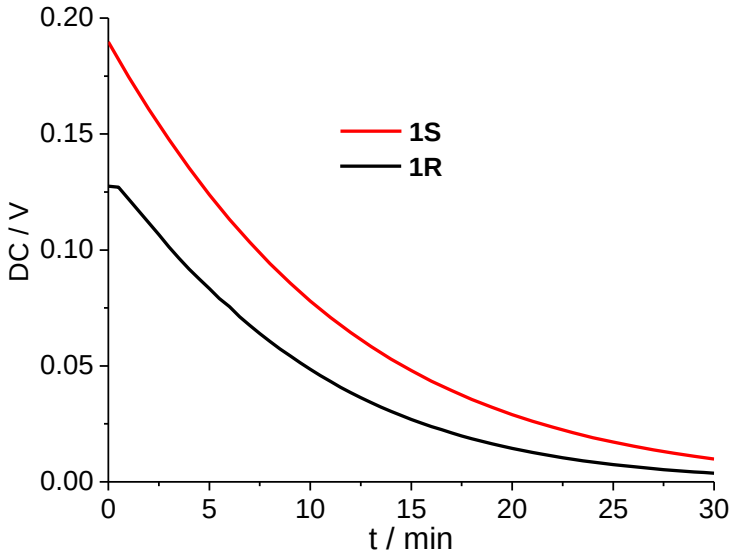

Figure S14 kinetic decay of CP-CL DC values at 500 nm of **1R**/**1S** in DMSO (5.0×10^{-4} M) after the addition of TBAF (2.0 equiv. per dioxetane group).

Absorption, CD, PL, and CPL Spectra of Dioxetanes and Benzoate Esters

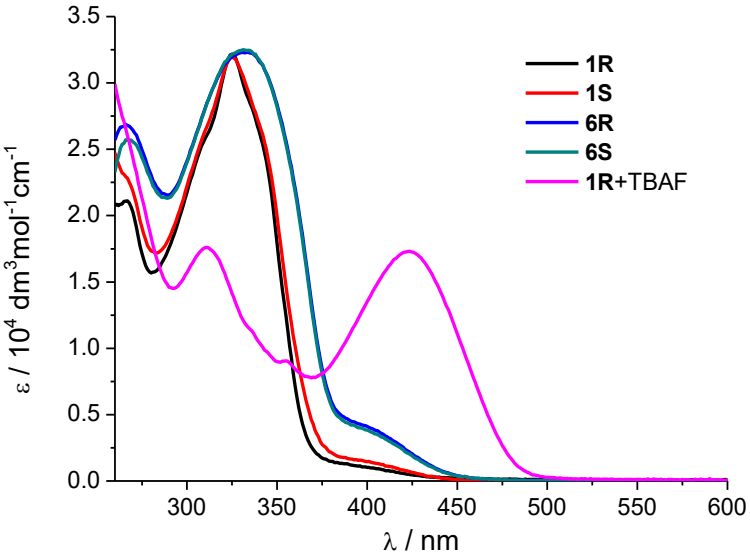

Figure S15. Electronic absorption spectra of **1R**/**1S**, **6R**/**6S** and **1R**+TBAF (2 eq.) in DMSO (1×10^{-5} M) at 298 K.

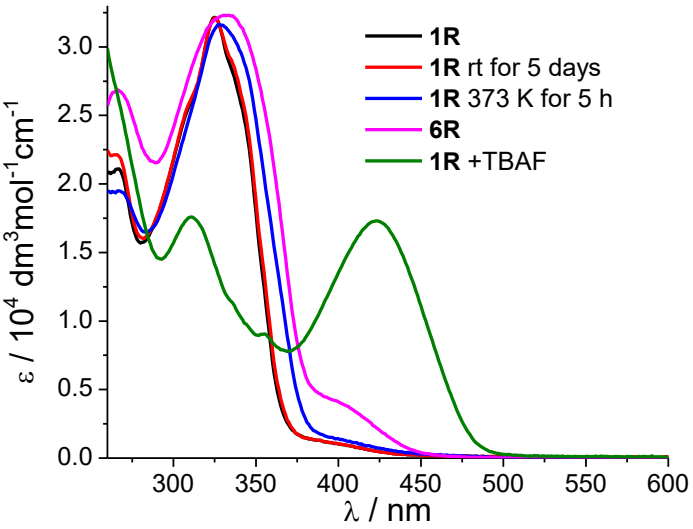

Figure S16. Electronic absorption spectra of **1R**, **1R** stored at rt for 5 days, **1R** heated at 100 °C for 5 hours, **6R** and **1R**+TBAF (2 eq.) in DMSO (1×10^{-5} M) at 298 K

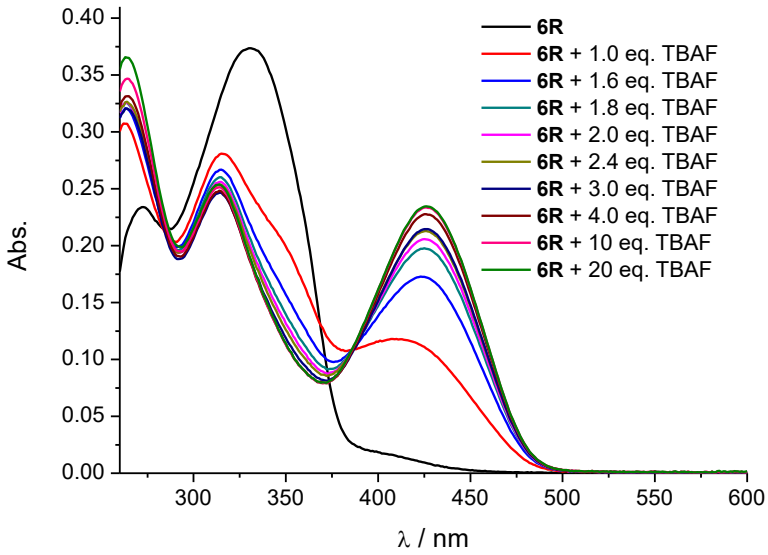

Figure S17. Electronic absorption spectra of the mixture of **6R** with different amount TBAF in DMSO (1×10^{-5} M) at 298 K.

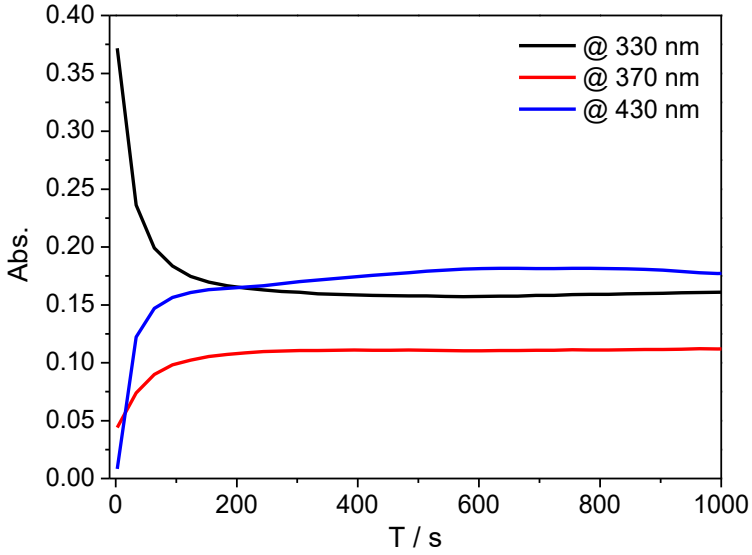

Figure S18. Time-course of the UV-vis kinetic profile at 330, 370 and 430 nm of the **1R** (1×10^{-5} M in DMSO) was added 2.0 equiv. TBAF.

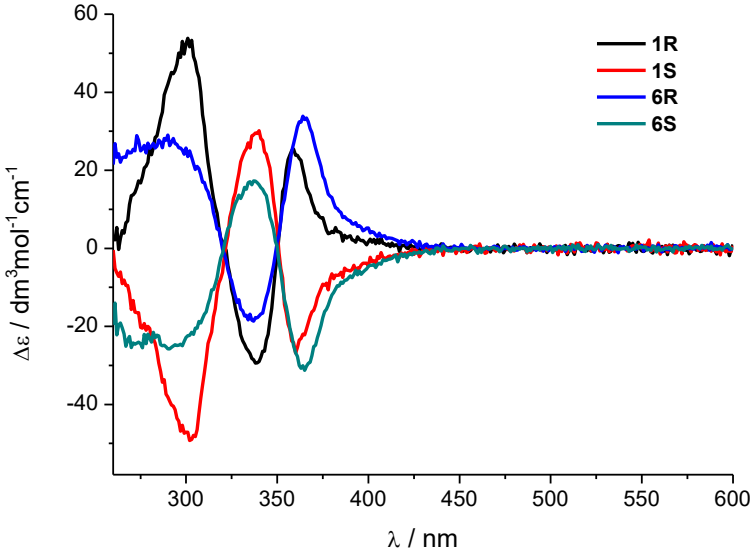

Figure S19. ECD spectra ($\Delta\varepsilon$) of **1R**/**1S**, **6R**/**6S** in DMSO (1×10^{-5} M) at 298 K.

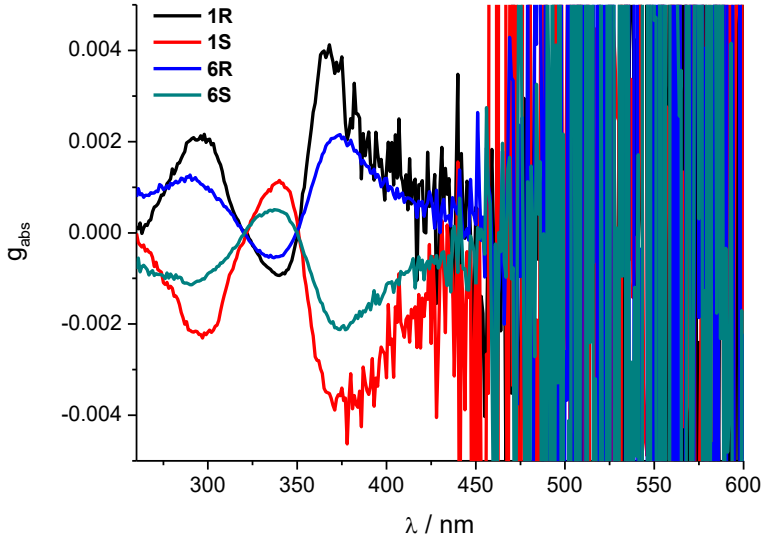

Figure S20. g_{abs} vs wavelength of **1R**/**1S**, **6R**/**6S** in DMSO (1×10^{-5} M) at 298 K.

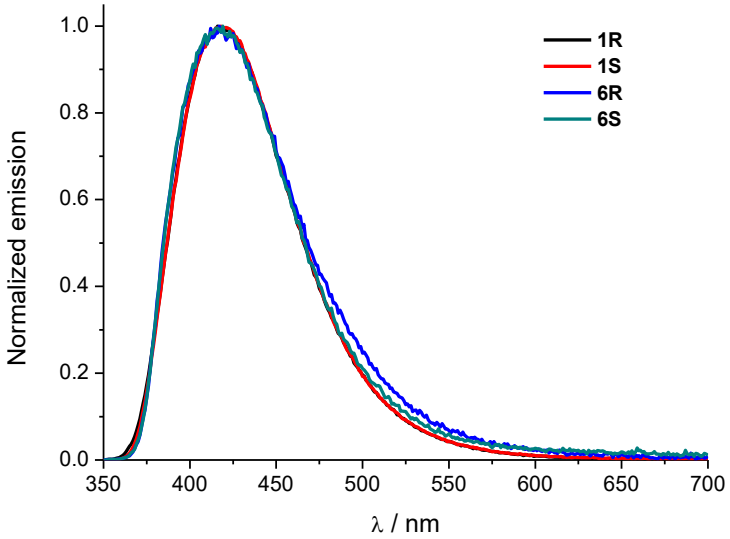

Figure S21. Photoluminescence spectra of **1R**/**1S** (λ_{ex} = 330 nm), **6R**/**6S** (λ_{ex} = 330 nm) in DMSO (1×10^{-5} M) at 298 K.

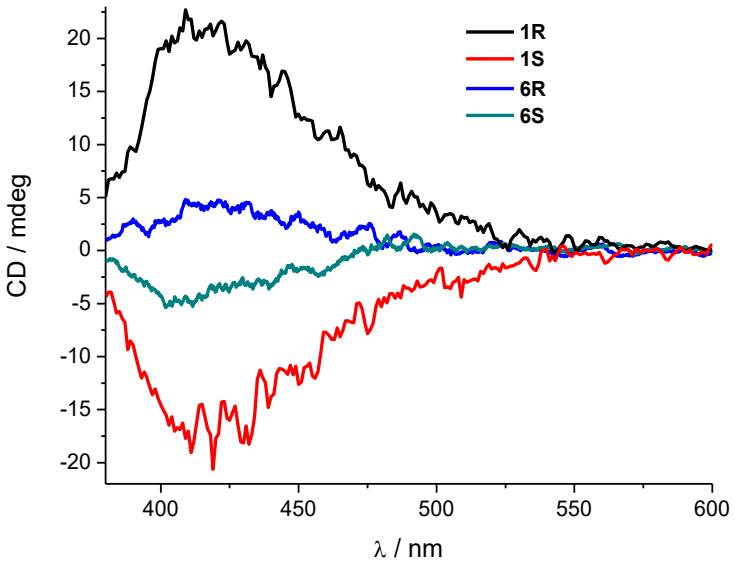

Figure S22. CP-PL spectra of **1R**/**1S** (λ_{ex} = 320 nm), **6R**/**6S** (λ_{ex} = 320 nm) in DMSO (1×10^{-5} M) at 298 K.

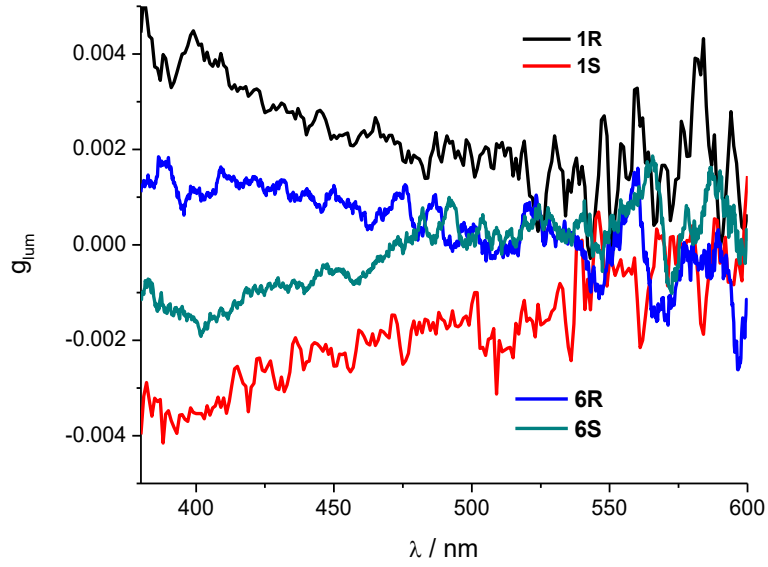

Figure S23. g_{lum} vs wavelength of **1R**/**1S**, **6R**/**6S** in DMSO (1×10^{-5} M) at 298 K.

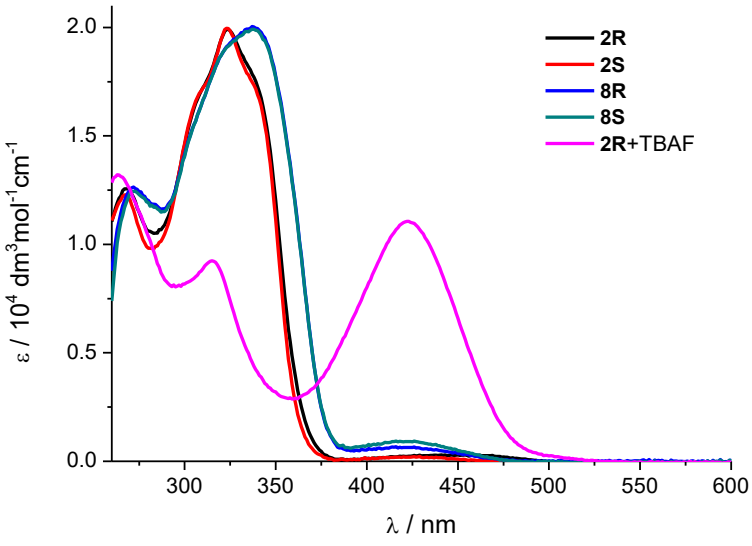

Figure S24. Electronic absorption spectra of **2R**/**2S**, **8R**/**8S** and **2R**+TBAF (1 eq.) in DMSO (1×10^{-5} M) at 298 K.

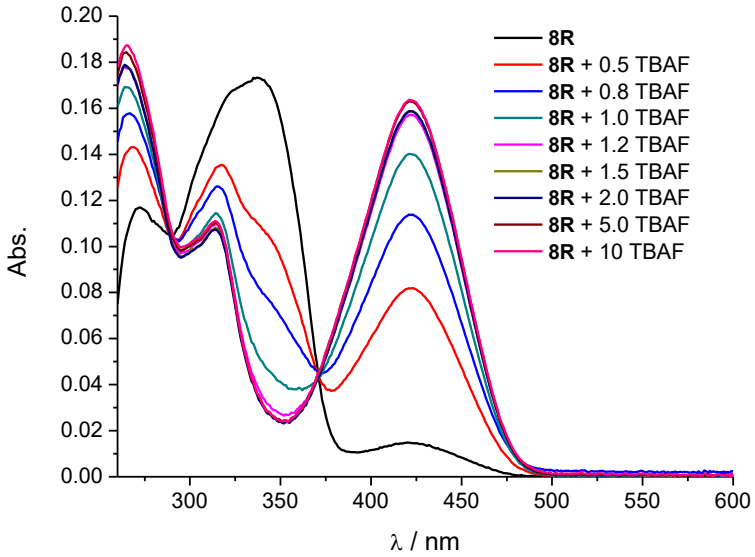

Figure S25. Electronic absorption spectra of the mixture of **8R** with different amount TBAF in DMSO (1×10^{-5} M) at 298 K.

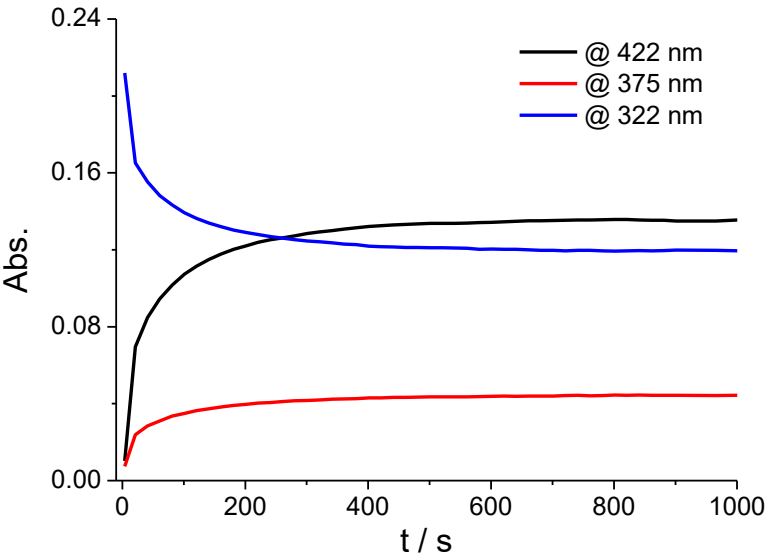

Figure S26. Time-course of the UV-vis kinetic profile at 322, 375 and 422 nm of the **2R** (1×10^{-5} M in DMSO) was added 1.0 equiv. TBAF.

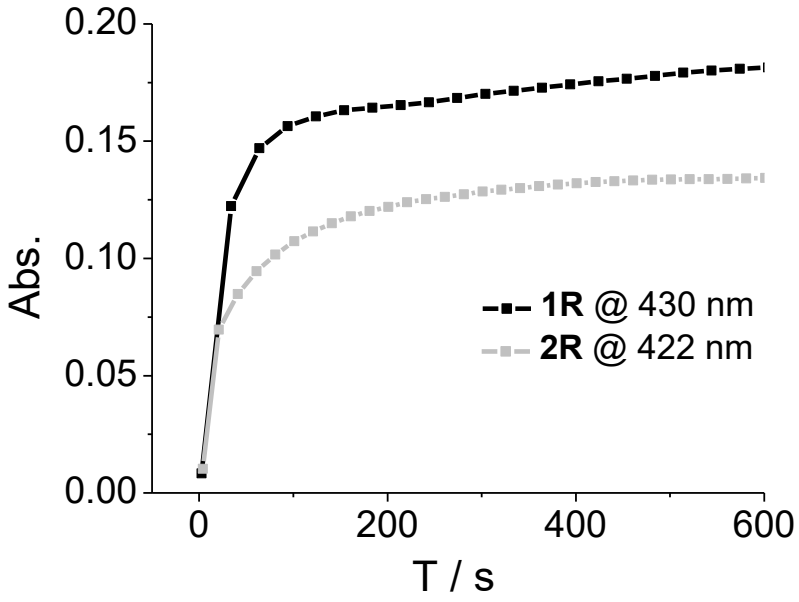

Figure S27.The absorption kinetic profile comparison of **1R** and **2R** at certain wavelength.

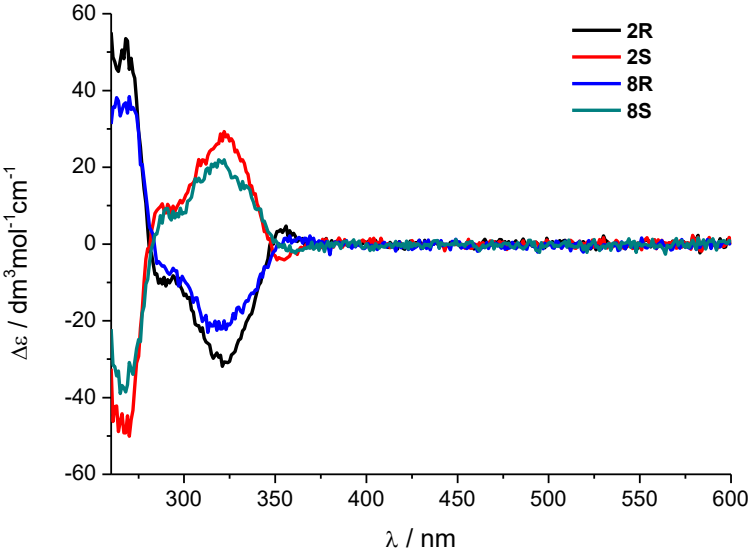

Figure S28. ECD spectra ($\Delta\varepsilon$) of **2R**/**2S**, **8R**/**8S** in DMSO (1×10^{-5} M) at 298 K.

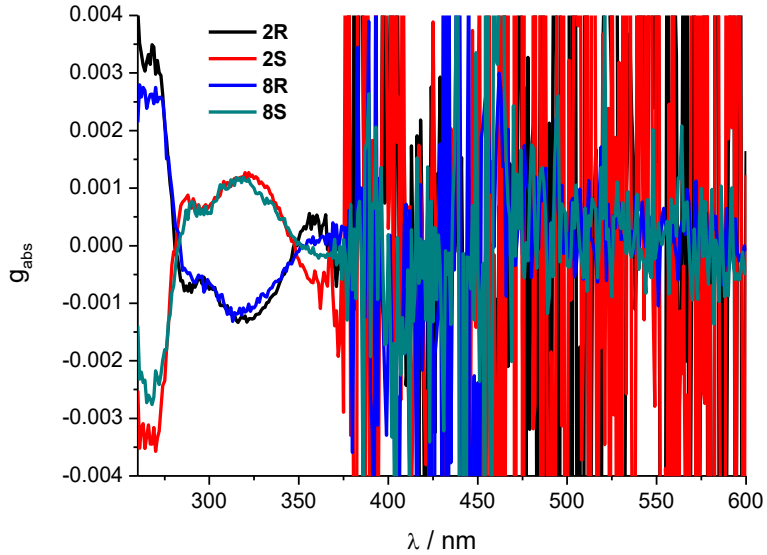

Figure S29. g_{abs} vs wavelength of **2R**/**2S**, **8R**/**8S** in DMSO (1×10^{-5} M) at 298 K.

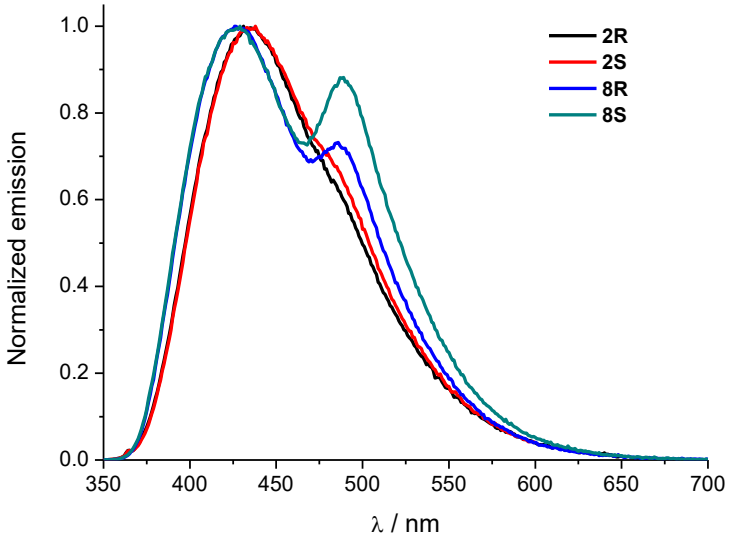

Figure S30. Photoluminescence spectra of **2R**/**2S** (λ_{ex} = 330 nm), **8R**/**8S** (λ_{ex} = 330 nm) in DMSO (1×10^{-5} M) at 298 K.

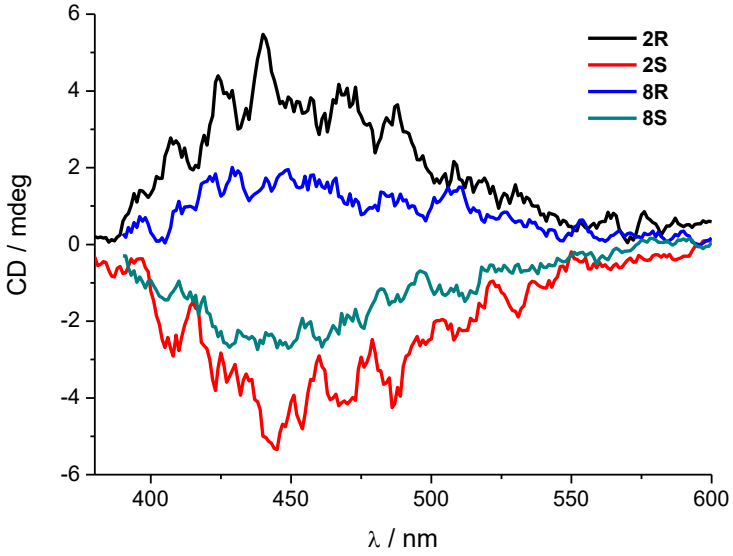

Figure S31. CP-PL spectra of **2R**/**2S** (λ_{ex} = 320 nm), **8R**/**8S** (λ_{ex} = 320 nm) in DMSO (1×10^{-5} M) at 298 K.

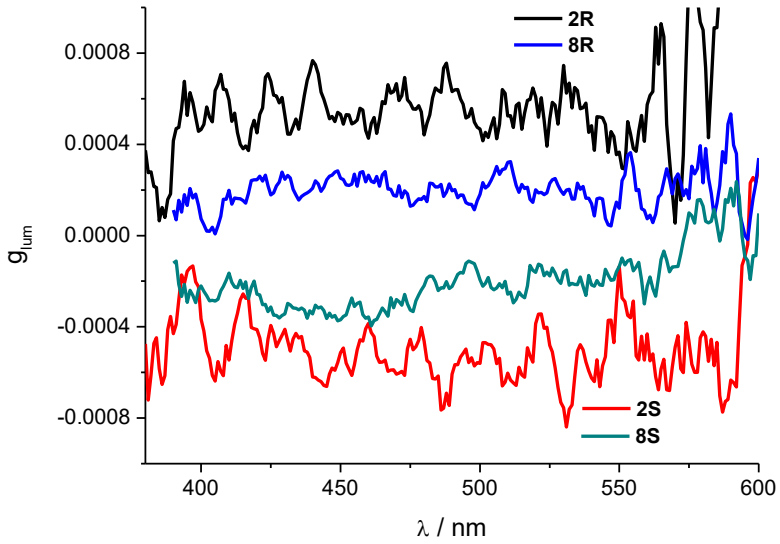

Figure S32. g_{lum} vs wavelength of **2R**/**2S**, **8R**/**8S** in DMSO (1×10^{-5} M) at 298 K.

Spectral Comparison of Mixtures with Different Sources

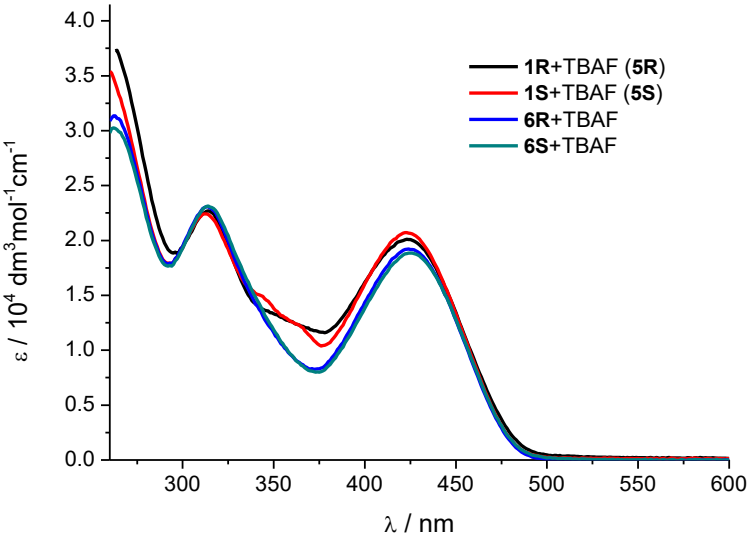

Figure S33. Comparison of absorption spectra of the spent reaction mixtures of **1R**/**1S**+TBAF (**5R**/**5S**) and **6R**/**6S**+TBAF in DMSO (1×10^{-5} M) at 298 K.

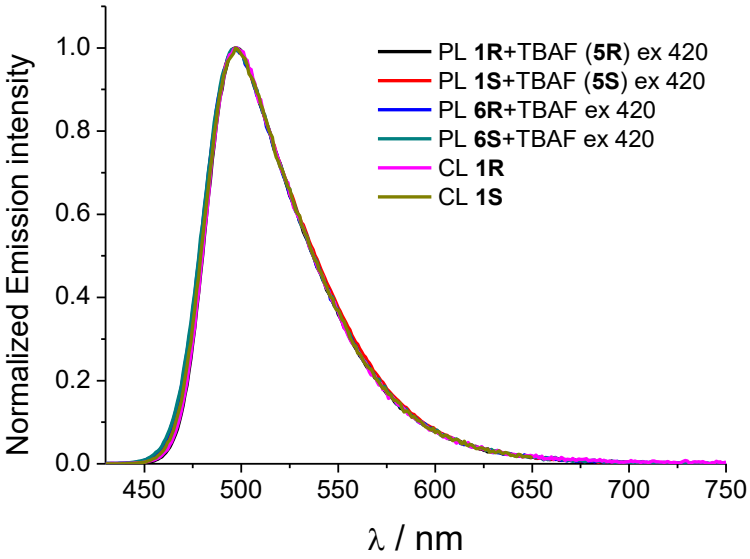

Figure S34. Comparison of photoluminescence spectra of the spent reaction mixtures of **1R**/**1S**+TBAF (**5R**/**5S**) (λ_{ex} = 410 nm) and **6R**/**6S**+TBAF (λ_{ex} = 410 nm) in DMSO (1×10^{-5} M) and chemiluminescence spectra of dioxetanes **1R**/**S** in DMSO (1×10^{-4} M) at 298 K after the addition of TBAF (1.0 equiv. per dioxetane group).

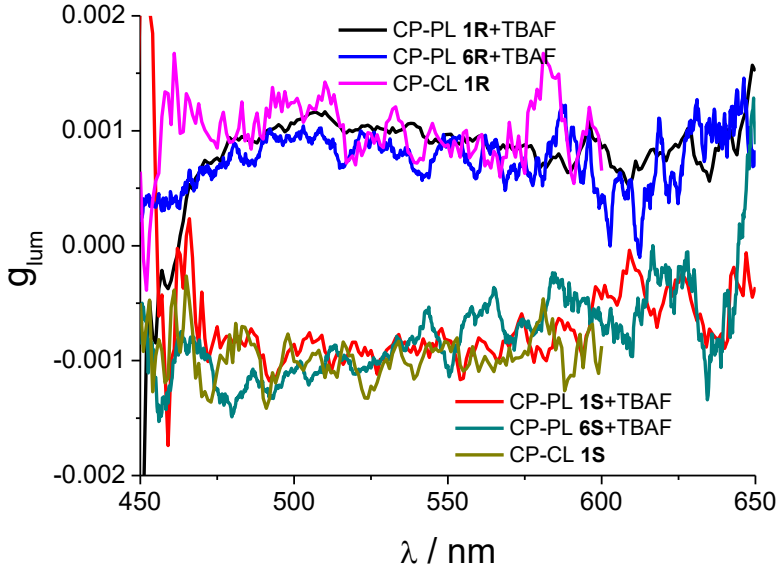

Figure S35. Comparison of g_{lum} plots of photoluminescence (λ_{ex} = 310 nm) of the spent reaction mixtures of **1R**/**1S**+TBAF (**5R**/**5S**) and **6R**/**6S**+TBAF in DMSO (1×10^{-5} M) and g_{CL} of **1R**/**1S** in DMSO (5×10^{-4} M) at 298 K after the addition of TBAF (2.0 equiv. per dioxetane group).

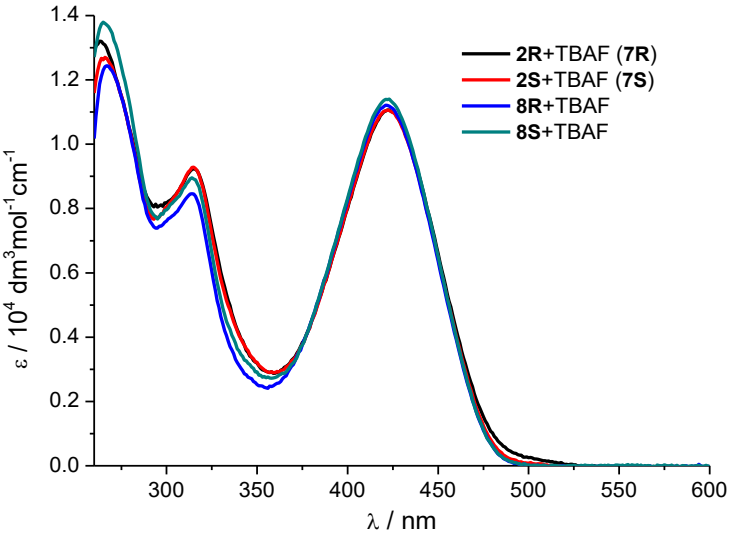

Figure S36. Comparison of absorption spectra of the spent reaction mixtures of **2R**/**2S**+TBAF (**7R**/**7S**) and **8R**/**8S**+TBAF in DMSO (1×10^{-5} M) at 298 K.

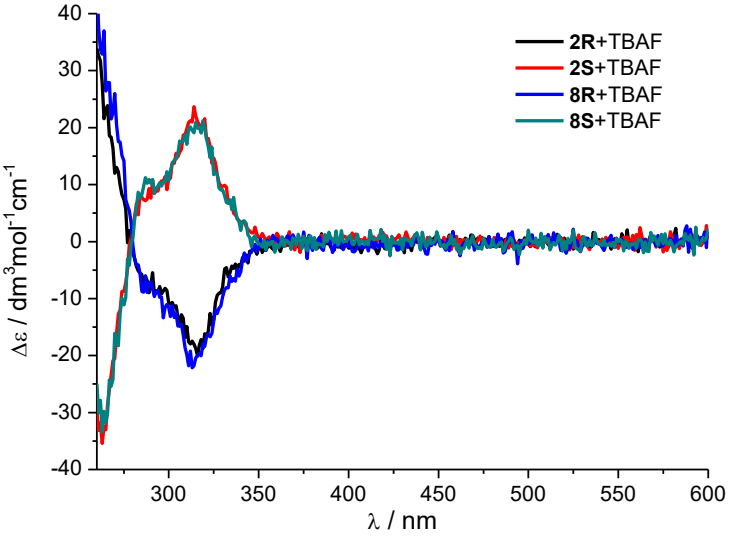

Figure S37. Comparison of ECD spectra of the spent reaction mixtures of **2R**/**2S**+TBAF (**7R**/**7S**) and **8R**/**8S**+TBAF in DMSO (1×10^{-5} M) at 298 K.

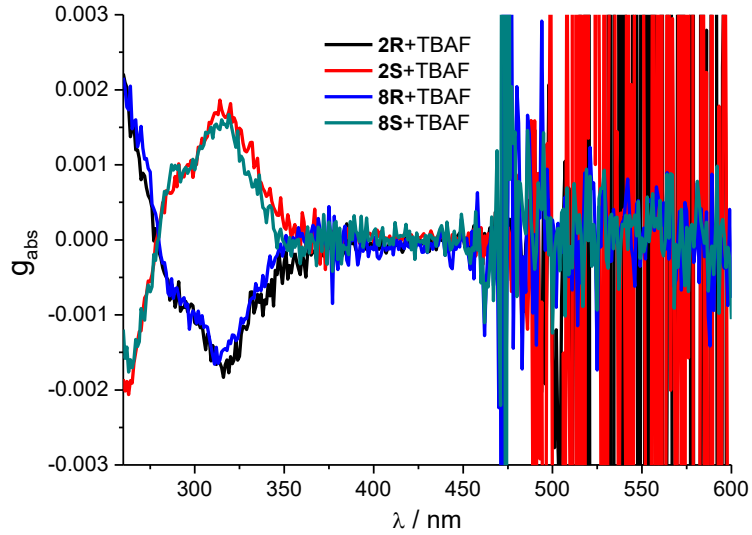

Figure S38. Comparison of g_{abs} plots of the spent reaction mixtures of **2R**/**2S**+**TBAF** (**7R**/**7S**) and **8R**/**8S**+TBAF in DMSO (1×10^{-5} M) at 298 K.

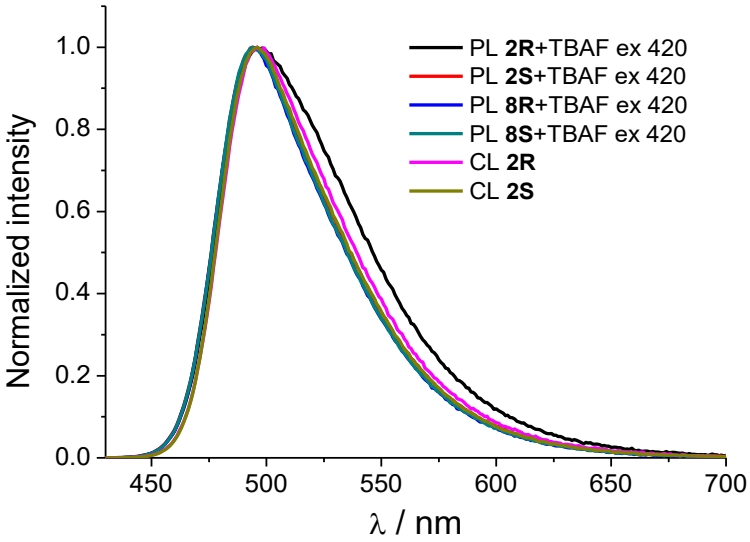

Figure S39. Comparison of photoluminescence spectra of the spent reaction mixtures of **2R**/**2S**+TBAF (**7R**/**7S**) (λ_{ex} = 410 nm) and **8R**/**8S**+TBAF (λ_{ex} = 410 nm) in DMSO (1×10^{-5} M) and chemiluminescence spectra of dioxetanes **2R**/**2S** in DMSO (1×10^{-4} M) at 298 K after the addition of TBAF (1.0 equiv. per dioxetane group).

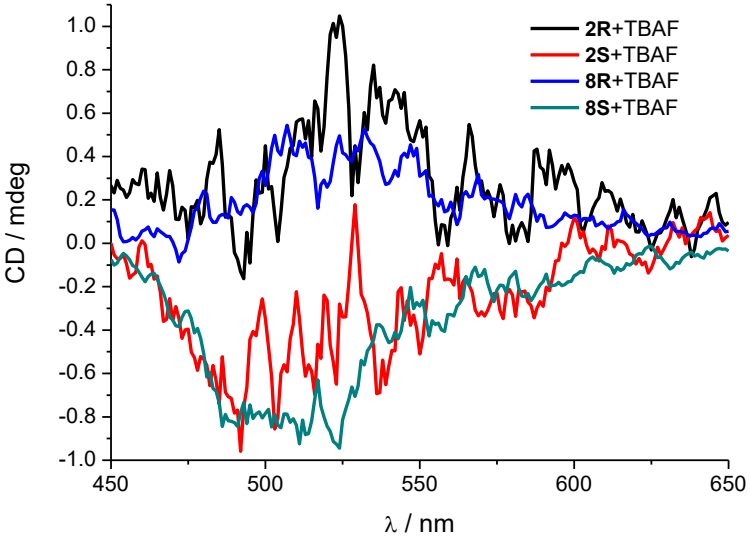

Figure S40. Comparison of CP-PL spectra of the spent reaction mixtures of **2R**/**2S**+TBAF (**7R**/**7S**) (λ_{ex} = 310 nm) and **8R**/**8S**+TBAF (λ_{ex} = 310 nm) in DMSO (1×10^{-5} M) at 298 K.

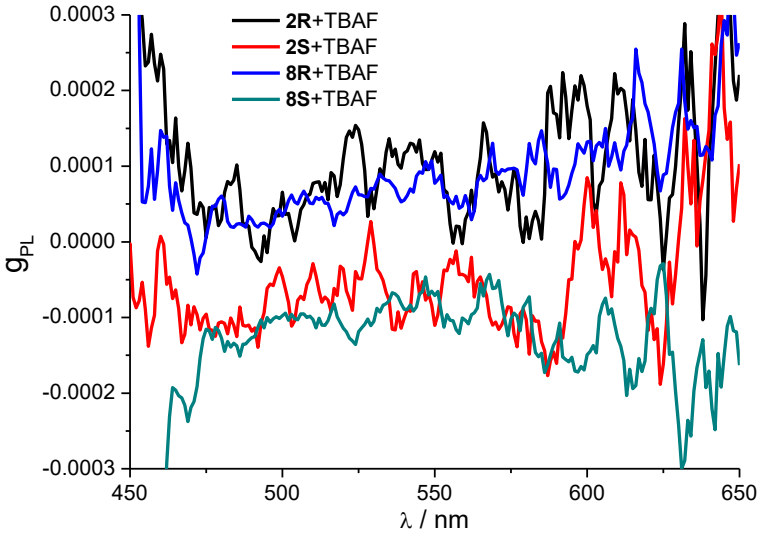

Figure S41. Comparison of g_{PL} plots of the spent reaction mixtures of **2R**/**2S**+TBAF (**7R**/**7S**) and **8R**/**8S**+TBAF in DMSO (1×10^{-5} M) at 298 K.

Computational Results

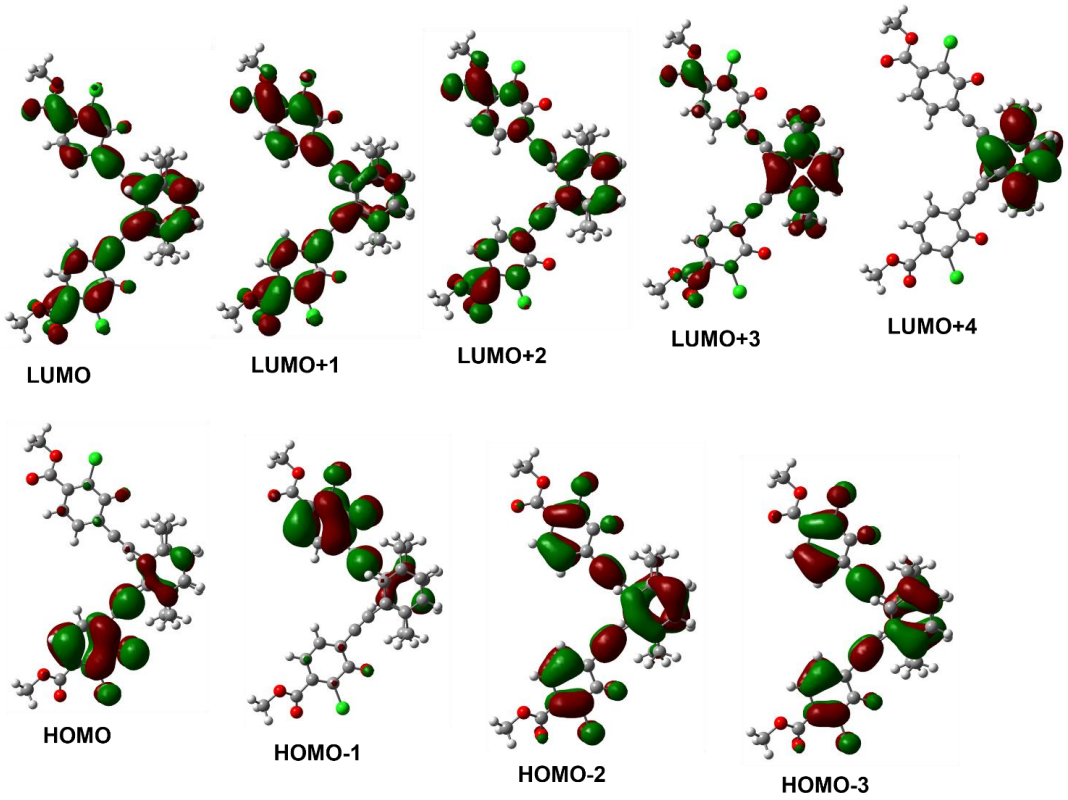

Figure S42. Frontier molecular orbitals of **5R**.

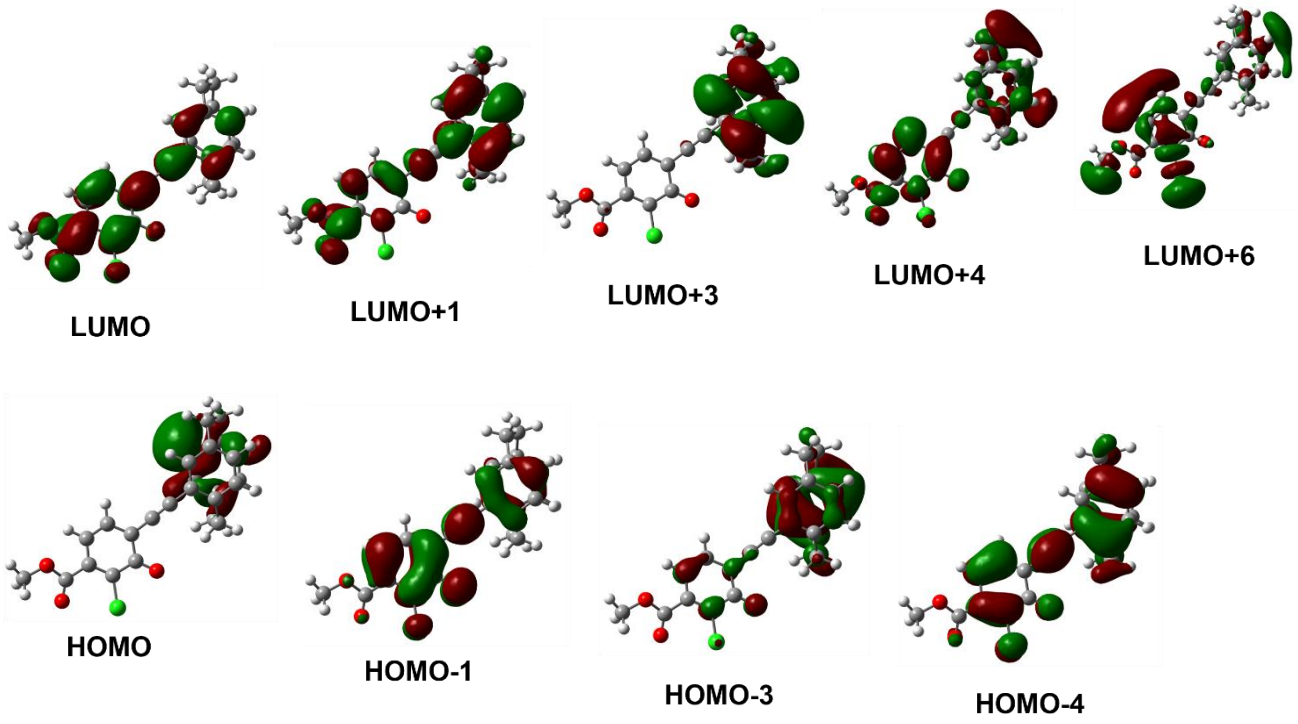

Figure S43. Frontier molecular orbitals of **7R**.

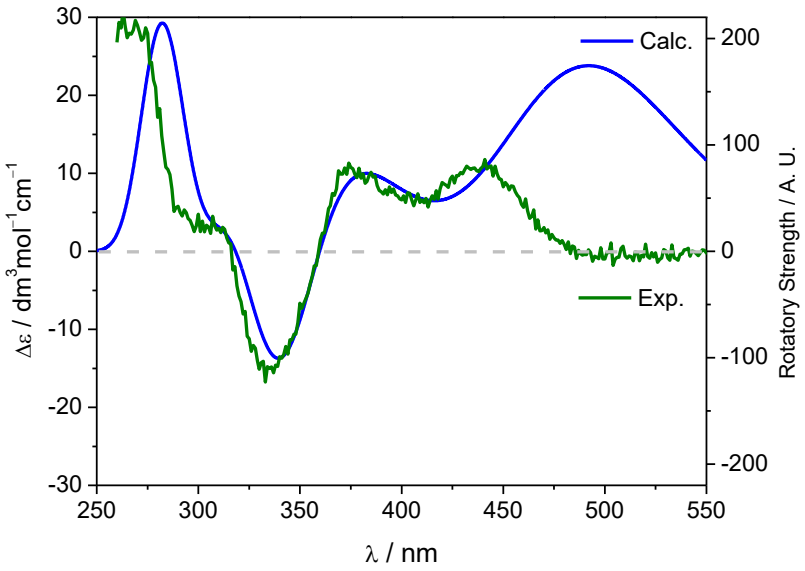

Figure S44. Comparison of the experimental and calculated TDDFT (BHLYP/SV(P) with DMSO continuum solvent model) ECD spectra of **5R**.

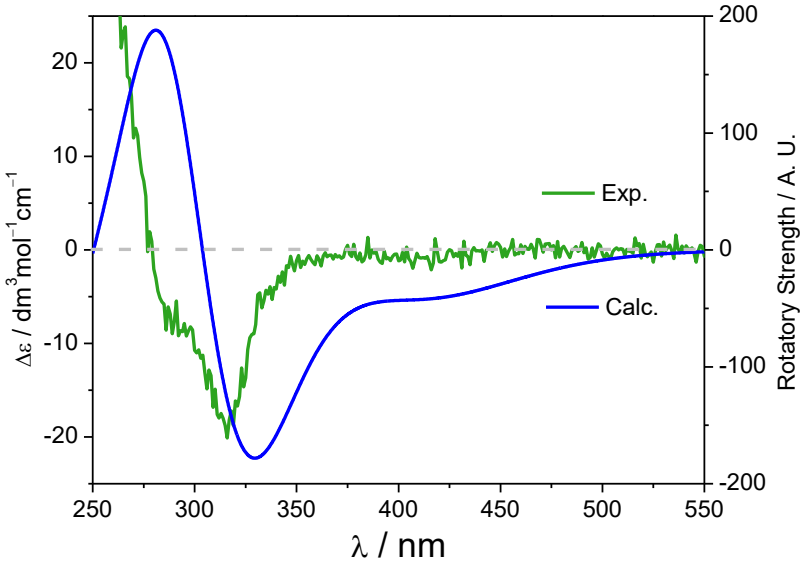

Figure S45. Comparison of the experimental and calculated TDDFT (BHLYP/SV(P) with DMSO continuum solvent model) ECD spectra of **7R**.

Table S5. Calculated absorption wavelength and the corresponding rotatory strength and electron transitions of **5R**.

	Wavelength	Rotatory strength	Ele. Dip. S.[a]	Mag(*v*). Dip. S.[b]	E.-M. angle[c]	Transition
1	492.38 nm	123.54	9.5684	0.1146	19.33	H→L (52.6%), H→L+1 (17.5%)
2	393.75 nm	42.53	0.1399	0.0029	79.45	H→L+1 (44.1%), H→L (29.3%)
3	392.32 nm	-21.43	0.1798	0.0038	111.09	H-1→L+1 (39.9%), H-1→L (34.5%)
4	359.96 nm	118.51	0.9397	0.0219	76.84	H→L+2 (16.9%), H-1→L+3 (14.9%)
6	356.03 nm	76.46	0.4041	0.0100	23.98	H-5→L+1 (24.4%), H-5→L (18.5%)
7	355.10 nm	-139.46	2.8211	0.0745	170.00	H→L+7 (35.6%), H→L+4 (22.1%)
8	352.39 nm	70.8	0.3682	0.0084	70.72	H-3→L (28.7%), H-5→L (8.4%)
9	345.17 nm	-161.22	1.7900	0.0487	164.56	H-2→L (34.3%), H-3→L+1 (11.9%)
10	325.02 nm	-12.32	0.0458	0.0015	129.7	H-9→L (25.9%), H-9→L+1 (19.0%)
11	322.12 nm	38.75	0.0415	0.0014	10.77	H→L+3 (28.2%), H-6→L (13.6%)
12	319.91 nm	-91.53	0.7575	0.0263	104.6	H-1→L+3 (26.1%), H-7→L (16.8%)
13	316.48 nm	85.89	0.268	0.0095	57.51	H→L+4 (54.7%), H-6→L (13.4%)
14	315.85 nm	21.79	0.2214	0.0078	79.87	H-1→L+4 (56.2%), H→L+4 (13.1%)
15	309.01 nm	-50.23	0.1335	0.0046	125.59	H-1→L+12 (19.7%), H-3→L+1 (18.6%)
16	307.90 nm	70.96	0.6802	0.0256	72.18	H→L+13 (37.1%), H→L+10 (15.6%)
17	302.64 nm	27.33	0.0615	0.0028	55.79	H-12→L+1 (13.5%), H-12→L (11.2%)
18	302.13 nm	57.25	0.5323	0.0200	72.67	H-1→L+5 (30.9%), H-1→L+12 (12.2%)
19	301.54 nm	-56.38	0.4217	0.0178	141.84	H→L+5 (25.7%)
20	298.64 nm	-134.11	0.685	0.0271	125.89	H-7→L+1 (17.5%), H-3→L+3 (14.7%)
21	297.86 nm	-47.93	0.6906	0.0261	96.35	H→L+13 (9.9%), H-3→L (9.0%)
22	295.74 nm	-49.56	0.084	0.0038	145.81	H-7→L (24.8%), H-2→L+1 (21.9%)
23	292.33 nm	134.67	0.7700	0.0328	41.56	H-1→L+9 (8.7%), H-1→L+5 (5.5%)
24	290.63 nm	60.12	0.5559	0.0262	73.05	H→L+10 (6.2%), H-1→L+5 (5.3%)
25	287.92 nm	-15.76	0.3069	0.0159	121.17	H-6→L+1 (19.7%), H-4→L+1 (10.5%)
26	284.97 nm	-28.25	0.1698	0.0078	107.82	H-4→L+10 (20.5%), H-5→L+10 (10.9%)
27	282.30 nm	88.91	0.5370	0.0240	71.10	H-7→L+1 (8.1%), H-2→L+4 (7.4%)

[a]The square of transition electronic dipole moment. [b]The square of magnetic electronic dipole moment in velocity representation. [c]The angle between the transition electronic and magnetic dipole moment.

Table S6. Calculated absorption wavelength and the corresponding rotatory strength and electron transitions of **7R**.

	Wavelength	Rotatory strength	Ele. Dip. S.[a]	Mag(*v*). Dip. S.[b]	E.-M. angle[c]	Transition
1	431.76 nm	7.50	6.1683	0.0724	89.37	H-1→L (83.1%)
2	427.38 nm	-20.45	0.5939	0.0075	93.66	H→L+3 (37.9%), H→L+7 (17.9%), H→L+5 (15.1%), H-1→L (10.2%)
3	408.61 nm	-15.73	0.0559	0.0007	112.33	H→L+1 (36.9%), H→L (19.3%), H→L+4 (10.9%), H→L+12 (7.8%), H→L+3 (6.9%)
4	339.27 nm	-6.40	0.0193	0.0004	121.88	H-2→L (71.0%), H-2→L+1 (21.0%)
5	320.03 nm	-155.85	1.2554	0.0273	121.41	H-3→L (68.6%), H-3→L+1 (11.8%)
6	316.22 nm	-8.78	0.0156	0.0007	111.42	H→L+12 (39.3%), H→L+1 (16.2%)
7	292.70 nm	108.24	3.5834	0.0940	57.76	H-4→L (51.0%), H-1→L+1 (17.2%)
8	290.36 nm	23.92	0.0470	0.0010	37.53	H→L+7 (35.6%), H→L+4 (22.1%)
9	285.95 nm	-32.70	0.0125	0.0007	91.53	H-1→L+1 (65.5%), H-4→L (14.6%)
10	277.13 nm	60.72	0.3456	0.0099	14.02	H-1→L+3 (31.2%), H-6→L (11.2%)
11	270.52 nm	-17.63	0.0470	0.0014	120.78	H-2→L+3 (57.4%), H→L+8 (22.7%)
12	264.99 nm	-12.89	0.0900	0.0023	147.35	H→L+8 (55.5%), H-2→L+3 (25.0%)
13	261.94 nm	25.06	0.0378	0.0010	36.63	H-2→L+1 (42.3%), H-1→L (13.8%)
14	254.53 nm	21.26	0.0382	0.0018	59.32	H-3→L+3 (9.1%), H-1→L+2 (8.9%)
15	251.35 nm	-13.94	0.0579	0.0020	126.86	H→L+4 (40.3%), H→L+5 (32.4%)
16	247.91 nm	-48.41	0.1946	0.0076	117.76	H-6→L (17.3%), H-3→L+1 (14.8%)
17	244.57 nm	98.93	0.1274	0.0054	13.00	H-3→L+1 (39.1%), H-1→L+3 (10.4%)
18	241.19 nm	17.02	0.0326	0.0016	51.08	H-10→L (38.6%), H-17→L (13.1%)
19	239.63 nm	-34.39	0.6620	0.0261	110.44	H-1→L+2 (45.0%), H-1→L+6 (8.4%)
20	238.83 nm	30.91	1.1046	0.0449	82.65	H-1→L+2 (19.7%), H-3→L+3 (14.9%)
21	236.13 nm	-109.14	0.3677	0.0161	163.96	H-1→L+4 (16.7%), H-3→L+3 (14.9%)
22	227.18 nm	21.92	0.2505	0.0101	83.65	H-3→L+5 (21.7%), H-2→L+5 (14.3%)

[a]The square of transition electronic dipole moment. [b]The square of magnetic electronic dipole moment in velocity representation. [c]The angle between the transition electronic and magnetic dipole moment.

Table S7. Cartesian coordinate of **5R** in ground state (M062X/6-311G(d,p)).

E(M062X) = -2757.625917 Hartree

atom	x	y	z
Cl	-7.59504600	0.60498400	-0.86962200
Cl	7.43083800	0.78556700	0.96875500
O	8.06957800	3.32397700	-0.40342100
O	-6.81779700	4.61750800	0.86425500
O	-7.79466100	3.60581600	-0.88517800
O	-5.22451800	-1.02162600	-0.35034500
O	5.11661500	-0.89821300	0.39306000
O	6.51438300	4.90277700	-0.07134000
C	9.05019100	4.35492000	-0.31483900
H	8.90477500	5.10560500	-1.09656200
H	10.01076500	3.85617800	-0.44116100
H	9.00714000	4.85644500	0.65524900
C	6.78537200	3.72819600	-0.22053200
C	5.78680000	2.62928900	-0.30185300
C	4.55255700	3.00765500	-0.87838100
H	4.41559400	4.03969000	-1.17088300
C	3.56351700	2.06176700	-1.07357700
H	2.62586700	2.34884900	-1.53881200
C	3.73546700	0.72539000	-0.69006800
C	2.73799600	-0.24554700	-0.92586800
C	1.93949000	-1.14205000	-1.11626400
C	1.16256700	-2.31498700	-1.29932800
C	1.73368200	-3.56688900	-0.94593700
C	2.88492600	-3.64688300	0.03229700
H	3.70093600	-2.96616600	-0.22463300
H	3.27536700	-4.66991200	0.02801700
C	2.44985200	-3.27534000	1.52970900
H	3.00417600	-3.93719500	2.20418500
H	2.79391400	-2.25857300	1.72201000
C	0.95456800	-3.37954100	1.75896200
C	0.14430300	-2.24348800	1.68484200
H	0.59706100	-1.26038800	1.74877400
C	-1.21459800	-2.32591600	1.32137200
C	-2.01772700	-1.17403600	1.12003100
C	-2.83629600	-0.29878300	0.91629400
C	-3.84982000	0.65044400	0.66289400
C	-5.06996400	0.16092500	0.01369800
C	-6.08551300	1.19287700	-0.16374300

C	-5.92295900	2.52490500	0.22303400
C	-6.94392800	3.57322800	-0.02711700
C	-7.70778000	5.70594600	0.63695100
H	-7.55548800	6.14302800	-0.35395900
H	-7.48154900	6.43935800	1.41135500
H	-8.75038000	5.38536800	0.71099700
C	5.96875000	1.30986800	0.11310300
C	4.95863700	0.26731500	-0.02132800
C	-0.19793800	-2.26934800	-1.66328200
H	-0.67332700	-1.29802000	-1.74129900
C	-0.98169000	-3.42487200	-1.72091900
C	-2.47908100	-3.35286600	-1.49283800
H	-3.01749100	-4.03622600	-2.15864800
H	-2.84628600	-2.34699900	-1.69908700
C	-2.90572100	-3.71491600	0.00937600
H	-3.73728400	-3.05022200	0.25854600
H	-3.27241300	-4.74653700	0.02686600
C	-1.75647500	-3.59553400	0.98597600
C	-1.02309800	-4.71965200	1.36672100
H	-1.45349600	-5.70395500	1.20042600
C	0.30958900	-4.62281300	1.76318100
H	0.89092000	-5.53043700	1.90298900
C	-0.30802800	-4.65269300	-1.70801300
H	-0.86809200	-5.57544700	-1.83490800
C	1.02647800	-4.71291300	-1.31059600
H	1.47955000	-5.68453300	-1.13051400
C	-3.70426800	1.99280300	1.03704400
H	-2.77233100	2.30045600	1.50067100
C	-4.70908100	2.91984400	0.83686000
H	-4.57983600	3.95054100	1.13171100

Table S8. Cartesian coordinate of **7R** in ground state (M062X/6-311G(d,p)).

E(M062X) = -1687.684534 Hartree

atom	x	y	z
Cl	-5.05532600	2.26039400	-0.35740100
O	-6.60664600	-1.89352200	0.12475200
O	-6.96473900	0.22806000	0.76478300
O	-2.15479100	2.05517200	-0.61606600
C	4.20581300	-1.16792200	1.81792200
C	5.43728900	-0.89973700	1.18491500
C	6.06793200	-2.00430200	0.34148000
H	6.28564800	-2.89653300	0.94237000
H	7.01851000	-1.65739300	-0.09017700
C	5.12241500	-2.47534500	-0.84594000
H	5.74902100	-2.87795500	-1.65535200
H	4.49928100	-3.29278600	-0.47684400
C	4.20612900	-1.36876000	-1.33461800
C	2.84009600	-1.39429000	-1.04950200
H	2.38034800	-2.31744900	-0.71740100
C	2.06874100	-0.21726600	-0.98242100
C	0.68605900	-0.26469200	-0.65625000
C	-0.51500700	-0.26338000	-0.46531200
C	-1.91471300	-0.29765200	-0.25969900
C	-2.67621400	0.95430900	-0.36804900
C	-4.11178500	0.77405200	-0.16256600
C	-4.72687100	-0.45404900	0.10582200
C	-6.17622100	-0.59992400	0.36848100
C	-7.97235900	-2.13241700	0.43935400
H	-8.17691900	-1.94881400	1.49857000
H	-8.15338300	-3.18088700	0.19823200
H	-8.63403700	-1.48980500	-0.14845700
C	3.39950200	-0.02995700	2.00879400
H	2.39424300	-0.14955300	2.42870800
C	3.72841700	1.26384000	1.53773800
C	2.63883400	2.24734000	1.15101700
H	2.90839600	3.27698000	1.42333900
H	1.72823100	1.99751500	1.70358100
C	2.25101200	2.26704500	-0.40925600
H	1.16747900	2.38389700	-0.49159500
H	2.71820800	3.14468000	-0.86982600
C	2.73212700	1.02899000	-1.12473700

C	4.00666200	1.01119100	-1.68989000
H	4.50593000	1.95817000	-1.87529600
C	4.73336300	-0.16807300	-1.81865200
H	5.77889500	-0.11593400	-2.10938000
C	5.07766700	1.49562000	1.23819800
H	5.41920200	2.49933100	0.98450600
C	5.94716800	0.40936700	1.08828500
H	6.97594300	0.59429000	0.76250000
C	-2.55141700	-1.51561400	0.01341300
H	-1.93593500	-2.40689500	0.08940300
C	-3.92034900	-1.61489600	0.18658600
H	-4.38486800	-2.56610600	0.40051500